GABRIEL GONZALO MACHADO

.

CORRELATIONS BETWEEN GEOLOGICAL TRACK AND BENTONITE QUALITY IN THE MERCOSUR TRADE BLOCK

São Paulo

2019

GABRIEL GONZALO MACHADO

CORRELATIONS BETWEEN GEOLOGICAL TRACK AND BENTONITE QUALITY IN THE MERCOSUR TRADE BLOCK

A thesis presented to the post graduation program of the mineral engineering & of the Escola Politécnica da Universidade de São Paulo as a requirement for the degree of Doctor of Science

São Paulo

2019

GABRIEL GONZALO MACHADO

CORRELATIONS BETWEEN GEOLOGICAL TRACK AND BENTONITE QUALITY IN THE MERCOSUR TRADE BLOCK

A thesis presented to the post graduation program of the mineral engineering & of the Escola Politécnica da Universidade de São Paulo as a requirement for the degree of Doctor of Science

Advisor:
Prof. Dr. Henrique Kahn
Co-advisor:
Prof. Dr. Francisco Valenzuela Diaz

São Paulo

2019

Este exemplar foi revisado e corrigido em relação à versão original, sob responsabilidade única do autor e com a anuência de seu orientador.

São Paulo, _____ de _____ de _____

Assinatura do autor: _____

Assinatura do orientador: _____

Catalogação-na-publicação

MACHADO, GABRIEL GONZALO
CORRELATIONS BETWEEN GEOLOGICAL TRACK AND BENTONITE QUALITY IN THE MERCOSUR TRADE BLOCK / G. G. MACHADO -- versão corr. – São Paulo, 2019.
128 p.

Tese (Doutorado) - Escola Politécnica da Universidade de São Paulo. Departamento de Engenharia de Minas e Petróleo.

1.Bentonita (aplicações industriais) 2.Caracterização tecnológica de minérios 3.Diagênese 4.Difração por raios X 5.Mercosul I.Universidade de São Paulo. Escola Politécnica. Departamento de Engenharia de Minas e Petróleo II.t.

Dedicated to my pillar during these tough four years; with love to you Josefina.

ACKOWLEDGEMENTS

In early 2015, the author of this thesis arrived to Sao Paulo as a foreigner embracing this challenging research project, without the support and guidance of everyone listed below, it would have been impossible to successfully achieve this enterprise, to all of them, I own eternal gratitude.

My advisor Prof. Henrique Kahn opened the door to the LCT and with it, came a wonderful team of researchers to aid me, for that I thank Juliana, Daniel, Renato, Carina, Manuela, Saulo, Guilherme, Fabrizzio, Paulo, Ilda, Ingled, Lino, Juscelino, Erilio, Adhemar, Fernanda, Thais, Gislayne, Mavinier. In the mining engineering department, I thank Eliana, Prof. Laurindo, Prof. Arthur, Prof. Homero, Fernanda, Alfredo, Juninho, Josi, Wellington, Jatoba, Andre Baradel and Yinka.

As co-advisor, Prof Francisco Valenzuela was a perfect match for our research topic along with his research group composed by Prof. Graça, Roberto and Wilson. In the chemistry department, I thank Prof. Jorgue Tenorio, Dr. Catia Graça, Dr. Paulo Moleira, Jorgue Coleti, Prof. Denise Crocce, Andre Vicente, Anna and Vitor. From other dependencies of the University of São Paulo I thank, Prof. Vera Constantino, Vanessa Roberta, Prof. Guilherme Ary Plonsky, Prof. Helio Wiebeck, Sheila Schuindt and Dr. Raphael Motta.

From other universities, research centers and other collaborators in Brazil, I thank André Calado, Prof. Andre Mexias, Prof. Romulo Angelica, Leopoldo Radtke, Profa. Simone Paz, Dr. Julio Harada, Arturo Cuicas, Juan Andrés Radina and Guillermo Mendez.

Researchers and collaborators from institutions abroad, Prof. George Christidis, Dr. Christian Detellier, Claude Fontaine, Dr. Jan Dietel, Dr. Stephan Kaufhold, Domingo Radina, James Sergeant and Silvana. To the *Coordenação de Aperfecionamento de Pessoal de Nivel Superior* (CAPES) for the financial support by means of a PhD scholarship and to those who have provided me with bentonite samples to work with.

Last but most important to my wife Josefina and my family Sofia, Gustavo, Petra, Eduardo, Patricia, Javier and all extended family for giving me the motivation to grow professionally.

"For the achievement of the triumph, it has always been indispensable to pass through the path of the sacrifices" (SIMÓN BOLÍVAR, 1783-1830)

This page was intentionally left blank.

ABSTRACT

It is undoubtable that the geological path followed by a bentonite natural occurrence, will set a birthmark in terms of grade and quality, the former being expressed in terms of mineralogical composition, smectite content and other aspects derived from the bulk sample characterization, and the latter being expressed in terms of the crystal chemistry of smectite species present and derived from the clay size fraction observations. The influence of parent rock composition, genesis mode, burial history and preservation conditions after alteration, would set the fingerprint on bentonite and inherent structural features in smectites species, which determines potential industrial and scientific uses.

The following thesis aims to evaluate physicochemical properties of 12 bentonite samples, coming from the six most relevant bentonite bearing geological areas located in the Mercosur economic block (Argentina, Brazil and Uruguay)[1]; in order to stablish possible correlations between distinctive geological contexts, and observed characteristics from whole rock providing information regarding grade and the clay size fraction will provide information regarding quality. Mineralogical composition corroborated the tendency to be influenced by the geochemical signature of parent rock firstly, and secondly genesis mode (probably due to lack of information in this aspect).

Age, on the other hand, could on the contrary, be a misleading parameter; in the sense that preservation is not necessarily time dependent. Poor grade and the presence of mixed layers and accessory clay mineral phases (mostly kaolinite but also I/S, illite and pyrophyllite) appear to be associated with hydrothermal to sedimentary alteration modes, higher grade bentonites with tendency to yield extreme relative values of physical properties, measured in layer charge, swelling and organic sorption, were found in association to diagenetic bentonites. In terms of smectite species, all members found belong to the montmorillonite-beidellite series, and rhyolitic to dacitic volcanic source, tends to alter into the

[1] Paraguay and Venezuela are also members of the Mercosur Economic trade block, but do not report Bentonite mining activity.

montmorillonite end member of the series; and accordingly, basic precursors (basalt) to intermediary (andesite), show a tendency to alter into transitional up to beidellite Fe-rich end members of the series respectively.

To evaluate implications on possible applications, crystal chemistry was evaluated over the <1 μm size fractions by XRD and XRF along with other accessory techniques (FTIR, SEM-EDS and size distribution analysis), finding a clear trend, between layer charge relative magnitude, as a function organo-sorption behavior; by simply evaluating the d-001 XRD reflections on oriented slides after first K-saturation and sequential ethylene glycol solvation, against (CTAC)-montmorillonite d001 basal reflection , being inversely proportional and resulting in a broad variety Organophilic XRD patterns, showing distinctive expandability behavior ranging from 15,2 Å To 21,68 Å. As a function of alkyl chain size and the known sorption isotherm, basically all patterns of organo-compound sorption where observed, going from lateral monolayer to paraffin type sorption behavior.

Key words: bentonites, di-octahedral smectites, diagenesis, layer charge, organoclays & Mercosur.

RESUMO

É inquestionável que o caminho geológico seguido pela ocorrência natural de bentonitas, irá indicar suas características em termos de teor e qualidade, o primeiro expressado em termos da composição mineralógica, conteúdo de esmectitas e outros aspectos derivados da caracterização da amostra cabeça, e o Segundo expressado em termos da química cristalina das espécies esmectiticas presentes e derivado das observações na fracção de tamanho de argilas. A influência da composição da rocha parental, sua gênese, o histórico de soterramento e das condições de preservação após processo de alteração, determinaria a "impressão digital" da bentonita e as características estruturais inerentes as espécies de esmectitas, que determina os usos potenciais e industriais.

O objetivo deste trabalho é avaliar propriedades físico-químicas de 12 amostras de bentonitas, provenientes de seis áreas geológicas mais relevantes localizadas no bloco econômico do Mercosul (Argentina, Brasil e Uruguai)[2]; o intuito é estabelecer possíveis correlações entre contextos geológicos distintos e características observadas em rochas (teor) e fração de tamanho de argila (qualidade).

A composição mineralógica corroborou a tendência de ser influenciada pela assinatura geoquímica da rocha parental em primeiro lugar, e em segundo lugar, por sua gênese (provavelmente devido à falta de informação neste aspecto).

A idade, por outro lado, poderia, pelo contrário, ser um parâmetro ilusório, no sentido de que a conservação não é necessariamente dependente do tempo. Baixo teor e baixo conteúdo de esmectita, assim como a presença de camadas mistas e fases argilosas acessórias (principalmente caulinita, mas também I/S, ilita e pirofilita) parecem estar associadas aos modos de alteração hidrotermal a sedimentar, bentonita de alto teor, com tendência a produzir valores relativos

[2] Paraguai e a Venezuela são também membros do Mercosul, mas não reportam atividade na produção de Bentonitas.

extremos de propriedades físicas, medidas em carga foliar, inchamento e sorção orgânica, foram encontradas em associação com bentonitas diagenéticas.

Em termos de espécies de esmectitas, todos os membros identificados como pertencentes a série montmorilonita-beidellita, e a fonte vulcânica riolítica a dacítica, tendem a se alterar para membro final da série montmorilonita, e consequentemente, os precursores básicos (basalto) e intermediário (andesito), mostram tendência a se alterar em membros transitórios e beidellita ricos em ferro, respectivamente.

Para avaliar as implicações nas possíveis aplicações, a química cristalina foi avaliada nas frações abaixo de 1 μm por DRX e FRX, juntamente de outras técnicas de apoio (FTIR, MEV/EDS e distribuição granulométrica), encontrando uma tendência clara entre a magnitude relativa da carga da camada, como uma função do comportamento da organo-absorção, simplesmente avaliando as reflexões basais em d-001 a partir de lâminas orientadas após a primeira saturação em potássio e solvatação sequencial de etileno glicol, contra reflexão em d-001 da (CTAC)-montmorilonita, sendo inversamente proporcional e resultando em uma ampla variedade de padrões de DRX organofílico, mostrando um comportamento de expansibilidade distinto, variando de 15,2 Å a 21,68 Å.

Como função do tamanho da cadeia carbônica e da isoterma de sorção conhecida, basicamente todos os padrões de sorção de organo-compostos foram observados, partindo do comportamento de sorção do tipo monocamada lateral para sorção tipo parafina.

Palavras chaves: bentonitas, esmectitas di-octaédricas, diagêne, carga foliar, organoargila & Mercosul.

TABLE OF CONTENT

LIST OF FIGURES

LIST OF TABLES

1 INTRODUCTION

Clays and Clay minerals, have been called to be the materials of the 21st century (BERGAYA; LAGALY, 2006) for they constitute a natural and diverse source of abundant, inexpensive and environmentally friendly materials. They are being used in countless scientific and industrial applications (GRIM, 1962; HARVEY; LAGALY, 2006; LAGALY; FAHN, 1983; MEUNIER, 1998; MURRAY, 2007; ODOM, 1984; OLPHEN, 1978) and an increasingly growing search for environmental uses (HARVEY; LAGALY, 2006)**.**

This family of minerals, may appear in the most varied geological systems, but specially in sedimentary environments, were they represent roughly 40% of overall whole rock composition (WEAVER; POLLARD, 1973), being illite the most common clay mineral phase followed by kaolinite, montmorillonite and mixed layer Illite-smectite. They may readily appear as natural nanocomposites, as it is the case of smectite series that constitute most relevant mineral phases within bentonites, providing all special features. Altogether, along with the capability to exchange cations in interlayer positions and absorb organic compounds, enabling hybrid materials by modifying the crystal structure and physical properties; bentonites represent a fundamental matrix for advanced applications, and therefore, it is of the strategic interest to a heavily industrialized country such as Brazil, to invest in the development of applied clay science.

The former statement, does not represent a singular view, since the early 90's, the Brazilian government has been sponsoring technical documents and programs oriented to stimulate applied research in this field (SISNANO, 2012; CABRAL; COELHO, 2013; COELHO, 2010; NANOBUSINESS, 2012; REZENDE, 1991; TOMIO, 1999), leading to an enhance academic production, very applied oriented in the following decades and reaching a peak recently to begin declining, probably due the current economic crisis or to the lack of tangible results (ANADÃO; WIEBECK; VALENZUELA-DÍAZ, 2011).

Despite the state effort to break the old unhealthy correlation between non-fuel commodities prices and national GDP (PRIDEAUX, 2009), by adding value to mineral commodities, It appears to be that most scientific production during this stage, had an extremely applied approach but very little effort has been put in

geological aspects controlling bentonite quality and grade, in a regional scale. Moreover, it is undoubtable that the geological path followed by a bentonite natural occurrence, in terms of the influence of parent rock composition, genesis mode, burial history and preservation conditions after alteration, would set the fingerprint on bentonite and inherent structural features in smectites species, which determines potential industrial and scientific uses (CHRISTIDIS; HUFF, 2009; MURRAY, 2007; GRIM; GUVEN, 1978). It is therefore, mandatory to explore these birthmarks in order to properly tailor applications as a function of structural features, and the way they tend to distribute in a bentonite natural occurrence.

The following study, aims to stablish a comparative framework for most relevant bentonite bearing mineralized areas located in the MERCOSUR economic trade zone, taking into account six different areas with distinctive geological contexts located in Argentina, Brazil and Uruguay, giving the fact that Paraguay and Venezuela, despite being members, do not report bentonite mining activities. Accordingly, more than 30 samples were collected, from which a representative set of 12 samples was thoroughly characterized from whole rock (grade) and the clay size fraction (quality), using standard clay characterization techniques and protocols, to observe possible correlations between bentonite features and geological path, afterwards, and comparative performance in organophillization with special focus in organic pollutant selective sequestration, applications were evaluated for the whole set of samples in order to contrast physicochemical trends observed in the regional framework against applied performance.

From X-ray diffraction (XRD) of randomly oriented powder and X-ray fluorescence (XRF) chemical analysis on bulk samples, grade and mineral phase quantification is accessed using a Rietveld refinement software by Bruker diffract. Topas V5.1. The presence of accessory minerals that would have implications in organophillization at the <1 μm size fractions where observed at this stage. Scanning electron microscopy (SEM/EDX), Thermogravimetric analysis (TGA), size distribution analysis by low angle laser light scattering (LALLS) and Fourier transform infrared spectrometry (FTIR), were also used as complementary methods. The structural formula, was estimated from the <1 μm size fractions by

XRF chemical analysis on fused beads, in order to gather information regarding isomorphic substitutions in terms of location and magnitude of layer charge. Although, it was found a clearer trend and easier to access, between layer charge as a function organo-sorption behaviour; by simply evaluating the 001 peak positions on oriented slides after first K saturation and ethylene glycol solvation, against organoclays oriented slides XRD traces.

1.1 Objectives

1.1.1 Main objective

Establish correlations between geological context and bentonite quality & grade, as a function of the six geological sub-areas evaluated in this study; in order to predict behavior for specific applications of high added value, strategic for the Brazilian industrial landscape and yet undeveloped locally.

1.1.2 Specific objectives

1. Fulfill a complete sampling campaign that would assure including most representative available bentonite sources in the region.
2. Perform a thorough structural characterization to stablish a comparative framework in terms of grade and quality as a function of 6 distinctive geological areas (12 sample framework).
3. Observe trends in terms of physical and chemical properties such as layer charge, swelling and organic sorption; in order to predict performance in specific industrial applications, that appear to be strategic for the Brazilian market.
4. Run bench scale experiments to test before mentioned industrial applications, to evaluate response of different bentonite matrixes as a function of observed trends in objectives 2 and 3. Only that this time a broader variety of bentonites are tested, coming from the same 6 geological areas (33 samples overall).

5. Establish correlations between the geological path followed by bentonite occurrences evaluated, and their potential uses in advanced industrial applications.

1.2 Justification and innovation

In the past ten years, Brazil has placed itself among the top ten global producers of raw bentonites; it has also been among the top five importers[3] and one of the largest high added value clay derived products importers. Investing in reaching strategic economic autonomy could be justification enough for the current research project. Particularly if we consider that Brazil is an efficiency driven rather than an innovation driven economy (SINGER; ARREOLA, 2014).

As for the scientific justification, bentonite formation processes and the inherent structural features present in smectites species, is still poorly understood, even after decades of applied clay research. Moreover, the six bentonite bearing geological areas considered for the scope of the present study, are not the exception with respect to geological uncertainty; in fact, the ambiguity reported in literature are an expression of the diversity of unknown variables ruling bentonite grade and quality in this region, particularly for bentonites located in Bahia and Paraiba. Moreover, the fact that these deposits have epicenter a considerable industrial consumption pole right here in Sao Paulo, makes this a scientifically applied task.

As for the innovation within this project, perhaps the overall approach is already substantially innovative: using advanced clay science characterization techniques from a mining engineering department, over samples collected in a regional scale including three countries, in order to build bridges between diagenesis and advanced applications, to finally conduct applied R & D and solve unattended applications; all together is an innovative and applied methodology. Nevertheless, there are more specific innovation to outstand:

[3] According to DNPM/DIPLAM reports & USGS-Mineral Commodity Summaries.

- The geochemical correlation of bentonites, contained in the current geographical setup.
- Using layer charge relative magnitude based on XRD oriented slide traces, in order to predict organic sorption behaviour and other applications performance.
- Using observed physicochemical characteristics of studied samples, in order to selectively remove hormone concentration in polluted water, as a mean to evaluate the influence of geological track for one specific industrial application.
- In overall, a bridge has to be built from genesis (past), passing to mining and processing (present) up to advance applications tailoring (future). In order to properly address the issue of bentonite grade, and quality, in the terms that these parameters have been defined in (see section 2.2.4). This approach is novel, at list to our knowledge.

1.3 Background

The idea of this investigation was born in South Brazil during 2011 while the author conducted his master thesis based upon a Bentonite deposit located in Melo, Northern Uruguay (MACHADO, 2012). With data available at that time, it was evident that high-added value products based on bentonites lack production locally, despite being a major a player in the world rank production and an apparently large market specifically for organoclays and polymer clay nanocomposites (CABRAL; COELHO, 2013; COELHO, 2010; CUTRIM; MARTÍN-CORTÉS; VALENZUELA-DÍAS, 2015; PEREZ; BAX; ESCOLANO, 2005; TOMIO, 1999; NANOBUSINESS, 2012), this last document, sponsored by the Brazilian Ministry of Industry and Foreign Commerce (MDIC), encourages the local production of polymer clay nanocomposites as barrier enhance agents, oriented to satisfy special industrial needs and the substitution of imported equivalents.

Later on in July 2013, during the 15th International clay conference (XV ICC) held in Rio de Janeiro (MACHADO et al., 2013), the opportunity was use to present a PhD. research project proposal at the *Universidade de São Paulo*, that

began in early 2015. The first half of the project was dedicated to collect samples and thoroughly characterize them to stablish mineralogical and chemical composition, crystal chemistry and physical properties (measured in swelling behaviour, Layer charge, and organic sorption). Using the first stage output, a second stage was undertaken, with the scope to test these observed trends, in terms of: processability, organophillization and selective organic pollutant sequestration; using as target 17β-Estradiol soluble hormone due to reported high concentrations in local water reservoirs and the environmental concern that represents.

Perhaps the greatest challenge of this doctorate relies on the fact that technical feasibility has to be simultaneously contrasted to economical one, giving the fact that by no means this is fundamental research. On the contrary, it is by definition an applied project aiming to conclude in tangible results. Accordingly, the evolution of the project was enriched along the way, not only by scientific products, but also from feasibility information and market research.

1.4 Scientific landscape of the topic

For the purpose of observing global trends in the scientific field associated to the present study, a series of core data was downloaded from Scopus and Web of science and processed with the software VOSviewer version 1.6.6, in order to filter the biometric data as presented in the next 3 figures.

Figure 1 illustrates a whole data search of 15.534 Items from Scopus citation database for clay minerals, filtered to top 100 key words co-occurrence, only to outstand the major relevance of bentonites among the broad variety and abundance of clay minerals.

Other interesting features in the tendency to repeat chemistry associated terms, such as pH, sorption isotherm, heavy metals, lead, cooper, etc. Roughly one third of the words are associated to characterization techniques, indicating the need of advanced characterization due to small particle size and chemical variability, as mentioned before.

Figure 1 - Top 100 key words, after searching: clay minerals in Scopus citation data base.

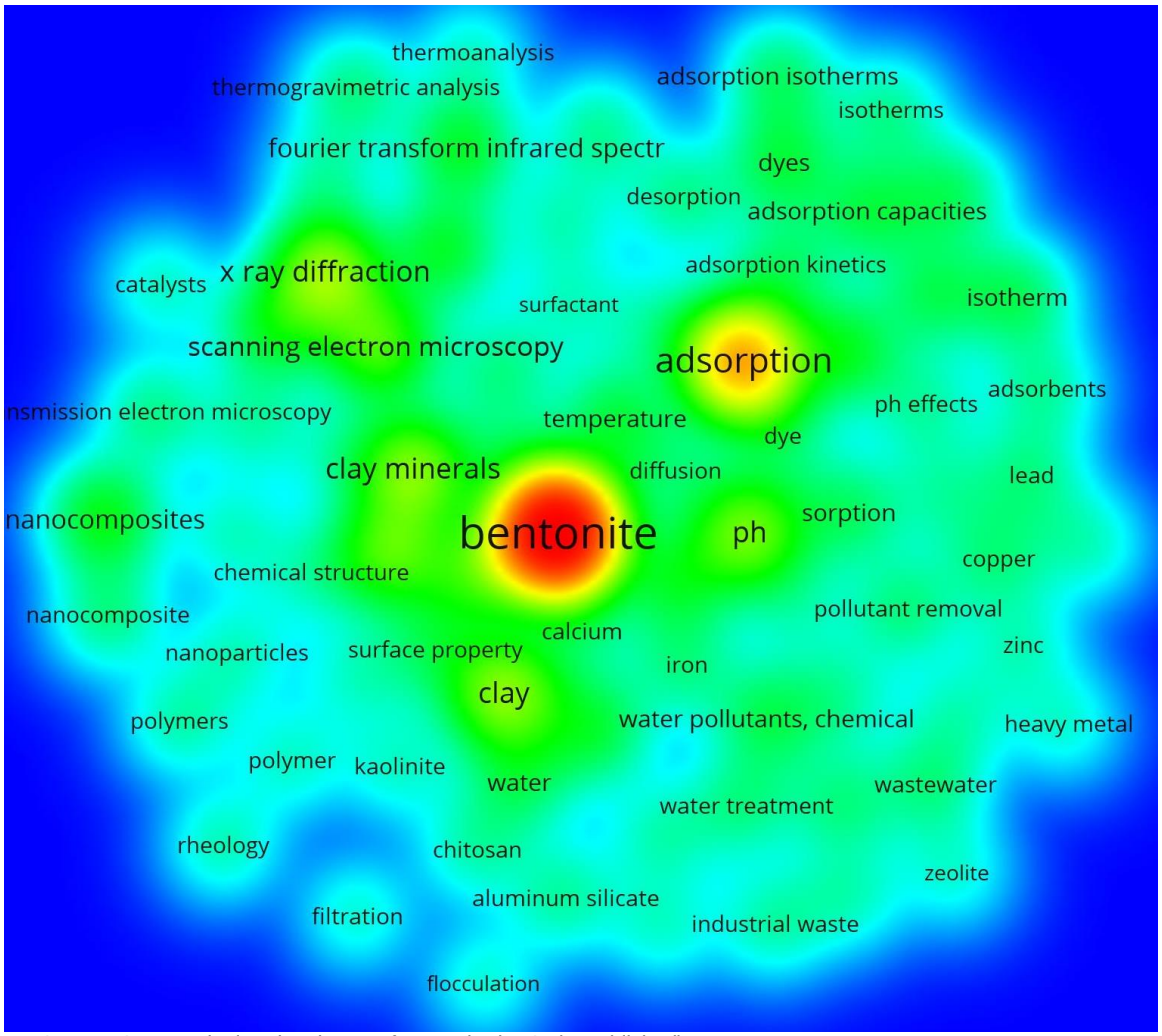

Source: Scopus citation data base. After Machado, G. (unpublished)

To picture the scientific landscape associated to bentonite applications specifically, and with the intention to remark the multidisciplinary nature of the topic. Figure 2, is the result of a search on Scopus citation data base over the words bentonite + applications, filtered in only words alit 150 times repeated, and cleaned by obvious terms, such as clays, phyllosilicates and others. From the graph is possible to derive that adsorption is the most cited property of bentonites probably due to the holistic use of the term, also, 3 distinctive areas of interest seem to be clustering. The blue segment groups advanced characterization techniques along with high tech applications, such as polymer-clay nanocomposites, the red associated water treatment derivatives and the green area, seems to group dyes and organo-interactions, along with absorption properties of bentonites. The relevance of X-ray diffraction as a fundamental tool to study bentonites, is possibly diminish by a duplicity in the data base.

Figure 2 - Top 35 associated words to bentonite research.

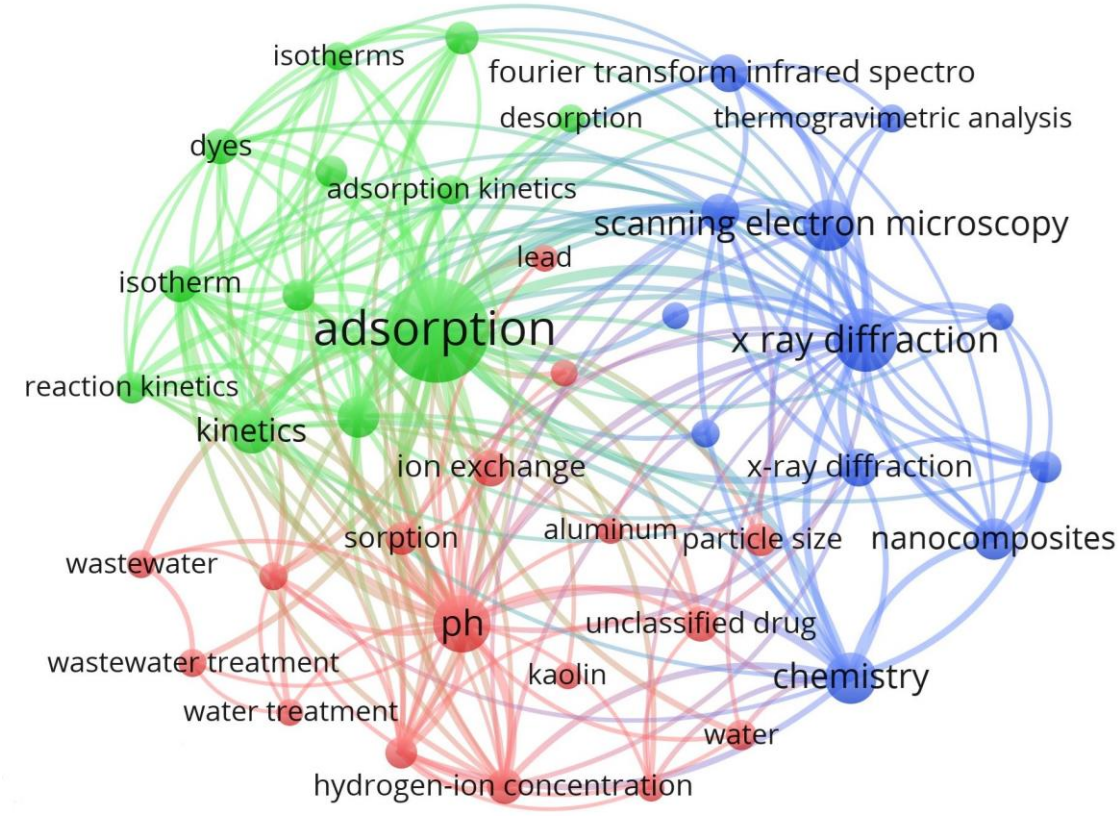

Source: Scopus citation data base. After Machado, G. (unpublished)

Geological research may be illustrated, in terms of most cited authors, countries, journals. They all offered interesting parameters to evaluate global tendencies. Figure 3, arranges authors by citations, on the search result: bentonite + genesis, showing only those authors with more than 70 appearances and resulting in a perspective for most influential authors over the topic. The blue cluster (below-left), groups the North American research group, and the yellow to the right the Spanish. Green and red are mostly European researchers, especially from the UK, France Germany and Greece. Unfortunately, there was duplicity in the data base between a Christidis G.[4] (72 citations) and a Christidis G.A. (116 citations). Correcting, Dr. George Christidis would be the most cited (288 citations), followed by Dr. Warren D. Huff (262) and Dr. Stig M. Bergström (182).

[4] Names as appear on Scopus citation core data base.

Figure 3 - Most influential authors on bentonite genesis.

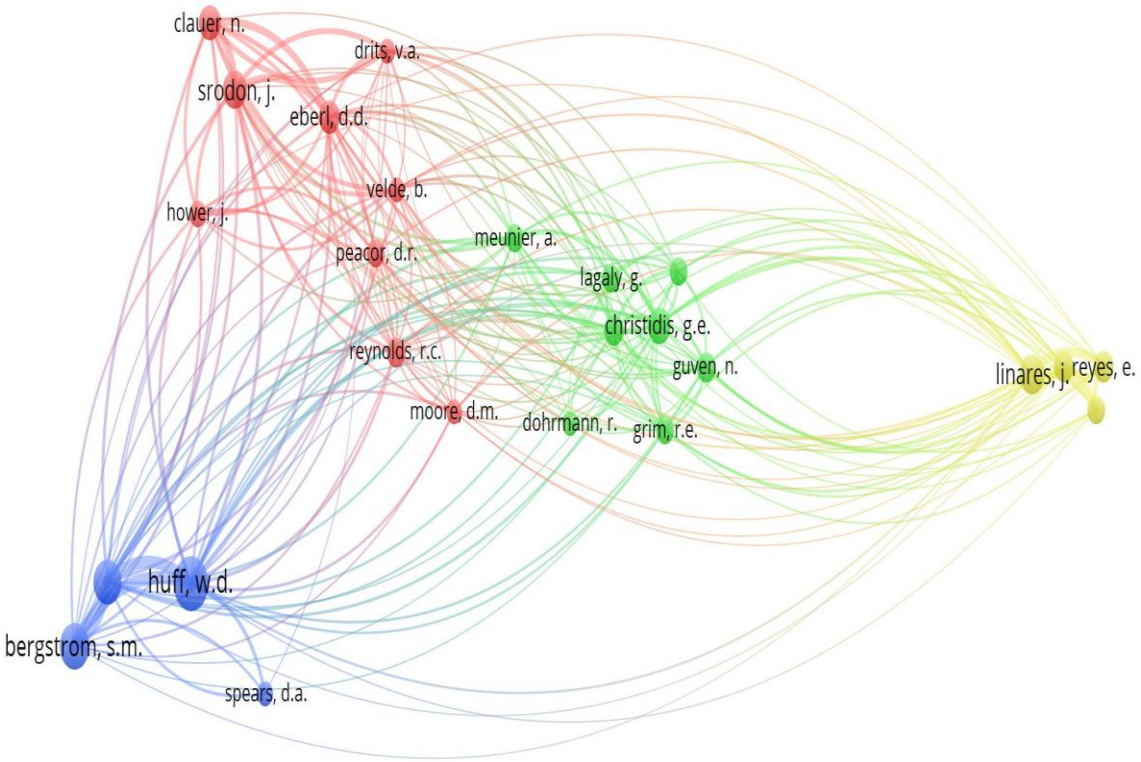

Source: Scopus citation data base. After Machado, G. (unpublished)

2 LITERATURE REVIEW

The multidisciplinary nature of the study and clay science *per se,* makes extremely difficult to review in full coverage all background knowledge used to write these pages. However, two bibliographical lines are presented as follows in order to offer a whole perspective of the state of the art of the associated scientific context. The first (section 2.1, p 28), is related to clay minerals and bentonite structure, geological aspects and relevant structural features of the di-octahedral smectite group and the second (section 2.2, p 48) is more aligned towards applications and market of bentonites specifically.

2.1 Regarding clays & clay minerals

The definition of ‘clay mineral’ is not free of controversy, different approaches may offer definitions as a function of their own perspective, for example; Guggenheim and Martin (1995) suggested that ‘‘phyllosilicate minerals are minerals which impart plasticity to clay and which harden upon drying or firing’’

Probably the most satisfying and updated definition was produced after several years debating in the definition, classification, and terminology of clays, clay minerals, related materials, and specific properties, by both, the AIPEA (*Association Pour l’Étude des Argiles*) and CMS (Clay Mineral Society) Nomenclature Committees (JNCs), proposing that the term signifies a class of hydrated phyllosilicates, making up the fine-grained fraction of rocks, sediments and soils (RAUTUREAU et al., 2017), since the origin of the material is not part of the definition, clay mineral (unlike clay) may be synthetic.

Some distinctions between clays and clay minerals are listed on Table 1. The term clay is used to describe a rock, while clay mineral refers to the mineral type specifically, therefore, a clay rock must contain clay minerals within. According to Bergaya; Lagaly (2006) the main properties of clay minerals are

- Nano-scale in one dimension.
- Anisotropy of layer and particle.
- With external basal (planar), edge and internal (interlayer) surface

- Modification by adsorption, ion exchange and grafting on external and internal surface.
- Plasticity.
- Generally, hardening when drying and firing.

Table 1 - Some distinctive parameters from clays to clay minerals, Bergaya; Lagaly, (2006)

Clay	Clay mineral
Natural	Natural and synthetic
Fine-grained (<2μm or <4μm)	No size criterion
Phyllosilicates as principal constituents	May include non-phyllosilicates
Plastic	Plastic
Hardens on drying or firing	Hardens on drying or firing

Fundamental units of clay minerals are:

- **The octahedral sheet:** Composed of closely packed oxygens and hydroxyls in which aluminum, iron, and magnesium atoms are arranged in octahedral coordination (see Figure 4 - left). When aluminum with a positive valence of three is the cation present in the octahedral sheet, only two-thirds of the possible positions are filled in order to balance the charges, then the mineral is defined as di-octahedral. If magnesium with a positive charge of two is present, all three positions are filled to balance the structure and the mineral in named tri-octahedral.
- **The tetrahedral sheet:** In this structure, the silicon atom is equidistant from four oxygens or possibly hydroxyls arranged in the form of a tetrahedron centered to the silicon atom. These tetrahedrons are arranged to form a hexagonal network repeated infinitely in two horizontal directions to form the silica tetrahedral sheet (see Figure 4 - right)
- Interstratification of octahedral and tetrahedral sheet (cont.)

Figure 4 - Diagrammatic sketch of the octahedral sheet (left) and the tetrahedral sheet (right).

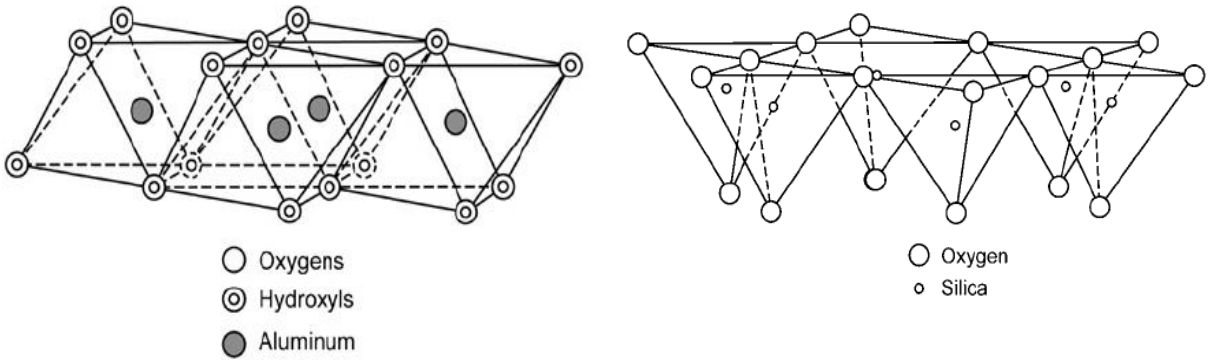

Source: (MURRAY, 2007a) pages 8 and 9.

With the exceptions of sepiolite and palygorskite, all phyllosilicates may be classified into two different crystal structures, according to combination of tetrahedral sheets bonded with an octahedral one, as illustrated in Figure 5.

Figure 5 - Typical phyllosilicate structures, as a functions of T (tetrahedral) to O (octahedral coordination.

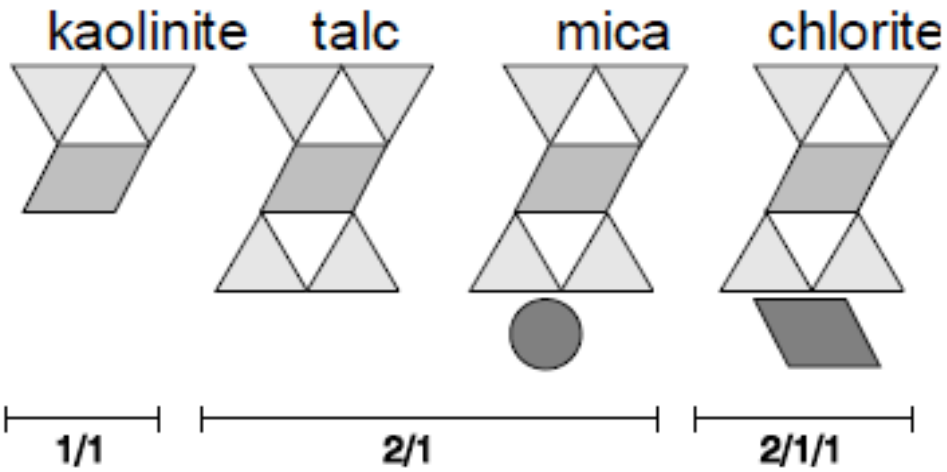

Source: The crystal structure of clay minerals through some exercises, by Alain Meunier (International Master in Advanced Clay Science Handouts, 2010)

From figure, is possible to distinguish the 1:1 layered structure type, (also called TO), and the 2:1 type (TOT):

- **1:1 type:** One tetrahedral sheet is bonded with an octahedral one. The layer is electrically neutral (trioctahedral: serpentine, berthierine; di-octahedral: kaolinite)
- **2:1 type:** two tetrahedral sheets are linked to the octahedral one in a “sandwich-like” structure. Three sub-types exist according to the presence

or absence of a layer charge and the way it is neutralized by an additional cation sheet (interlayer or “brucite” layer): neutral (tri-octahedral: talc; dioctahedral: pyrophyllite); layer charge compensated by interlayer cations (di- and tri-octahedral micas, vermiculites, smectites); layer charge compensated by a “brucite” layer (di and tri-octahedral chlorites).

- **2:1:1 type:** Trioctahedral chlorites are the most common representatives (BAILEY; 1975). Their crystal structure derives from the combination of a talc-like 2:1 layer with a brucite-like octahedral sheet. Cation substitutions give the talc-like layer a negative charge of about −1 and the brucite-like sheet an equivalent charge but of opposite sign. Most of the negative charge in the 2:1 layer is the result of substitution of Al^{3+} for Si^{4+} in tetrahedral sites.
- **None layered type:** The octahedral sheets are continuous only in one dimension in ribbons and because the tetrahedral sheets are also divided into ribbons by inversion of every two or three rows of tetrahedral. These structural features create channels between the ribbons. Palygorskite (Figure 6) is dioctahedral and sepiolite (Figure 7) trioctahedral. Both minerals have elongated habits often forming bundles of lath-like or fibrous crystals

Figure 6 - Crystal structure of palygorskite

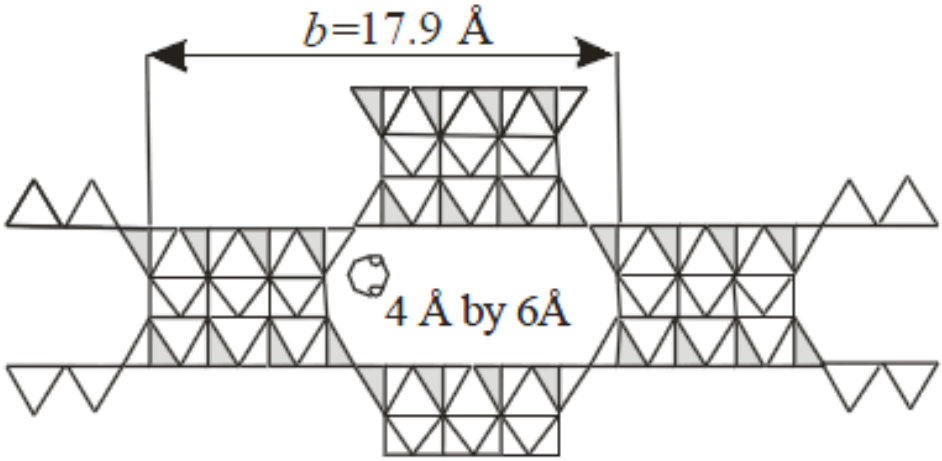

Source: Christidis (2011)

Figure 7 - Crystal structure of sepiolite

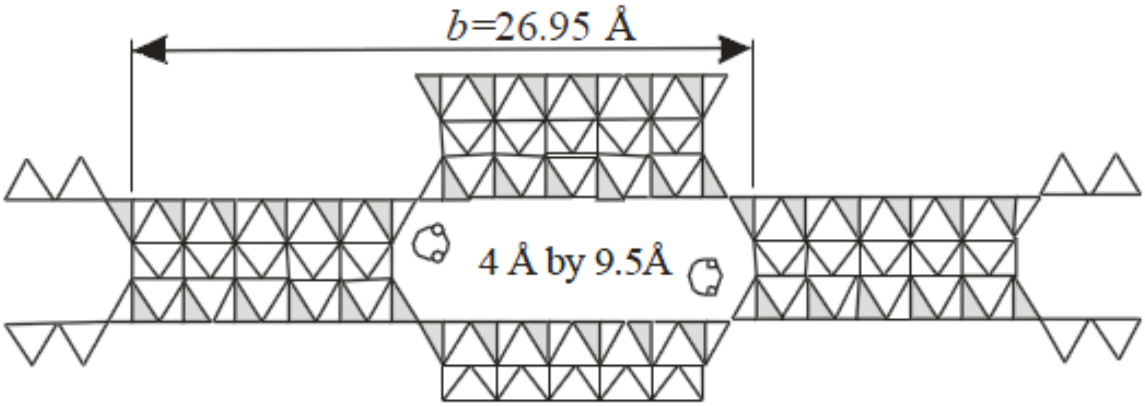

Source: Christidis (2011)

2.1.1 Clay minerals classification

Phyllosilicates of any size, such as macroscopic mica, vermiculite, and chlorite may be regarded as clay minerals. A similar concept was advocated by Weaver (1989) who suggested the term ‘physils’ for the whole family of phyllosilicates (including palygorskite and sepiolite) irrespective of grain size. The next two tables, list all phyllosilicates divided into planar hydrous phyllosilicates (Table 2) and none planar hydrous phyllosilicates (Table 3).

Table 2 - Classification of planar hydrous phyllosilicates

Interlayer material*	Group	Octahedral character**	Species
		1:1 Clay minerals	
None or H2O only,	Serpentine-	Tri	Amesite, berthierine, brindleyite, cronstedtite,fraipontite, kellyite, lizardite, nepouite
x 0	kaolin	Di	Dickite, halloysite (planar), kaolinite, nacrite
		Di-tri	Odinite
		2:1 Clay minerals	
None, x 0	Talc-pyrophyllite	Tri	Kerolite, pimelite, talc, willemsite
		Di	Ferripyrophyllite, pyrophyllite
Hydrated exchangeable cations,	Smectite	Tri	Hectorite, saponite, sauconite, stevensite,swinefordite
		Di	Beidellite, montmorillonite, nontronite, volkonskoite
Hydrated exchangeable cations	Vermiculite	Tri	Trioctahedral vermiculite
x 0.6–0.9		Di	Dioctahedral vermiculite
Non-hydrated monovalent cations	True (flexible) mica	Tri	Biotite, lepidolite, phlogopite, etc.
		Di	Celadonite, illite, glauconite, muscovite, paragonite, etc.
Non-hydrated divalent cations, x 1.8–2.0	Brittle mica	Tri	Anandite, bityite, clintonite, kinoshitalite
		Di	Margarite
Hydroxide sheet, x variable	Chlorite	Tri	Baileychlore, chamosite, clinochlore, nimite, pennantite
		Di	Donbassite
		Di-tri	Cookeite, sudoite
		Regularly interstratified 2:1 clay minerals	
x Variable		Tri	Aliettite, corrensite, hydrobiotite, kulkeite
		Di	Rectorite, tosudite

Source: Martin et al.,(1991), after Bergaya; Lagaly, (2006)

***X ¼ net layer charge per formula unit.**

Tri ¼ trioctahedral, di ¼ dioctahedral

Table 3 - Classification of non-planar hydrous phyllosilicates

Modulated component	Linkage configuration	Unit layer c and b value	Traditional affiliation	Species
1:1 Minerals with modulated structures				
Tetrahedral sheet	Strips	0.7 nm	Serpentine	Antigorite, bementite, caryopilite, ferropyrosmalite, friedelite, greenalite, manganpyrosmalite, mcgillite, nelenite, pyrosmalite, schallerite
	Islands	0.7 nm	Serpentine	
	Other		None	None
2:1 Minerals with modulated structures				
Tetrahedral sheet	Strips	0.95 nm	Talc	Minnesotaite
		1.25 nm	Mica	Eggletonite, ganophyllite
	Islands	0.96–1.25 nm	Mica/ complex	ferristilpnomelane, ferrostilpnomelane, lennilenapeite, parsettensite, stilpnomelane, zussmanite
	Other	1.23 nm	None	Bannisterite
		1.4 nm	Chlorite	Gonyerite
Octahedral sheet	Strips	1.27–1.34 nm	Pyribole	Falcondoite, loughlinite, palygorskite, sepiolite, yofortierite
1:1 Minerals with rolled and spheroidal structures				
None	Trioctahedral		Serpentine	Chrysotile, percoraite
	Dioctahedral		Kaolin	Halloysite (nonplanar)

Source: Martin et al.,(1991), after Bergaya; Lagaly, (2006)

Is important to keep in mind that not only alternation of tetrahedral and octahedral sheets may experience different grade of ordering in the long range stocking sequence, but also isomorphic substitutions tend to be of the most varied nature behaving as solid solutions and sheets working as building units, not necessarily in a regular way; Figure 8 presents a good example with observed tendency on the kaolinite to serpentine solid solution transition as a function of Si/Al/Mg relative contents.

Figure 8 - Ternary plot Al, Mg and Si representing solid solution diagram for some clay minerals.

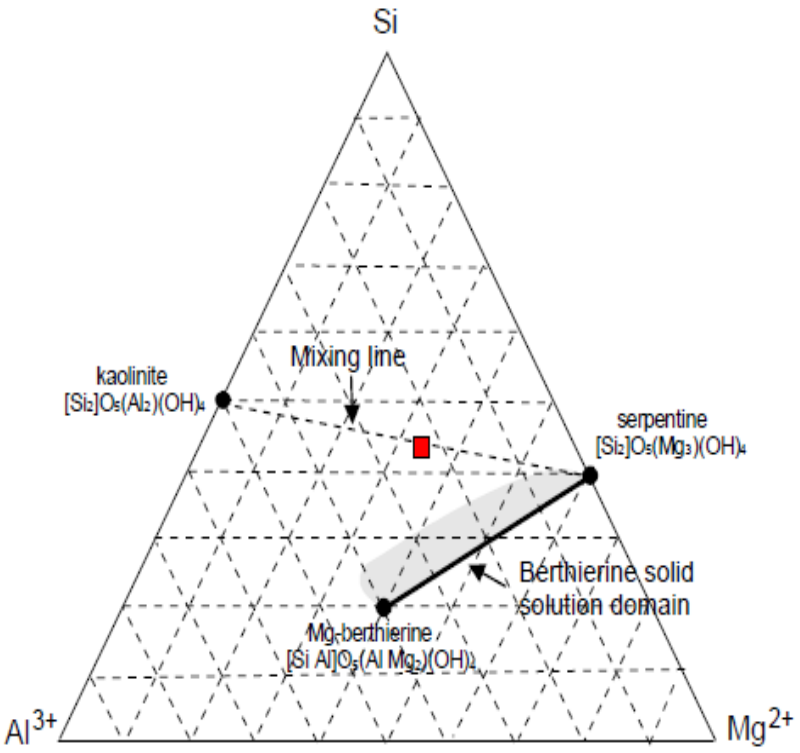

Source: (MEUNIER; VELDE, 1989)

The black thick line and the grey area represent the theoretical and experimental solid solution domains respectively. The theoretical composition of berthierine varies along the line according to the general formula (Equation 1):

Equation 1

$$[Si_{2-x}\,Al_x]\,O_5\,[(Fe^{2+},\,Mg)_{3-y-z},\,Fe^{3+}{}_y,\,z)]\,(OH)_4,\ (\text{where } X=6+y-2z)$$

2.1.2 Geological aspects of bentonite occurrences

By definition, bentonites derive from the alteration of volcanic ash or tuff regardless of the formation mode, bentonite forming processes can be classified into four different modes (GRIM; GUVEN, 1978). Although in-situ diagenetic alteration accounts for most know occurrences, hydrothermal and diagenetic alteration are well known thoroughly described in the literature (CHRISTIDIS; HUFF, 2009; MURRAY, 2007; MEUNIER, 2005; GRIM; GUVEN, 1978); less common bentonite genesis processes have also been described or are being debate.

In a general way, formation modes proposed by Grim; Guven (1978) still remain as fundamental mechanism, although the fourth genesis type proposed by this authors (miscellaneous and uncertain modes of origin) has been widely enriched in the literature.

2.1.3 Bentonites geological context in the Mercosur area.

Six distinctive geological areas are being considered for the purpose of this study as showed in Figure 9, they constitute major sources of raw bentonite located in the Mercosur area. Although this bentonite production zones are hereby described as *geological areas* and named after their general geographical location, it is relevant to explain that the grouping criteria applied for such a distinction is merely logistic, for some of these areas may present heterogeneous geological characteristics among samples from the same area, as it is better explained in section 3.1, such is the case for the Parana basin and Mendoza-San Juan and Paraiba. The reason being is the applied nature of this research, in the sense that all of this bentonite sources have epicenter in the central-southern area of Brazil that constitutes the main marketplace for all of this clay sources.

Figure 9 - Geological areas object of this study, in the South American geopolitical context.

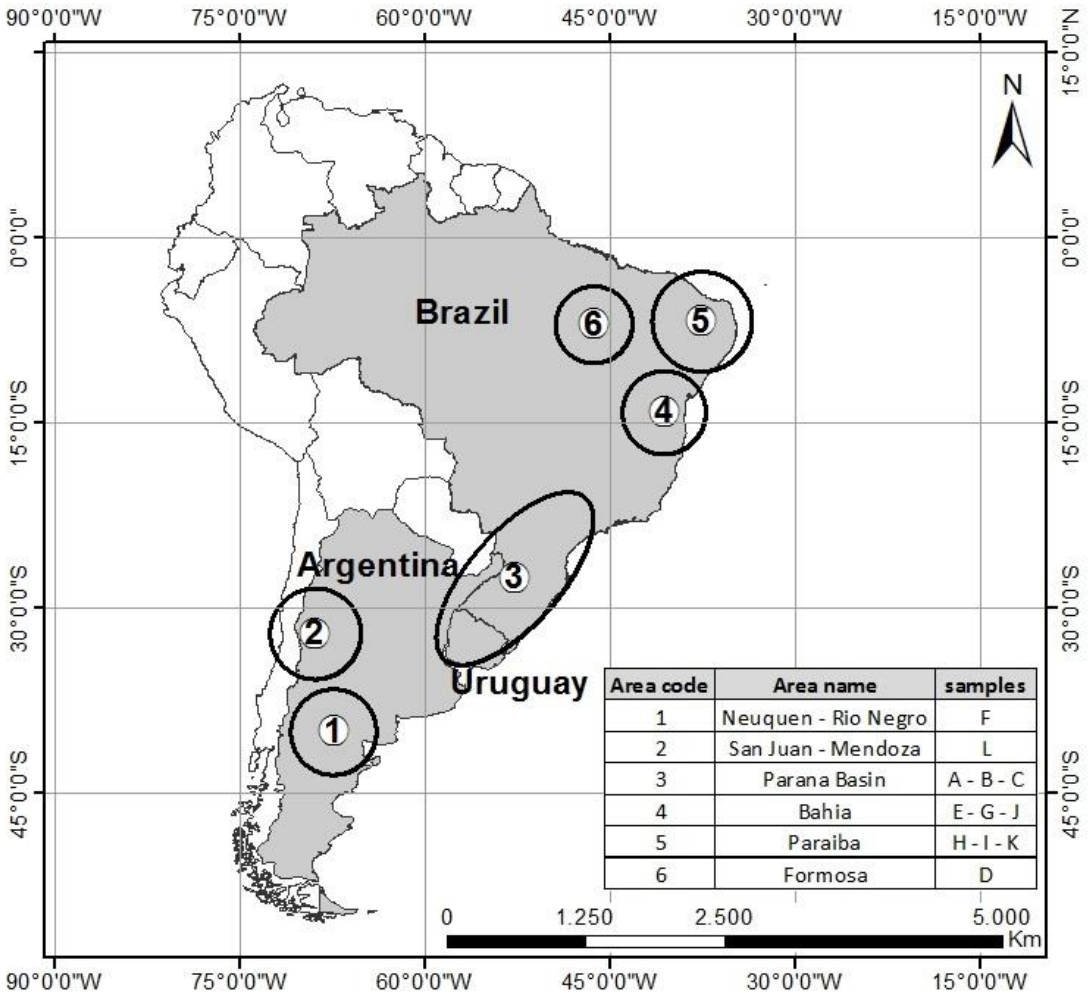

Source: G. Machado (2018; unpublished)

2.1.3.1 Geological Area 1- Neuquén-Rio Negro (Argentina):

Also described in the literature as Patagonian or north Patagonia bentonites, belong to Paleocene and Eocene formations (BORDAS, 1943), and they have been described as a result of in situ alteration and post weathering degradations (GRIM; GUVEN, 1978) on andesitic to basaltic volcanic source (IMPICCINI; VALLÉS, 2002) in a marine to transitional environment. This bentonite beds are usually interbedded with unaltered ash (LOMBARDI, 2003). Hereafter this region will be referred as the geological area number 1.

2.1.3.2 Geological Area 2 - San Juan-Mendoza (Argentina):

In this region, several formation processes and corresponding ages have been reported. The region contains some of the very few know bentonite deposits

that can be classified as detrital bentonites altogether with in-situ altered layers from rhyolitic to dacidic volcanic tuffs dated on the Triassic (BORDAS, 1943; GRIM; GUVEN, 1978) Hydrothermal alteration of rhyolitic to rhyodacitic pumices and breccias from the Pleistocene (ALLO; MURRAY, 2004), 2004). The same region also contains at list twenty Ordovician K-bentonites deposits in the Argentine pre cordillera, underlying Gualcayamo formation (FANNING et al., 2004; HUFF et al., 1998) For the purpose of this study we use the first description that fits best to the corresponding sample (L), hereafter this region will be referred as the geological area 2.

2.1.3.3 Geological Area 3 - Parana Basin (Brazil, Uruguay & Argentina)

Bentonites located in the Parana basin have been reported as a product of in-situ alteration of volcanic ashes deposited in a lagoonal to transitional environment that belongs stratigraphically to Late Permian (Tatarian) Rio do Rastro Formation, which is the equivalent to Yaguari Formation in Uruguay (MAYNARD;GAINES, 1996; FORMOSO et al., 2000; PIRES;GUERRA-SOMMER, 2004; ROCHA-CAMPOS et al., 2011). The volcanic source Choiyoi igneous province from San Rafael block located in central Western Argentina should be considered as source for the ash fall deposits during the Permian section of the Parana Basin, along the Pacific margin of Southwest Gondwana and the geological evolution of neighboring Paleozoic Foreland basins in South America and Africa (ROCHA-CAMPOS et al., 2011). A bentonite bed located in Bañado de Medina, Northern Uruguay, has been correlated to a regional scale of rhyolitic volcanic source occurrences, where the volcanic source was probably located in southwestern Argentina and Chile, during early to mid-Permian (FORMOSO et al., 2000), This bentonite deposit, has been correlated to those found nearby Acegua, Southern Brazil, based upon mineralogical similarities and chemical signature of heavy minerals and rare earth elements (CALARGE et al., 2003; MEUNIER et al., 2006). It was described as an essentially monomirerallic clay containing dioctahedral smectite mainly with Ca^{+} exchangeable cations in the interlayer position, this implies that it may constitute one of the oldest bentonite deposits known and yet it’s been kept under remarkably well preserved due to the special geological context linked to a intercratonic basin (Paraná Basin) and more locally

due to a series of faults that protected the rather thin bed from erosion. Therefore it represents an outstanding source for academic research to achieve more knowledge about the digenetic process itself and also the way physical and chemical properties can vary as a function of their spatial distribution, and it may constitute one of the oldest known bentonite deposits showing no signs of Illitization or degradation due to an extraordinary preservation, possibly related to the protective role played by the intercratonic section of the Parana basin (MACHADO et al., 2016). They suggested that variations in major element, REE and minor element abundances throughout the massive clay deposit indicate two successive ash falls. Moreover, the abundance of trace elements indicates a fractionated volcanic glass derived from rhyolitic magmas produced in a subduction/collision geological context.

About the volcanic source and in a more regional scale, a precise work was presented by (ROCHA-CAMPOS et al., 2011). These researchers stated that the Choiyoi igneous province from San Rafael block located in central western Argentina (Patagonia) should be considered as source for the ash fall deposits during the Permian section of the Parana Basin, along the Pacific margin of Southwest Gondwana and the geological evolution of neighboring Paleozoic Foreland basins in South America and Africa.

Figure 10 shows a geographical influential spectrum of the volcanic ash source. Although Melo has been dated as Permian, it is also accepted that volcanic activity in Northern Patagonia reached an activity peak in the Triassic and early Jurassic (PIRES; GUERRA-SOMMER, 2004) and these events have been described as highly explosive due to the felsic nature of the magmas (AXELROD et al., 1976).

Figure 10 - Rhyolitic volcanism, in the Choyoi province towards the Parana Basin.

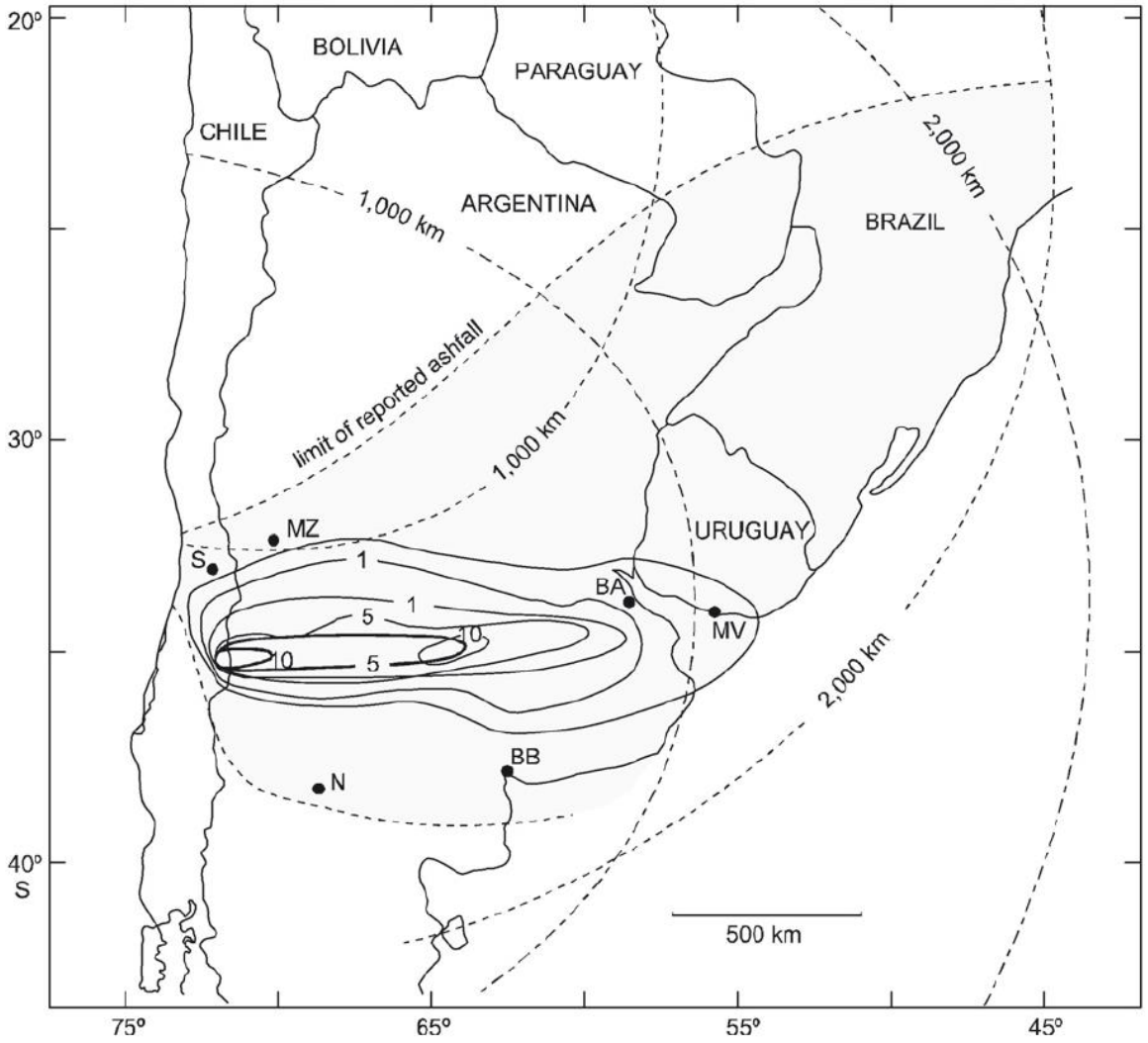

Source: Circles at 1000 and 2000 Km radius centered on the San Rafael area and Northeastern Choyoi igneous province towards the Parana Basin; Base map: ash distribution during the Quiza pu eruption of 1932 (HILTRECH AND DRAKE, 1992). Coarser contour lines: ash fall thickness by (LARSSON, 1937). MZ: Mendoza; BA: Buenos Aires; MV: Montevideo; S: Santiago, N: Neuquen; BB: Bahia Blanca. Through less intense, the eruption exemplifies dispersion of ash over distances comparable with those of Choiyoi Volcanism After. (ROCHA-CAMPOS ET AL., 2009).

The bentonite occurrence has been first reported by (GOÑI, 1952) and then by (BOSSI, 1966). The research performed by (CALARGE; MEUNIER; FORMOSO, 2003), proposes the idea of layer charge heterogeneity for this deposit as a function of swelling capability. Although, these authors describe the stratiform bentonite as a 1,5 m thick smectite rich bed, which contains less than 5% non-clay minerals; in contrast (MACHADO, 2012), showed that the highly pure bentonite bed can be up to 5 m thick and its mineralogical composition vary widely as a function of depth, particularly at the top.

2.1.3.4 Geological Area 4 - Bahia State (North-East Brazil)

Bentonites located near Vitoria da Conquista in Bahia state of Brazil, have been gaining relevance in the scientific community and local market in the past decade, particularly with respect to acid activated bentonite products and Iron Industry applications (CABRAL; COELHO, 2013; DNPM, 2015); there is plenty of literature dealing with bentonites from Bahia, but unfortunately most of it is applied oriented, leaving only a few technical documents available regarding genesis and geological context. Nevertheless, it seems to be clear that they resulted from the alteration of a basic parent rock (CARVALHO, 2017; CBPN, 2014; VIANA et al., 2003). Age has been suggested to be from the Neoproterozoic (CARVALHO, 2017; SILVA-VALENZUELA et al., 2018; VIANA et al., 2003), early Precambrian (KÖSTER et al., 2015) and from the Tertiary, for a nearby bentonite with similar characteristics (GRIM; GUVEN, 1978).

Genesis mechanism and post events remain uncertain, although it has been described as sedimentary, lateritic and hydrothermal, this last formation mode seems to be coherent with kaolinite content found in samples coming from the area (13.3 Wt (%), 32.9 Wt (%) and 19.5 Wt (%)), typical of hydrothermally altered bentonites (GARRELS, 1984; HOWER; MOWATT, 1966; MILLOT, 1970; GRIM; GUVEN, 1978).

2.1.3.5 Geological Area 5 - Paraiba State (North-East Brazil)

Several bentonite occurrences of have been reported since the early 60’s (CALDASSO, 1979; PINTO; PIMENTEL, 1968). All outcrops in the region have been found in the surroundings of Campina Grande, Paraiba state of North-East Brazil. More specifically in Jua, Lages, Bravo, and more recently Cubati and Pedra Lavrada (CUTRIM; MARTÍN-CORTÉS; VALENZUELA-DÍAS, 2015; MIRELLA et al., 2014; SILVA; COSTA, 2013; TONNESEN, 2010). They have been described as the alteration product of Basaltic Tuff and Lapilli from the Tertiary (BEURLEN, 1995; GOPINATH, 1979; GOPINATH; SCHUSTER; SCHUCKMANN, 1981, 1988); not without certain debate regarding genesis. Caldasso, (1979) Proposed a sedimentary genesis type, (PINTO; PIMENTEL, 1968) offered an hydrothermal hypothesis, while (BEURLEN, 1995) describes a diagenetic process by in situ-alteration in lacustrine environment.

2.1.3.6 Geological Area 6- Formosa (Maranhão State Northern Brazil)

Bentonites located in the northern Brazilian state of Maranhao, have been reported first as smectite rich deposits in technical reports from the early 90´s (REZENDE, 1991) and then properly as bentonites (MORAES et al., 2010), in association with Basalts from the Tertiary. Later, by da PAZ; Angélica; Neves, (2012), stated that the dominant smectite species in this deposits are Mg-montmorillonite and suggested that possible formation mechanisms to be taking into consideration would be either by hydrothermal alteration or sedimentary. There is still room for research regarding genesis of this mineralized area and the previous two, but there is sufficient geochemical information for the purpose of this study. A summary of all samples with respect to geological areas is presented in Materials and Methods (section 3).

2.1.4 Related studies on layer charge

Mermut et al., (1994) constitutes a fundamental reference used as a ground base to interpret interactions between montmorillonite and amines as a function of layer charge, despite all debate regarding layer charge determination by alkylammonium Ions (LAIRD, 1999; MERMUT; LAGALY, 2001), the evaluation of structural formula, alkylammonium methods of determining layer charge and the K saturation method are suitable tools to approach to study of layer charge and its implications on practical applications of clay minerals. And specially the one offered by (JAYNES; BOYD, 1991). This work was also used as a reference of related studies about organophillization.

Christidis; Eberl (2003) proposed one of the methods used in this research to estimate layer charge and charge heterogeneity. The mentioned publication explains how from 29 well characterized samples loaded on a data base, is possible to compare XRD patterns after potassium saturation and ethylene glycol solvation to obtain layer charge magnitude and heterogeneity from profile fitting or by peak position criteria. Other relevant studies on layer charge are the presented by Czímerová; Bujdák; Dohrmann (2006), Kaufhold (2006), Laird; Scott; Feuton (1989) and Petit et al. (1998)

Christidis & Huff (2009) addressed the topic of layer charge and provided a broad overview about the variables which control bentonite formation and alteration. This publication showed evidence for cryptic variations in bentonite deposits (Figure 11) as was reported by Christidis; Makri; Perdikatsis (2004) in a bentonite deposit located in Milos-Greece and by Meunier; (2005) in a 1 m thick bed in Charentes, France.

Figure 11 - Variation of C.E.C and the (Al_2O_3+Fe_2O_3)/MgO ratio with depth in smectites from a bentonite deposit located in Charentes, France

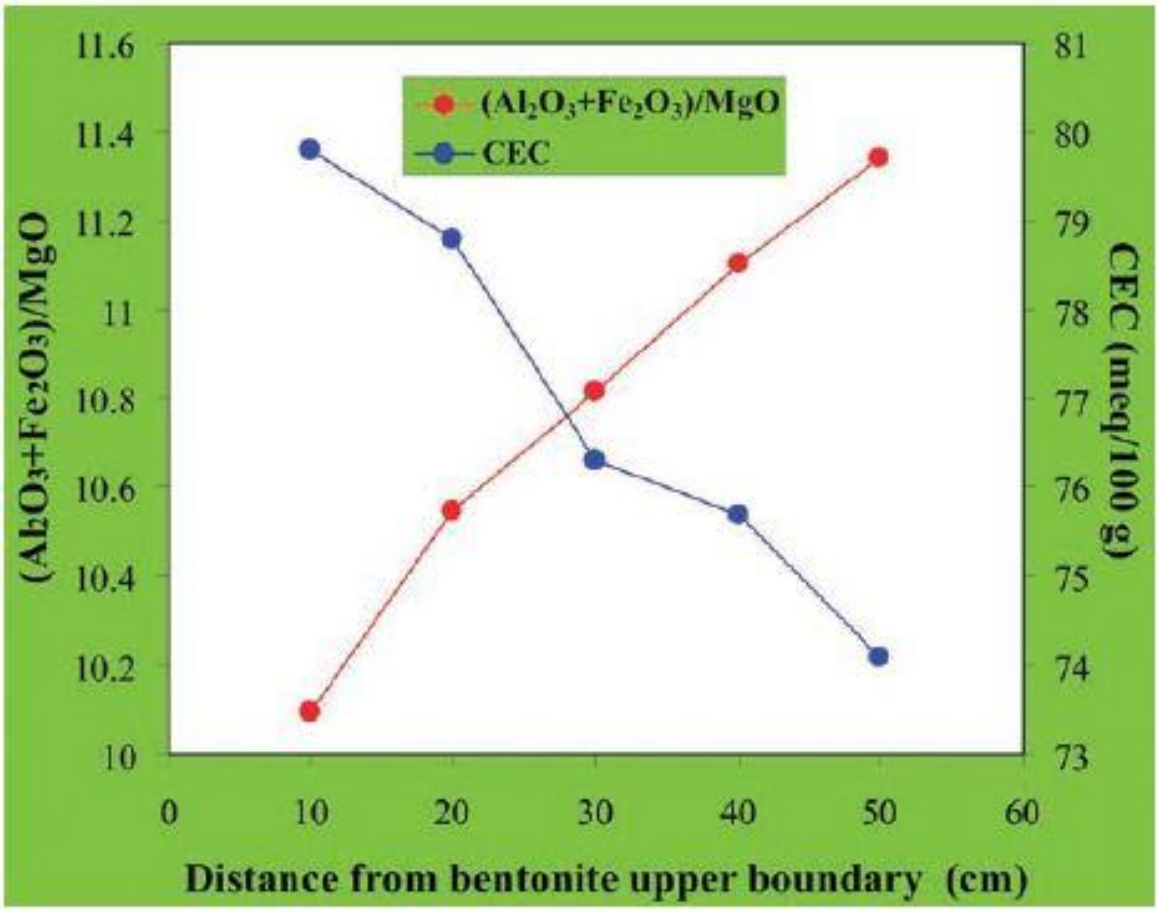

Source:(MEUNIER, 2005) after (CHRISTIDIS; HUFF, 2009)

The research developed by Machado; Christidis; Dani, (2012), at the Technical University of Crete in collaboration with the UFRGS, “Spatial variation of layer charge in Melo bentonite deposit located in northern Uruguay”, and the implications on physical properties and organophillization, will constitute the fundamental methodological approach to obtaining most critical parameters from the clay matrix and also offers and advance data from one of the bentonite deposit that is used in this project (MACHADO, 2012; MACHADO et al., 2013).

A partial result of this project can also be cited by MACHADO et al.,(2016) as a relevant background on the topic of layer charge as a parameter to stablish uses of bentonites but also how to treat & process as a function of the spatial distribution. The work entitled “Spatial distribution of layer charge in a bentonite deposit. a powerful tool for mine planning”, presented and published at the *XIII Jornadas Argentinas de Tratamiento de Minerales*, proofed that diagenetic processes and alteration implicit on Bentonite occurrences, tend to have a gradual cryptic, and rational distribution; directly relative to formation environment characteristics and preservation afterwards. Some direct implications could be applied to bentonite mining. It is the usual practice to estimate the quantity of reactants when trying to stimulate cation exchange according to the smectite proportion within the bentonite. Physical parameters like layer charge are considered to be fixed. Figure 12, shows XRD traces of 5 oriented slides, over the < 1 µm size fraction, for a whole profile (borehole), after sequential K-saturation and ethylene glycol solvation, indicating the tendency to decrease layer charge around the middle of a stratiform bed.

Figure 12 - Layer charge distribution as a function of depth - Melo bentonite deposit, Uruguay.

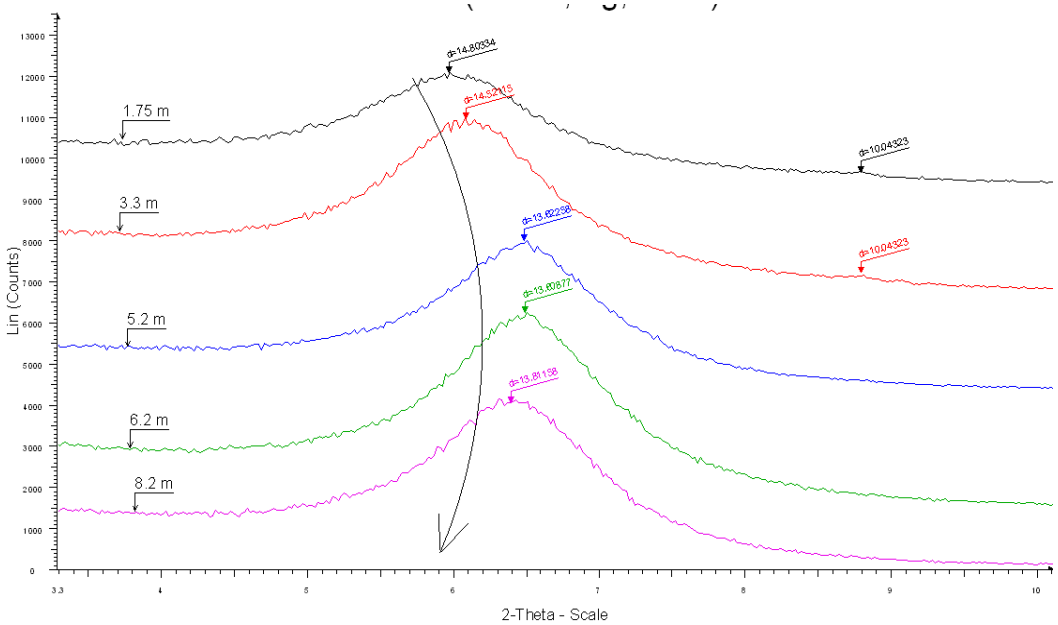

Source: Maxhado (2013). Presented at the 15th International Clay conference in Rio de Janeiro, 2013

Figure 13 shows a set of figures illustrating the way layer charge is spatially distributed along the mentioned occurrence, a normal expansion from air dried to ethylene glycol treated sample of 1.5 Å, expandability corresponding to 2EG-EG. As for the organophillic clay expandability, the peak at 17.46 Å is characteristic of a bilayer amine intercalation. At a first glance, all organophillic XRD patterns show a similar expandability in terms of their d001 ($C_{12}H_{28}ClN$)-montmorillonite peak position, ranging from 17.05 Å to 17.68 Å. They could all be considered as bilayer sorbed organoclay according to the size of the alkyl chain used and the known sorption isotherm. Despite the slight d-spacing differences among samples, there is a well-defined positive relationship between layer charge and position of the 001 peak of the organophillic smectites. This is a clear indication that the position of the 001 peak is related to the magnitude of layer charge.

Figure 13 - Compendium of graphical evidence regarding layer charge spatial distribution.

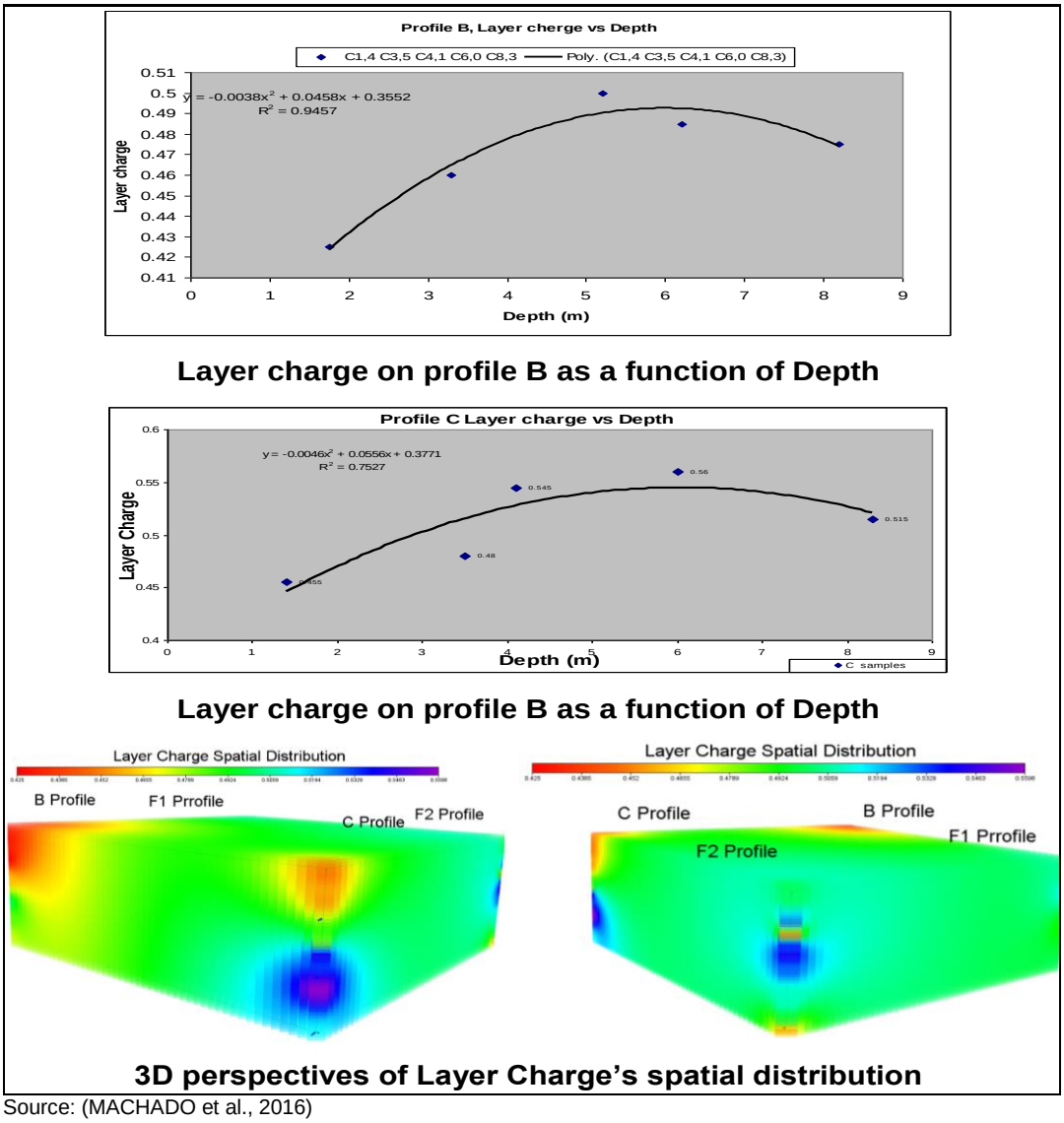

Source: (MACHADO et al., 2016)

An interesting trend was observed when the peak position was plotted vs depth; the d-spacing increases towards middle of the bentonite bed, and decreasing again towards the bottom, similar to the variation of layer charge.

2.1.5 Regarding smectite chemical composition and structural formula

The unit formula or structural formula for smectites has been widely studied in the literature (SCHULTZ, 1969; KÖSTER et al., 1999; ONAL, 2006). Normally, the data obtained by XRF chemical analysis on < 1 μm samples would be sufficient to access the chemical composition of smectite species, and will also provide enough information about the octahedral and tetrahedral elemental

distribution, and consequently, layer charge, based on known general rules that cannot be accessed throughout XRD techniques (CZÍMEROVÁ; BUJDÁK; DOHRMANN, 2006; DAZAS et al., 2015; KAUFHOLD, 2006; LAIRD; SCOTT; FEUTON, 1989)

2.1.6 Characterization techniques applied to clay minerals

Proper characterization of phyllosilicate minerals represents a challenging task, not only due to their natural nano scale size (in one dimension only), but also due to their tendency to exhibit broad chemical composition ranges derived from solid solutions and their ability to form polyphased crystals by interstratification (MEUNIER, 2005).

Probably the base document to approach technique selection, and comprehend in full view advantages and limitations of possible characterizations techniques and protocols would be the Handbook of clay science. (BERGAYA; LAGALY; BENEKE, 2006), for it constitute a complete summary of applied techniques, no doubt remains that the most widely used technique for clay characterization, is X-ray diffraction (MOORE; REYNOLDS, 1997), and complementary tools may be found in (BRAXOLEY; CHIPERA; BISH, 2001; KLEEBERG; MONECKE; HILLIER, 2008; O'CONNOR; CHANG,1986; SRODON et al., 2001; ZWELL; DANKO, 1975). Fourier transform Infra-Red (FTIR) (MADEJOV et al., 2001; WANG; ZHANG; REDFERN, 2003). Scanning electron microscopy (SEM) (BOHOR; HUGHES, 1971), X-ray florescence (XRF)(KANNGIESSER, 2003).

Thermal analysis of organoclays (YARIV, 2004). Regarding Rietveld approach for quantitative mineral analysis (KLEEBERG; MONECKE; HILLIER, 2008; TOBY, 2006; UFER et al., 2008).

2.1.7 Rietveld refinement:

The Rietveld refinement technique for powder-diffraction data was proposed and developed by Hugo Rietveld during the late 60's and early 70's and still today, it is the topic of great study and debate. The basic idea behind the Rietveld method is to calculate the entire powder pattern using a variety of

refinable parameters and to improve a selection of these parameters by minimizing the weighted sum of the squared differences between the observed (VON DREELE; 2003). It is not the only mineral quantification approach based on XRD data processing, three main techniques are currently in use for clay mineral quantification:

A. Single peak/natural standard technique, which relies upon a selected individual peak as a measure of mineral abundance, and upon natural specimens as standards (HILLIER, 2000; ŚRODOŃ et al., 2001)

B. whole pattern/natural standard technique, which obtains intensities of the phase in a mixture by fitting the entire XRD pattern with patterns of pure standards (SMITH et al., 1987; BATCHELDER; CRESSY, 1998; CHIPERA; BISH, 2002)

C. Whole pattern/computed standard techniques that includes the Rietveld analysis and it consists in fitting the experimental pattern with the patterns of pure phases calculated from crystallographic data (BISH; HOWARD, 1988)

The main drawback of the Rietveld method for clay mineral quantification comes along with complex structures such as mixed-layering, polytypism, as well as tri-dimensional defects (ŚRODOŃ, 2006). In order to overcome this problem, numerous studies are aming to the development of computed crystallographic models, which describe various types of structural disorder (BERGMANN; KLEEBERG, 1998; UFER, 2004; UFER et al., 2008). Until now, no structural model is available to describe mixed-layering by Rietveld analysis, but is under development (UFER ET AL., 2009), most widely used models for smectites are those proposed by Ufer, (2004).

2.2 Regarding applications of bentonites

Much has been written regarding the remarkable properties of bentonites and their broad spectrum of industrial applications, attending an impressive amount of industries, innumerable specific functionalities (GRIM, 1962; OLPHEN, 1978; LAGALY; FAHN, 1983; ODOM, 1984; MURRAY, 2007) and an increasingly

growing search for environmentally friendly uses (HARVEY; LAGALY, 2006)**.** The physical and chemical properties of bentonites that provides such versatility, is given by the smectite mineral group contained in bentonites, not only in terms of smectitic phase content (most commonly found species are members of the montmorillonite to beidellite series of dioctahedral smectites), but also due to structural features within smectites. Therefore, a very clear distinction between grade and quality is presented along with the mineral characterization.

Moreover, the geological track followed by a bentonite deposit will determine all relevant variables of the smectite phases present in the mineral assembly, such as the cation exchange capacity, layer charge, morphology, crystal chemistry, etc. Most relevant variables controlling bentonite grade and quality are parent rock composition, bentonite forming processes type, age and post-diagenetic events such as weathering and burial history (CHRISTIDIS; HUFF, 2009). However, not always these birthmarks rule the way deposits are being exploited, neither have they ruled market destinations, particularly in small-scale mining operations (CLEM, 1961; HARVEY; LAGALY, 2006).

2.2.1 Related studies on organophillization

Most organic reactions in nature occur at the nano scale, in terms of particle size that means most of this type of interactions have place within the range of the so called clay size fraction of minerals. Therefore, clay minerals, hydrated oxides, and hydroxides, mainly of Si, Al, Fe and Mg, and some geo-organic polymers are responsible for most surface and colloid reactions on earth, including adsorption of organic matter by its components (YARIV; CROSS, 2002).

The main aspects of hydrophilicity to hydrophobicity transition when interacting organic compounds within the structure of 2:1 clay minerals is influenced by layer charge and crystal chemistry according to Yariv; Cross (2002), vermiculites and montmorillonites are with no doubt the most relevant minerals phases when it comes to organoclays research. Nevertheless, nontronites, beidellite and saponite are also well documented. Perhaps the most important feature of this text is the fact that one can understand how the nature and location of octahedral and tetrahedral substitutions are the major players on the way a

specific play with interact with organic compound. On the other hand, characterization techniques suitable for the evaluation organoclays are NMR, TGA, FTIR and Thermo-IR Spectroscopy (YARIV; CROSS, 2002).

The dynamics of organic cations onto clay structures are described and modelling are described by Nir; Rytmo; Undabeytia, (2002). Basic evaluation parameters and principles regarding role of layer charge in organic contaminants sorption have been studied by Jaynes; Boyd (1991) and Lagaly; Fahn (1983). Other Important parameter were discussed by other authors:

- Clay sorbents: the mineralogy, processing and applications by MURRAY (2007);
- Sorption and detoxification of toxic compounds by bi-functional organoclays, by Gerstl et al. (2004);
- Clays for pollution control by Churchman et al., (2006)
- Uses of organo clays by L. Deligianni, A. Ekonomakou, Bentonite Division - Silver & Barite Group (2010);
- A Brazilian review article is very appropriate to understand preparation approaches and protocols by de Paiva; Morales; Valenzuela Díaz (2008).

2.2.2 Related studies regarding clay-polymer nanocomposites (CPN)

This amazing phenomenon has called scientific attention since the beginning of the 20th century. Already in the 60´s the ability of smectites to induce polymerization of certain unsaturated monomers in the interlayer space of Smectites was demonstrated by Blumstein (1965). But it was not until the beginning of the 80´s when Toyota launched great applied research inventory on clay based nanocomposites and six years later the first car containing PCN was on the streets. That event triggered nano-clays research and a remarkable number of patents and publications

The Brazilian government has encourage the development of CPM industrial by means of technical documents sponsored by the "*Mininsterio do Desenvolvimento, Industria e Comércio Exterior do Brasil",* claiming feasibility on

the local market (NANOBUSINESS, 2012); important features like National consumption of CPN and regional demand distribution, also a raw feasibility study is presented, proposing a plant installation taking into account infrastructure and projected market size up to 2025, Silva; Ferreira, 2008. Ruiz-Hitzky; Van Meerbeek (2006) establishes a base line work to comprehend basic principles and conventions on this issue, besides, there is quite a great deal of ethical resources on its work.

Kutz (2011) offers a broad perspective of thermoplastics, advantages and downsides of each polymer that could be used as a matrix and most relevant dynamics of injection and extrusion processes. Polymer/clay nanocomposites preparation methods and characterization are extremely susceptible to aggregation of clay particles, melt fluid dynamics and other mechanical variables according to Okamoto; Ray (2009), this work offers a complete overview regarding preparative methods and structures of PCN, materials properties and melt Rheology.

Detailed information about the diffusion coefficient for gas and liquids are offered for all possible polymer matrixes, allowing a good understanding of how to manipulate interaction parameters in order to achieve optimum barrier properties in PCN (DRUMMY et al., 2007, CARRADO; SANDY, 2007). Rubber clay nanocomposites are ruled by similar principles to those observed in CPN, although one must consider a greater diffusion coefficient in association with the rubber molecule size and lower homogenization efficiency (GALIMBERTI, 2011).

After organophillization where a hydrophobic surface among the clay particles. The aim is to have a compatibility interaction within the polymer melt in the plastic polymerization approach and in solution intercalation approach the polymer will be dissolved into a solvent with dispersed clay; disordered clay sheets will be swollen easily in solvents such as acetone, chloroform and toluene. After polymer is absorbed into delaminated sheets, the entropy gained by solvent´s molecules evaporation will allow remaining polymer chains to diffuse between layers (VITTAL, 2009).

Many factors will have influence on results like: temperature, melt rheology of polymer/clay composite, polarity of the polymer matrix, charge density, organic

modifier, and others. Therefore, depending on the nature and properties of clay and polymer as well as preparation methodology of nanocomposite, different composite microstructures can be obtained.

Polymer selection with those matrixes that can be used for the packaging industry and usually the desired reinforcement is measured in the improved capability to create a gas barrier. Many studies have reported the barrier properties of polymer/clay nanocomposites against the diffusion of gases and vapors (TORTORA et al., 2002; RAY et al., 2003; LANGE; WYSER, 2003; GIANNELIS, 1996; KOH et al., 2008) Local demand/supply balance can be summarized as follows:

- Polyethylene (PEs)(low and medium density) produced in Brazil by BRASKEM and QUATTOR (3.035.000 T/year)
- Polypropylene (same companies 1.965.000 T/year)
- Polystyrene (four different companies 580 T/year), PET or PVC[5].

2.2.3 Related studies on acid activation.

Carrado; Komadel (2009) addressed the topic of acid activation of bentonites and Polymer-Clay Nanocomposites and provided a broad overview about the variables which control this processes. The handbook of clay science, also has a chapter dedicated to the topic, written by the same author (KOMADEL; MADEJOVÁ, 2006), locally, a good overview with a soft chemistry approach is offered by (VALENZUELA DÍAZ; DE SOUZA SANTOS, 2001)

2.2.4 Bentonite grade & quality

By definition bentonite grade in the industrial minerals glossary is directly proportional smectite content (KOGEL, 2006), although commercial bentonite products are commonly classified by grades according to the specific application; E.g. pharmaceutical grade, foundry grade, polymer grade, etc. These

[5] All data regarding local polymer production was extracted from (NANOBUSINESS, 2012)

ramifications are due to the fact that not only mineralogical composition with respect to the smectite group is relevant; other aspects, such as whole elemental compositions, morphology, the presence of penalty minerals or other clay minerals, major interlayer cation and more, are relevant when to goal is to obtain certain performance on diverse systems. For the purpose of this document, bentonite grade is approached by stablishing the smectite group content, the di/tri-octahedral nature of smectites and the implications derived from other minerals contained in each sample, and will be based on whole rock analysis. Consequently, bentonite quality is based on structural features and physicochemical parameters of smectites based in observations over the < 1 μm size fraction.

Assessment is the determination of physical and chemical properties of an industrial rock or mineral in order to confirm if it can be used in certain applications. Usually the raw material has to fulfill certain specifications, dictated by international bodies, e.g.: DIN, BSI, ASTM, API, OCMA, etc.

However, in certain occasions specifications are simply dictated by commercial customers, in which there is plenty of literature in association to each applied technique, such is the case of PVP surface area (BLUM; EBERL, 2004) based on whole sample; and traditional assessment of a bentonite (INGLETHORPE et al., 1993, CHRISTIDIS; SCOTT, 1993). Traditional assessment involves determination of both, quality and grade.

3 METHODS & MATERIALS

Giving the complexity and large geographical setup of this research project, a bottom-up approach will be used to validate data. The first step is presented as a thorough characterization carried out over the 12 samples framework, containing at list one specimen from each geological area in order to explore correlations or trends, between the geological path and physical and chemical properties observed, then sections 4.7 and 4.9, a broader sampling universe of 33 samples coming from the same geological areas, is used to evaluate the parent rock type based on trace and REE's and certain implications that the geochemical fingerprint could have on applications.

3.1 Bentonite sources

It would be improper to reveal information specifying the source in a comparison analysis for several reasons, among which we would like to outstand the following:

- In first place, some of these bentonites are commercial products competing among themselves for market shares as a function of their quality.
- Secondly, a few of those samples belong to mines whose owners have not given expressed consent to the divulgation of this data.
- Lastly, some of these deposits are not being commercially exploited or have a low profile in the market environment regardless of the specific bentonite quality. Nevertheless, these results will establish criteria to decide which bentonite sources will be selected as a function of crystal chemistry and other features, for the next step.

Accordingly, all samples will be referred hereafter, in an aleatory alphabetical denomination from "A" to "L". To explain the process of bentonite characterization by step, the procedure is illustrated using a single patterns favoring the most complex ones, for further analysis and overall comparative conclusions. Figure 9 (section 2.1.3), shows the relative geographical locations for the six studied geological areas, while the following Table 4, associates them with respect to their geological context, in terms of what is considered to be most

relevant variables affecting bentonite quality and grade, summarizing what was extracted from the literature.

Table 4 - List of 12 samples used to stablish a grade/quality framework.

Sample	Area name	Area Code	Age	Parent rock	Formation Mode	Pos-Events
F	Neuquen-Rio Negro	1	Paleocene-Eocene	Andesite	InSitu Alteration	preservation
L	San Juan-Mendoza	2	Triassic	Rhyolite/Dacite	Detrital	Heavy tectonism
A	Parana basin	3	Mid-Permian	Ryolite/Dacite	InSitu Alteration	Intercratonic preservation
B	Parana basin	3	Mid-Permian	Ryolite/Dacite	InSitu Alteration	wethering/Illitization
C	Parana basin	3	Mid-Permian	Ryolite/Dacite	InSitu Alteration	wethering/Illitization
E	Bahia	4	Tertiary	Basalt	In situ or Hydrothermal*	Uncertain
G	Bahia	4	Tertiary	Basalt	In situ or Hydrothermal*	Uncertain
J	Bahia	4	Tertiary	Basalt	In situ or Hydrothermal*	Uncertain
H	Paraiba	5	Tertiary	Basalt	Uncertain	Uncertain
I	Paraiba	5	Tertiary	Basalt	Uncertain	Uncertain
K	Paraiba	5	Tertiary	Basalt	Uncertain	Uncertain
D	Formosa	6	Triassic	Basalt	Hydrothermal or whethering*	Wethering

*bibliographical research showed uncertain or contradictory
List of samples arranged by geological Area

The previous chart limits the geographical precedence of each sample, by the Geological Area, and no detailed information regarding the source (beyond the content in Table 4) is provided. Nevertheless, a certain distinction is made for samples coming from the same area having heterogeneous formation mode, age, parent rock or post-formation events; such as the case in Paraiba (Area 5), Parana Basin (Area 3) and San Juan-Mendoza (Area 2)

Table 5, presents a complete list of 33 collected samples, not fully characterized, neither studied for the porpoise of this study, but they are listed here because they were used to stablish a geochemical fingerprint based on trace and rare earth elements and some application trials, giving the fact that most of them belong to the same geological areas, and those who don’t (group 7) are international referential bentonites.

Table 5 - Complete list of samples

Area Code	Sample	Area name	Age	Parent rock	Formation Mode
1	F	Neuquen-Rio Negro	Paleocene-Eocene	Andesite	InSitu Alteration
1	P	Neuquen-Rio Negro	Paleocene-Eocene	Andesite	Unkown
1	Q	Neuquen-Rio Negro	Paleocene-Eocene	Andesite	Unkown
1	W	Neuquen-Rio Negro	Paleocene-Eocene	Andesite	Unkown
1	AC	Neuquen-Rio Negro	Paleocene-Eocene	Andesite	Unkown
2	L	San Juan-Mendoza	Triassic	Rhyolite/Dacite	Detrital
2	M	San Juan-Mendoza	Triassic	Rhyolite/Dacite	InSitu Alteration
2	N	San Juan-Mendoza	Triassic	Rhyolite/Dacite	InSitu Alteration
2	O	San Juan-Mendoza	Triassic	Rhyolite/Dacite	Unkown
2	R	San Juan-Mendoza	Triassic	Rhyolite/Dacite	Unkown
2	T	San Juan-Mendoza	Triassic	Rhyolite/Dacite	Unkown
2	AF	San Juan-Mendoza	Triassic	Rhyolite/Dacite	Unkown
2	AH	San Juan-Mendoza	Triassic	Rhyolite/Dacite	Unkown
2	AJ	San Juan-Mendoza	Triassic	Rhyolite/Dacite	Unkown
2	AL	San Juan-Mendoza	Triassic	Rhyolite/Dacite	Unkown
3	A	Parana basin	Mid-Permian	Ryolite/Dacite	InSitu Alteration
3	B	Parana basin	Mid-Permian	Unkown	Unkown
3	C	Parana basin	Mid-Permian	Unkown	Unkown
4	E	Bahia	Tertiary	Basalt	In situ or Hydrothermal*
4	G	Bahia	Tertiary	Basalt	In situ or Hydrothermal*
4	J	Bahia	Tertiary	Basalt	In situ or Hydrothermal*
4	Y	Bahia	Tertiary	Basalt	In situ or Hydrothermal*
4	AO	Bahia	Tertiary	Basalt	In situ or Hydrothermal*
5	H	Paraiba	Tertiary	Basalt	Uncertain
5	I	Paraiba	Tertiary	Basalt	Uncertain
5	K	Paraiba	Tertiary	Basalt	Uncertain
5	AP	Paraiba	Tertiary	Basalt	Uncertain
6	D	Formosa	Triassic	Basalt	Hydrothermal or whethering*
7	AA	Unkown	Unkown	Unkown	Unkown
7	AB	Unkown	Unkown	Unkown	Unkown
7	AE-A	Unkown	Unkown	Unkown	Unkown
7	AE-B	Unkown	Unkown	Unkown	Unkown
7	AM	Unkown	Unkown	Unkown	Unkown

*****bibliographical research showed uncertain or contradictory

**Samples belonging to area code 7 are well known international commercial references

3.2 Establishing bentonite grade

Size distribution analysis (LALLS), randomly oriented powder X-ray diffraction (XRD) and whole rock X-ray fluorescence spectroscopy (XRF) chemical analysis were carried out at first, for they would provide information used to define milling protocol in order to avoid excessive energy that could damage crystal structures, particle size separation strategy as a function of particle population/s, mass absorption coefficient and chemical filter for X-ray diffraction (XRD).

After all major mineral phases are identified on the bulk (ROP) XRD patterns, a crosschecking stage is necessary based on molar sum contrasting

bulk XRF chemical data and identified phases on XRD traces, chemical misfit can outstand the presence of trace mineral below the detection limit of XRD or amorphous phases, in which case the semi-quantitative analysis was complemented by means of scanning electron microscopy coupled with EDS, Fourier transformed infra-red (FTIR) or simply strategic size separation in order to enrich target trace minerals followed by XRD.

Mineral quantitative analysis based on full profile fitting of randomly oriented samples, was carried out according to Srodon et al., (2001) and Ufer et al., (2008) using TOPAS structure files data base by BRUKER, with slight adjustments on smectite structure files according to the methodology proposed by Neumann; Avelar; da Costa (2014). In order to enhance profile fitting as a function of chemical variability due to isomorphic substitutions in di-octahedral and tri-octahedral positions, based on the information provided by chemical analysis over the <1 μm size fraction.

3.3 Establishing bentonite quality

Swelling behavior of smectite species and its implications on layer charge, interlayer cation and crystal chemistry, were evaluated mainly by means of XRD on oriented glass slides combined with chemical results over the clay size fraction. EG treatment was performed in rounds of no more than 5 samples at a time to avoid EG evaporation, samples were put in a glass desiccator at 60° C for 24 hrs.

Na and K saturation was performed on the <1 μm fractions using 1M NaCl and KCl solutions respectively. The samples were saturated for at least 4 times, the last one overnight under mechanical agitation. Each time the solution was changed. After saturation, the samples were rinsed shortly by dispersing the clay fractions with an ultrasound device and finally washed four times with ethyl alcohol.

The sequential K-saturation and EG treatment was used to build a comparative layer charge magnitude model, regardless of charge location, based on the method proposed by (CHRISTIDIS; EBERL, 2003), without using the software enclosed for layer charge value calculations, based on XRD simulated traces calculated from three component interlayering. Therefore, it only accounts

for comparative results with respect to evaluated samples under the same conditions.

Swelling observations based on EG oriented slide XRD traces, will indicate predominant interlayer compensating cation and will be correlated with chemical information in order to evaluate coherency in the data set. Layer charge may also influence swelling behaviour, tending for higher electrostatic interaction to beat in higher layer charge values and therefore, indirectly proportional to swelling; the contrary can be expected for lower layer charge smectites

Structural formula consideration are dropped according to Schultz (1969), Köster et al., (1999) and Onal, (2006) from the data obtained by XRF chemical analysis on < 1 μm samples. The method from the last author will also provide enough information about the octahedral and tetrahedral distribution of the layer charge, parameter which cannot be accessed throughout XRD techniques.

No correction was performed to SiO_2 values at the clay size fraction; hence the objective is not to establish a reliable structural formula for smectite species, but to observe geochemical trends.

3.4 Main characterization techniques

Hence this research work aims to stablish comparative correlations, special effort was given to equally prepare and analyze all samples. Moreover, replicas where conducted for all analytical techniques applied, with the exception of randomly oriented XRD patterns that where collected in triplicates. Preparation began by drying 1 kg/sample at 60 ^{o}C during 24 hrs., then crushed in a ceramic ball mill at 120 rpm up to 100% Wt < 149 μm (100 mesh Tyler) in dry sieve. Afterwards, powders were spit in a Microscal Ltd. spinning riffler type FTOB, into twenty parts.

Three out of twenty parts were used for sedimentation in order to produce <1 μm size fraction rich in smectites, leaving the remaining bulk material to be pulverized using a Herzog pneumatic pulverizing mill (HSM-100) on tungsten carbide up to 100% Wt < 74 μm (200-mesh) for XRF, SEM and FTIR and smaller amounts up to < 10 μm to be used in powder XRD for optimum setup (DERMATAS et al., 2007; O'CONNOR; CHANG, 1986; KLEEBERG et al., 2008)

3.4.1 Sample preparation

Apart from procedures above, whole samples where gently ground with pestle and mortar; subsequently they were sieved to obtain diameter above 53µm (Ø>53 µm) size fraction for the observation of heavy minerals. Afterwards the Ø>1 µm size fraction was obtained by mechanical agitation during 24 hrs. and sedimentation according to Stokes law using deionized water (Figure 14). Ethylene glycol treatment was done in rounds of no more than 5 samples at a time to avoid evaporation of ethylene glycol; samples were put in a glass desiccator at 60° C for a period ranging 16 hrs. to 24 hrs.

Figure 14 - Pictures of sedimentation lay out and some characterization devices.

Above: sedimentation setup, Left below: SEM samples mounted on stubs, right below: XRD randomly oriented powder pressed samples

Na^+ and K^+ saturation was performed on the <1 µm fractions using 1M NaCl and KCl solutions respectively. The samples were saturated for at least 4 times, the last one overnight under mechanical agitation. Each time the solution was changed. After saturation, the samples were rinsed shortly by dispersing the clay fractions with an ultrasound device and finally washed four times with ethyl alcohol.

3.4.2 X-ray diffraction (XRD)

X-ray diffraction (XRD) was carried out in a diffractometer Bruker D8 Endeavour with Cukα: wavelength 1.54 Å, radiation (40 Kv, 40 mA), multilayer graphite monochromator, LYNXEYE XE detector and 2.3 mm soller slits for both, incident & diffracted bean. Bulk samples were prepared as randomly oriented powder (ROP) by backload on holders having 10 mm of sample surface, and less than 1 µm size fraction as oriented slides (OS) on glass rounded slides of 25 mm. Most XRD protocols were followed according to Moore; Reynolds (1997) and Chipera; Bish (2001), except for ethylene glycol solvation (EG) according to Mosser-Ruck et al., (2005) and K-saturation for oriented slides preparation followed by EG treatment and derived considerations regarding layer charge magnitude as proposed by Christidis; Eberl (2003).

Phase Identification was performed using the software by Bruker Difrac.Eva 4.1.1., and crystallographic information files PDF4 (2012) data base, semi-quantitative phase analysis by Rietveld method was performed using the software by Bruker diffract Topas V5.1. Table 6 shows a summary of XRD experimental conditions for all treatments, as well as the abbreviations in which results will be presented hereafter.

Table 6 - Ray diffraction experimental conditions

Experiment	Abbreviation	2 Theta range	Step Size	¯ime per Step (Sec)
Randomly oriented powder	ROP	From 2° to 75°	0.02	3
R. O. P. (Replicas)	ROP(r)	From 2° to 75°	0.02	2
Air dried (oriented slides)	AD	From 1° to 45°	0.02	2
Ethylene glycol solvated O.S.	EG	From 1° to 45°	0.02	2
Na^+ Saturation O.S.	Na-sat	From 1° to 45°	0.02	2
K^+ Saturated+ EG O.S.	K-sat+EG	From 1° to 45°	0.02	2
Organophilic clay oriented slide	K-sat	From 1° to 45°	0.02	2

Source: Gabriel G. Machado (unpublished)
Note: All oriented slides where done over the less than 1 µm particle size.

Adopted nomenclature is detailed bellow:

- R.O.P.= randomly oriented powder X-ray diffraction experiment
- O.S.= oriented glass slide X-ray diffraction experiment
- EG= ethylene glycol solvated on oriented slide X-ray diffraction experiment

- K-sat= Potassium saturation X-ray diffraction experiment, as explained in the previous section.
- Na-sat= Sodium saturation X-ray diffraction experiment
- K-sat + EG= K-saturated and then ethylene glycol solvated as proposed by (CHRISTIDIS; EBERL, 2003)
- AD= Air dried X-ray diffraction experiment
- REP= Replica of an X-ray diffraction experiment or X-ray florescence.
- Nat= Natural air or non-air dried X-ray diffraction experiment
- O.C.= Organoclay X-ray diffraction experiment on oriented glass slide (meaning XRD pattern of a previously organo intercalated sample)
- PCN = Polymer clay nanocomposite preparation

3.4.3 X-ray fluorescence (XRF)

Chemical analysis of whole rock and <1μm size fraction was determined using the X-ray fluorescence spectroscopy technique (XRF), on a S8 Tiger WDXRF Bruker spectrometer. A total of 33 samples were analyzed in replicas, 5 more random control readings and several re-doings, for a grand total of 75 experiments were carried out, all prepared as fusion beads. Loss on Ignition (LOI) was determined before melting following the procedure explained in next paragraph. Fired powders after determination of LOI were mixed with lithium tetra borate ($B_4Li_2O_7$) flux under the following conditions:

I. Mixing proportion whole rock:flux was 7:1 .
II. Mixing proportions for most <1 μm fractions was 7:1, although some samples had a different proportion this ratio was kept and used in the instrument software settings to calibrate concentrations.
III. Samples were gently ground, and weighed, then $B_4Li_2O_7$ was added progressively to obtain a homogenous powder, subsequently the

mixtures were placed in platinum crucibles and finally three drops of lithium bromide (BrLi) were added and the samples were melted.

Selectively, some stardardless whole elemental analysis were carried out, over the same fusion beads in order to close the sum gap, when mayor ten elements were not sufficient for a satisfactory bulk chemical overall composition.

3.4.4 Loss on ignition (L.O.I.)

L.O.I was estimated for all samples and 10 aleatory selected duplicates by following these steps:

I. Porcelain crucibles were weighed after drying in an oven at 110º C.

II. Each crucible was labeled and filled with a powder either of whole rock or <1µm particle size, dried for at least 3 hrs. at 105º C and weighed. Then the dry weight of the samples was recorded.

III. Subsequently the powders were fired for 2 hrs. at 1020º C. Finally, from the difference of the weight after drying and after firing, the LOI was estimated.

3.4.5 Particle size distribution analysis

Particle size distribution analysis was performed for all bulk samples by low angle laser light scattering technique (LALLS) on a Malvern Mastersizer 2000, first on bulk with no dispersant added on deionized water and applying 1 minute of intermittent ultrasonic treatment, pumping speed was left a constant speed at 2500 rpm.

The PSD (particle size distribution) of each sample would give valuable information regarding mineral size populations and would set the frame or sedimentation strategy as a function of particle size distribution. A few samples over the <1 µm to evaluate the efficiency of the sedimentation procedure and to distinguish heterogeneous populations among based on the crystal size for present phases acquired after Rietveld refinement.

PSD was adopted as a pre-step to define sample preparation strategy according to the technique proceeding. Figure 15, shows comparative graph for

12 samples, containing at list 1 specimen of each geological area, arranged from south to north. It is possible to obverse already, lower d-50 in samples F and L, belonging to areas 1 and 2 respectively.

Figure 15 - Statistical diameters D(10), D(50) and D(90) for 12 samples arranged from south to north

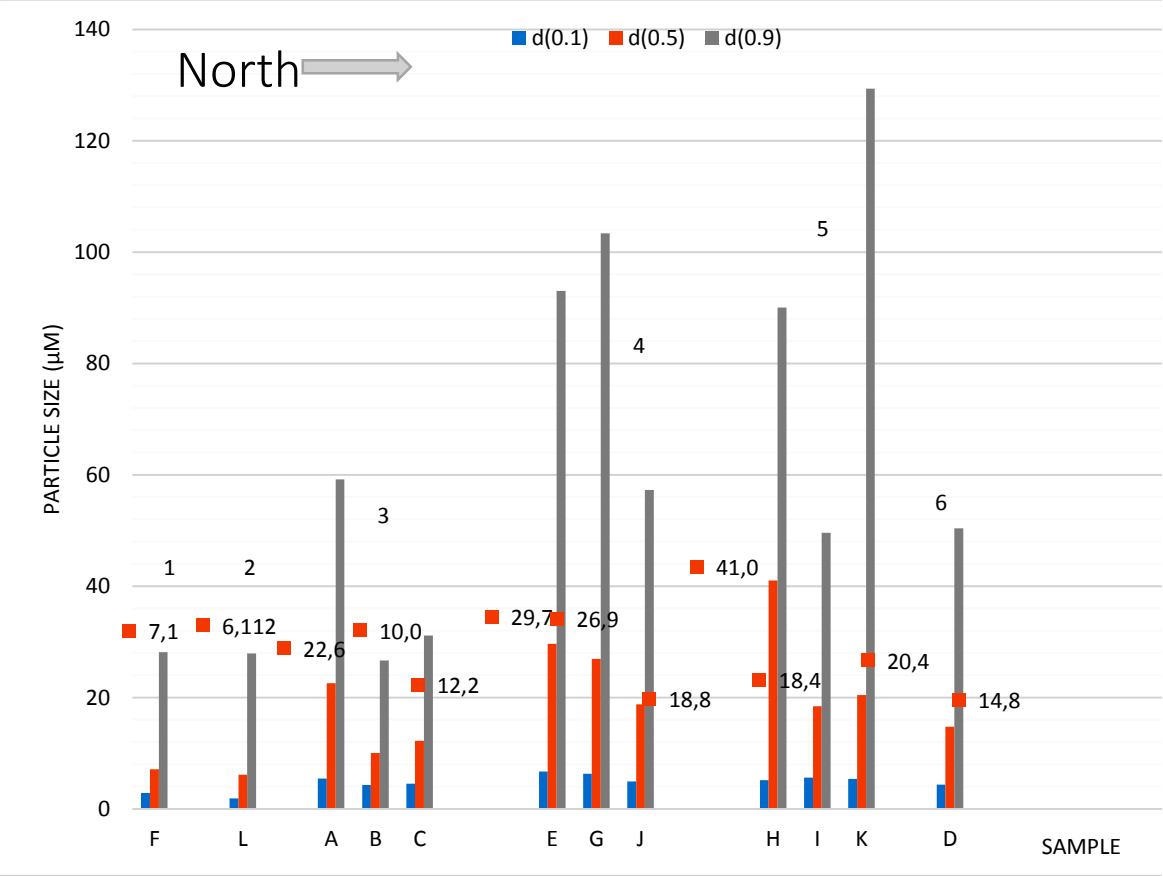

Note I: the value located on top of bars, is the mean particle size magnitude for each sample beneath.
Note II: The number located on top of mean size values, correspond to the Geological area for each sample beneath.

3.4.6 Other techniques

As mentioned before in Chapter 2, several accessory characterization techniques were used during this study, hence they do not represent the foundations of presented results, they will only be briefly described. Scanning electron microscopy (SEM/EDX), thermogravimetric analysis (TGA), Fourier transform infrared spectrometry (FTIR), high performance liquid chromatography, inductively coupled plasma optical emission spectrometry (ICP-OES) and optical microscopy, were also used as complementary methods, and therefore, briefly described as follows:

- High performance liquid chromatography was conducted on a Shimadzu series 20A with a C18 column (VP-ODS 250Lx0.2), mobile phase: Me OH: H_2O (70:30 v/v), Injection volume = 100 µL Ambient temperature. Detection wavelength: 280 nm.
- Inductively coupled plasma optical emission spectrometry (ICP-OES): Trace and REEs elements were accessed by means of ICP-OES and 4 acid digestion on a Horiba Jobin Yvon Ultima2.
- Fourier Transform Infrared (FT-IR): was collected in a Bruker Tensor 27 Ft-IT using the OPUS data collection and analysis program. Samples were prepared by the KBr pressed-disc technique under 5 TN of pressure with 200gr of KBr and 0.5 mg of clay, to perform routine scanning of the spectra in the MIR region.
- Optical microscopy: The optical microscopy was performed with a Leica DMLP optical microscope. Freshly cut bentonite samples were mounted on petrographic slides with a special glue to avoid fracture when swelling. Then they were dry polished to ~ 100 µm thickness.
- TGA: 15 samples of polymer clay nanocomposites were analysed on a NETZSCH STA 449F1 thermo-gravimetric analyser under synthetic air. The thermal analysis was performed up to 600° C on a heating ramp of 10 C° per minute. Samples where cryogenically cut using approximately from 15 mg to 30 mg.

3.4.7 Layer charge & unit formula

Based on these structural features of smectite species, is possible to project expected performance in terms of industrial applications, therefore a special effort is given to the estimation of the layer charge and the unit formula (also structural formula) accessed by two methods.

One of them involved observing XRD patterns after potassium saturation and ethylene glycol solvation of the clay samples and subsequent comparison with XRD simulated traces calculated from three component interlayering (CHRISTIDIS; EBERL, 2003). The profile fitting is done with an Excel sheet that

was an output of this investigation and offers at the same time two different ways to compare the measured XRD values to the data base of the layer charge program (1) - whole profile fitting (2) - peak position fitting.

The second method uses the structural formula calculation (BROWN; NEWMAN, 1987; EBERL et al., 1986; KAUFHOLD, 2006; ONAL, 2006; SCHULTZ, 1969) from the data obtained by XRF chemical analysis results in < 1 µm samples. This last method will also provide enough information about the octahedral and tetrahedral distribution of the layer charge, parameter which cannot be accessed throughout XRD techniques.

A slight correction can be done to SiO_2 values of chemical data in order to establish a reliable structural formula for the smectite members. In the XRD traces it is possible to notice the presence of quartz[6] and as a consequence, to correct the smectite formula due to the existence of silicates (mostly amorphous) even at the clay size fraction, the same applies for oxides typically Fe^{+}, found also at the sub-micron size fraction, in which case the standard method used for relative quantification would be the XRD internal standard method, but was not carried out for the porpoise of this study, neither is considered, the oxidation state or specific location of $Fe^{+2/3}$ isomorphic substitutions.

3.5 Organophillization

Comparative criteria applications performance was evaluated throughout organic sorption behavior of natural (without previous Na^{+} activation) smectite rich concentrates (< 1 µm). The organo-compound used was a commercial product by Clariant Ltd, Genamin CTAC 50 ET, which is a cetyl trimethyl ammonium chloride cationic surfactant (CTAC). All variables were fixed: CTAC concentration, aging time, pH control, Clay concentration, size fraction, etc. Preparation protocols according to Lagaly; Ogawa; Dékány (2006).

[6] Although this XRD traces wouldn't be useful for mineral quantification, for they were collected in oriented slides over the clay size fraction.

Subsequently the samples were washed five times with methanol and oriented slides were prepared using methanol containing organophilic clays. Due to the volatility of methanol the samples were dried rapidly (2,5 hr.) and then they were placed in a desiccator to avoid moisture adsorption before collecting XRD pattern. The sorption of organic compounds was evaluated in terms of the expansion of the d001 basal reflection after organophillization and according to the size of the alkyl chain used, and the known sorption isotherm proposed by Jaynes; Boyd (1991) precise protocol is detailed as follows:

I. About 0,5 g of the <1μm samples were saturated three times with Na+ using 30 ml of NaCl. After last saturation, the samples were left overnight under mechanical agitation.

II. After washing the samples with deionized water four times, they were dispersed in CTAC solution 5 times. After the last run the centrifuge tubes where covered and kept for 24 hrs at 60 °C.

III. Subsequently the samples were washed five times with methanol and oriented slides were prepared using methanol containing the organophilic clay. Due to the volatility of methanol the samples were dried rapidly (2,5 hr) and then they were placed in a desiccator to avoid moisture adsorption caption until X-ray diffraction analysis.

IV. Cetyl trimethyl ammonium chloride solution was prepared by dissolving 18, 5 gr of the cetyl trimethyl ammonium chloride into a mixture of 500 ml of deionized water and 100 ml of ethanol. Keeping a record of the pH change, 47.1 ml of 2M HCl was added to the solution up to a pH value of 7,3. and then 27.5 ml of 0,1 M HCl were used to avoid exceeding neutral pH. After 5 min of stable pH measurements, the solution was completed with deionized water up to 1L and was stored for the organophillization experiments.

The picture in Figure 16, shows the sequence of previous organophillization presenting distinctive hydrophobic to hydrophilic behaviour, as a function of quats (quaternary ammonium compound) sorption, different polarity and carbon chain length, hence the distinctive hydrophobicity by bottle.

Figure 16 - Pictures of various organoclays.

3.6 Organic pollutant sequestration

Bentonite applications in water treatment are diverse; many functionalities may be expected from smectites, according to a given system. For the purpose of the present study, and aiming to stablish trends or correlations between structural features observed over the 6 geological areas considered, we approach an organic pollutant issue of local concern, which not only challenges nowadays treatment technologies, but also has a dramatic historical tendency to increase with time.

Alarming hormone concentrations levels have been reported in drinkable water reservoirs in Brazil, particularly in the Campinas area, Sao Paulo state (AQUINO; BRANDT; CHERNICHARO, 2013; MONTAGNER; JARDIM, 2011; SODRÉ; LOCATELLI; JARDIM, 2010; STUMPF et al., 1999), one of the most common species, due to its usage in Birth control pills, is the17β-estradiol. On the other hand, it has been reported that certain organoclays have the capability to collect hormone species (CAI et al., 2010), by absorption onto interlayer positions driven by hydrophobicity.

Artificially polluted deionized water was used for all experiments and the hormone concentration fixed at 1 ppm, in order to emulate reported concentrations in the Sao Paulo state waste waters containing β-estradiol. Bio reagent powder suitable for cell culture by sigma Aldrich (E2758).

Experiments were carried out in bench scale testing of a broad variety of organoclays enhanced for the selective sequestration of 17β-estradiol, no variables are presented at this stage (dose, time, pH), for it is relevant to show presented at this stage for it is relevant to expose this the evolution of protocol parameters in results and conclusions.

In order to characterize the removal efficiency of 17β-estradiol, a Shimadzu series 20A, high performance liquid chromatography device was used under the following operating conditions:

- C18 column (VP-ODS 250Lx0.2)
- Mobile phase: Me OH: H_2O (70:30 v/v)
- Injection volume = 100 µL
- Ambient temperature
- Detection wavelength: 280 nm
- Limit of detection (LOD in ppm) = 0.086986396 (86.99µg L-1)
- Limit of quantification (LOQ in ppm) = 0.260959187 (260.96 µg L-1)

Figure 17, shows the calibration scheme for the quantification of the given species as a function of relative peak intensity measures by the high performance liquid chromatography, and the calibration curve giving an almost perfect correlation for instrumental measurement is located in the appendix

Figure 17 - Calibration for the quantification of 17β-Estradiol on HPLC.

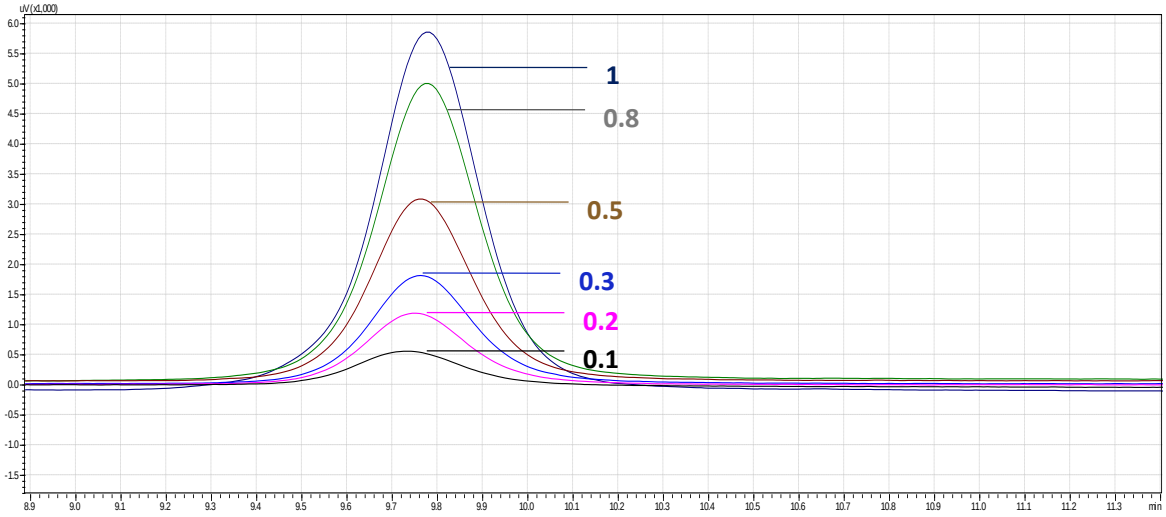

In order to optimize experimental procedures at this stage, the Doehlert experimental planning approach (Figure 18) was implemented considering the three most influential variables of our set: pH (minimum: 2 maximum: 9), clay dosage (minimum: 0.5 gr/l, maximum: 2 gr/l) and reaction time (minimum: 24 hrs, maximum:72 hrs.) in order to determine the experimental variables and interactions that have significant influence on the result, measured in one or several responses; to eventually fix this variables to deepen into clay source and organo compound type.

Figure 18 - Doehlert experimental planning for 17β-estradiol sequestration trials

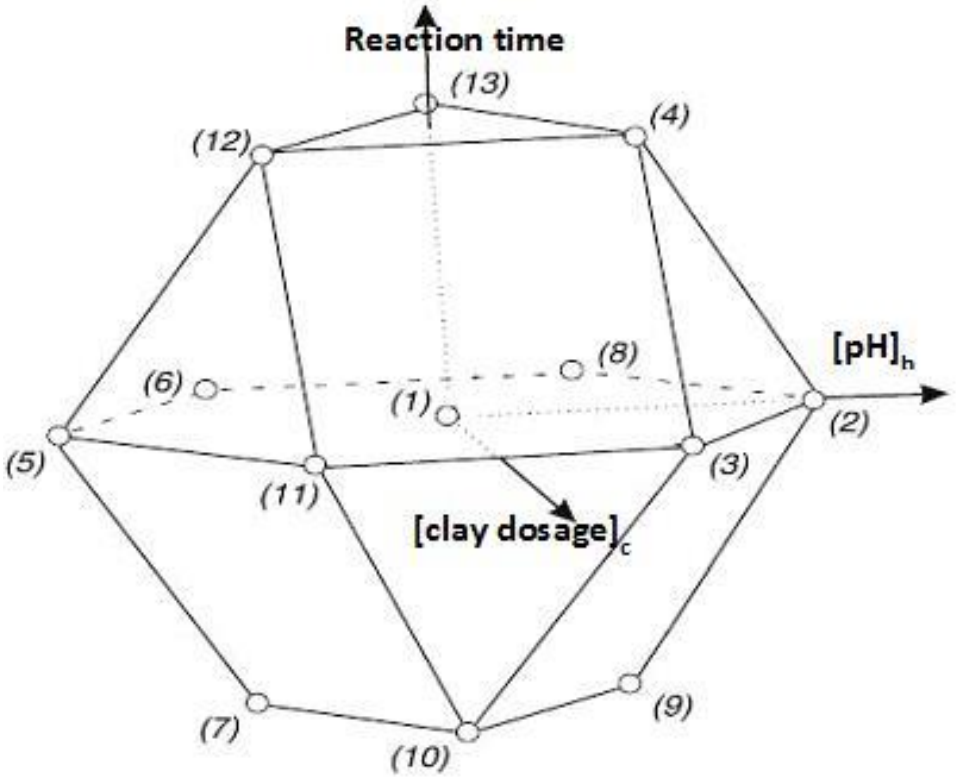

Source: Machado et al., (2018) unpublished work.

RESULTS

The following chapter is presented in the traditional sequence of techniques applied to clay minerals complete mineral characterization on the 12 samples framework as presented in Table 4, with the exception of sections 4.9 and 4.11.1 that refer to the whole set of 33 samples collected as described in Table 5, in order to broader the evaluation spectrum, but keeping the reference with respect to the six geological areas object of this study. Thereafter, and into chapter 5, discussions and considerations regarding grade and quality must unify all results and derive conclusions combining information from all achieved data.

Sections 4.8 and 4.9 are addressed to stablish whether the trends observed during the characterization, will be useful to predict comparative bentonite performance as a function of layer charge, swelling and organophillization (measured in d001 expansion after OC treatment), regardless of the mineralogical composition of whole rock materials, because they were equally purified to enrich smectite content over the clay size fraction. Octahedral Fe oxidation state and content, as well as tetrahedral Fe component are also disregarded in this study neither the influence of Iron rich smectites when performing described procedures.

3.7 Particle size distribution analysis by LALLS

The size distribution analysis showed a clear tendency to group into two characteristic cumulative volumes as a function of size distribution curves. As illustrated in Figure 19, southern bentonite samples “F” and “L” from geological areas 1 & 2 respectively, yielded significantly smaller mean size values than other samples, there is a tendency also to increase mean size value as northern location with the exception of sample “D” that showed an intermediate mean size value (14.8 µm).

Figure 19 - Size distribution analysis for all samples (LALLS).

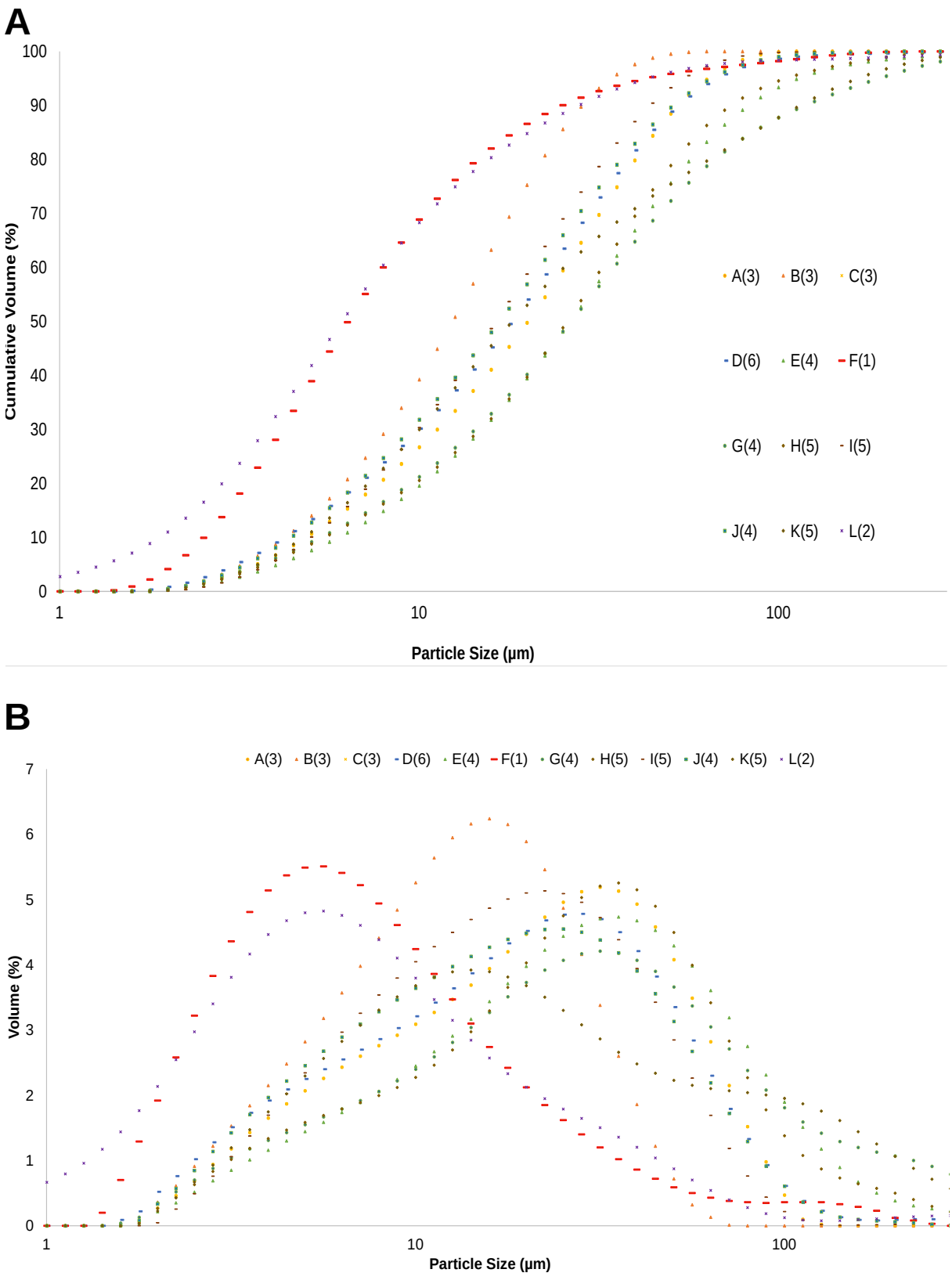

A) graph plots the cumulative volume (%under) against particle size, while B) plots volume vs particle size.

D(50) ranged from 6.1 µm for sample “L” up to 41 µm for sample H; likewise, there is a correlation between mineralogical composition with respect to higher d(50) values, especially those samples containing considerable amounts of quartz (23 Wt% for H sample), evidenced in the size population observed in Figure 19-B, around 100 µm.

3.8 Mineral phase identification by ROP XRD

Mineral phase ID based on XRD ROP patterns was executed as presented in Figure 20 for all samples (see Appendix C). Sample “B” Is presented as an example for it constitutes one of the most challenging phase ID fits due to the presence of clay mineral mixtures kaolinite (PDF 75-15932) and montmorillonite (PDF 13-0135), along with several accessory phases. Collected under the conditions described at Table 6. The inner zoomed box remarks the dioctahedral nature of present montmorillonite, irregular broadness of the d(060) is due to overlapping position in this region with the same reflection belonging to kaolinite

Figure 20 - Phase ID based on randomly oriented powder diffraction pattern for B sample

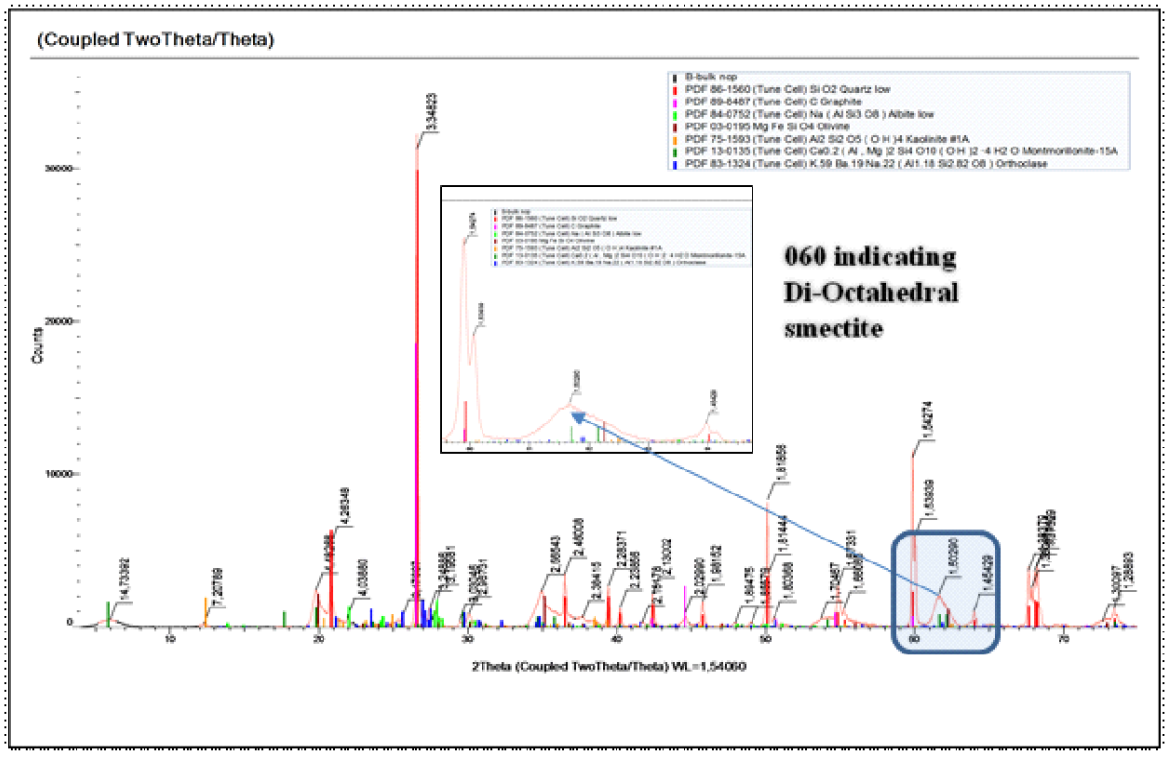

The tri or dioctahedral nature of smectite species present in all samples, was evaluated in the d(060) area ranging from 58º to 64º 2θ, and considering all possible contributions in this region from quartz d(211) at 1.549 Å, kaolinite d(060) maximum: 1.489 Å and other clay minerals detected (pyrophyllite, Illite and I/S mixed layers) in the region as explained by Srodon et al., (2001); finding mostly Al, Mg and Fe rich dioctahedral smectites from the montmorillonite to beidellite solid solution series (d(060): 1.49-1.505 Å) and in a minor extent contributions from Fe-dioctahedral smectites (d(060): 1.51-1.52 Å) (YAMADA et al., 1991; MOORE; REYNOLDS, 1997). No trioctahedral species where observed. Samples “D”, “E”, “G”, “H”, “I” and “J” (all coming from geological areas 4, 5 and 6) indicated the presence of Fe-dioctahedral smectites and Fe content from the < 1 µm chemical data also evidenced the presence of heterogeneous isomorphic Fe substitution presumably in octahedral position.

3.9 Mineral quantification by Rietveld refinement

Finally, and only after having a proper idea of most important crystal structures influencing the XRD bulk ROP pattern, TOPAS software was used to access a mineral phase semi quantitative analysis by Rietveld refinement. Figure 21shows a final fit for B sample matching considerably accurate with respect to the values given in Table 7(for all samples see Appendix C).

Although, samples “B” and “C” where suitable to express a complex XRD pattern for XRD on the Reitveld refinement they did not represent a major challenge. It was at sight of mixed-layering, Na-montmorillonites rich samples, Mg-montmorillonite samples and particularly at the presence of heterogeneous isomorphic octahedral substitutions. Where a great deal of work and learning to master Topas as a tool, represented a time consuming task. A mayor problem was the absence of proper structure files to explain all before mentioned phenomenon.

Figure 21 - Reitveld refinement fit for B sample on Topas V5.1

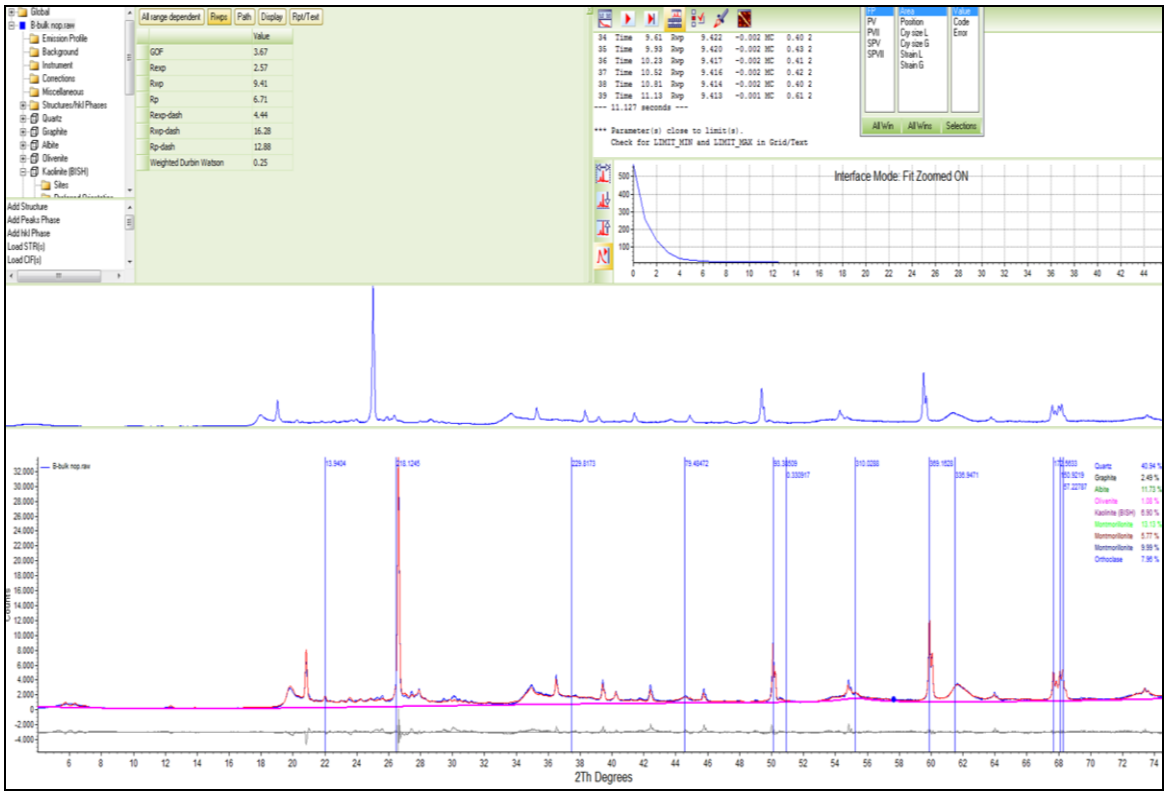

Table 7 - Quantitative mineral analysis results, after crosschecking Rietveld-Topas results against XRF-XRF molar sum.

Mineral / Sample	A	B	C	D	E	F	G	H	I	J	K	L
Montmorillonite	84,2	29,4	24,6	64,5	83,2	70,4	44,8	44,9	55,0	50,0	54,0	75,5
Quartz	9,4	40,5	40,7		1,1	7,0	20,5	23,0	38,0	30,0	29,3	
Hematite				6,8	1,0		1,8					3,5
Kaolinite		6,9	5,9	23,3	13,0		32,9	21,5		19,0		
Rutile						1,5						
Albite		11,7	14,8	5,4								
Cristobalite						4,3						12,5
K-Felspar	2,5	8,0	10,9		2,0			5,0			16,8	3,1
Andesine												3,4
Clinoptilolite												1,5
Pyrophyllite						3,5						
Anortite						13,3		5,5	3,0	1,0		
Graphite		2,5	1,6						4,5			
Barite	2,0											
Opal-CT	1,9											
Olivine		1,1	1,5									
Geological Area	**3**	**3**	**3**	**6**	**4**	**1**	**4**	**5**	**5**	**4**	**5**	**2**

Note: feldspar species were distinguished from the chemical composition aimed with SEM observations and opal-CT from quartz by combining XRD with SEM.

The reason for intentionally presenting the above graph and the one that follows in a raw un-treated way (in terms of image presentation), is to outstand all features of the software, top-right box shows convolution steps and conditions, to the top-left are crystal structures and quality parameters of the refinement.

Observing the low angle region on Figure 22 - Reitveld refinement for sample “J”, is possible to understand why more than one structure file is needed to fit smectitic phase with heterogeneous layer charge location and distribution, expressed in the broadness of peaks Figure 23, shows pattern that required the formulation of own structure files giving the fact that this sample is loaded with other clay minerals, kaolinite, illite and in a minor grade illite-smectite mixed-layering structures (only evident in the clay size fraction).

In order to have a refinement quality control parameter, two values are kept recorded, the first one commonly known as goodness of fit (GOF) and is provided by most refinement softwares, as a standard it was stablished to keep this value somewhat near 3 or less. The second is the RWP factor having an acceptable value beneath 10 (TOBY, 2006). Both are presented in Figure 23 - Reitveld refinement of samples K and I as examplesFigure 23 at the top of each refinement graph.

Figure 22 - Reitveld refinement for sample “J”

Figure 23 - Reitveld refinement of samples K and I as examples

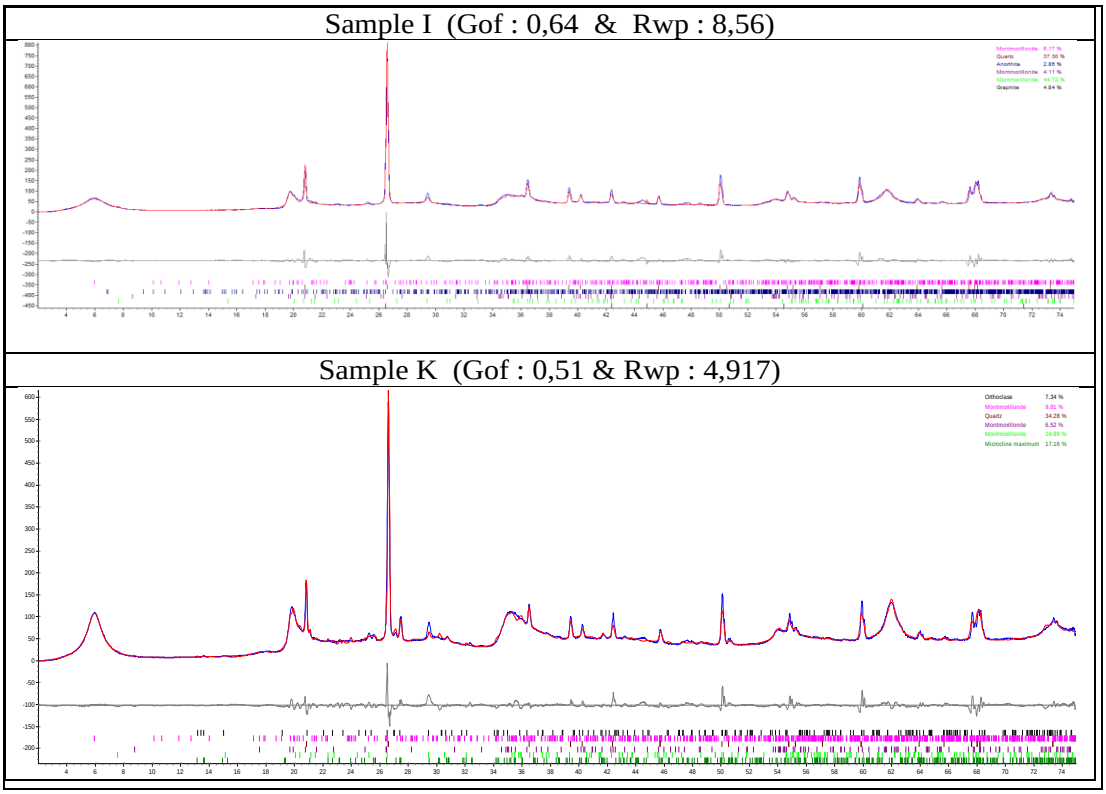

The blue/red pattern overlaying illustrate the experimentally collected trace against the simulated one based on crystallographic structures showed at the top right label. The grey line beneath both patterns illustrates the residual component from both patterns fit. And colored vertical lines indicate peak positions of considered structures.

XRD techniques used to comprehend swelling behavior, layer charge and smectitic phase quality are most of time base upon OS (oriented slides) preparation and treatment. Something to keep in mind is the fact that the preparation of oriented slides will depend on the initial solution particle concentration, therefore a different preparation can only be compared in terms of shape and peak positions, not from relative intensities for statistically it would be a fundamental error.

Perhaps is meaningless to expose in the plain document all graphical sketches from bentonite traces fitted by Rietveld, therefore only most challenging ones ore complex structures are presented hereby, three CIF files were solo used for all smectite fitting, although all fundamental parameters had to be refined in order to achieve an acceptable fit; on the other hand site coordination of isomorphic substitution in both cases (octahedral and tetrahedral), were also refine to fit, exporting a scan file in order to create a new version of structure (modified) file.

Distinguishing opal-CT from cristobalite was mainly by means of the broadness vs intensity evaluation of the d(101) reflection (ELZEA; ODOM; MILES, 1994). Traces of illite and illite-smectite mixed layers were found in samples “A”, “B” and “I” but only on oriented slides, this phases on bulk composition were probably below the detection limit of the technique (roughly 3%) and almost impossible to detect accurately in such a mixture by means of alternative quantitative approaches.

3.10 XRD over the clay size fraction

Observations on the clays size fraction (< 1µm) reveals information regarding crystal chemistry of smectite species and consequently, it allows stablishing correlations towards swelling and sorption behaviour. Comparing XRD oriented slides (OS) traces, in possible to access a comparative parameter of layer charge (magnitude), organophillization, and swelling capability, as it is presented in Figure 24. In order to illustrate observed results, four very distinctive samples (in terms of observed trends) are presented as in a comparative frame of 6 different treatments (Table 6), over the low angle region.

Figure 24 - All oriented slides zoomed at the d(001) for samples 4 representative samples

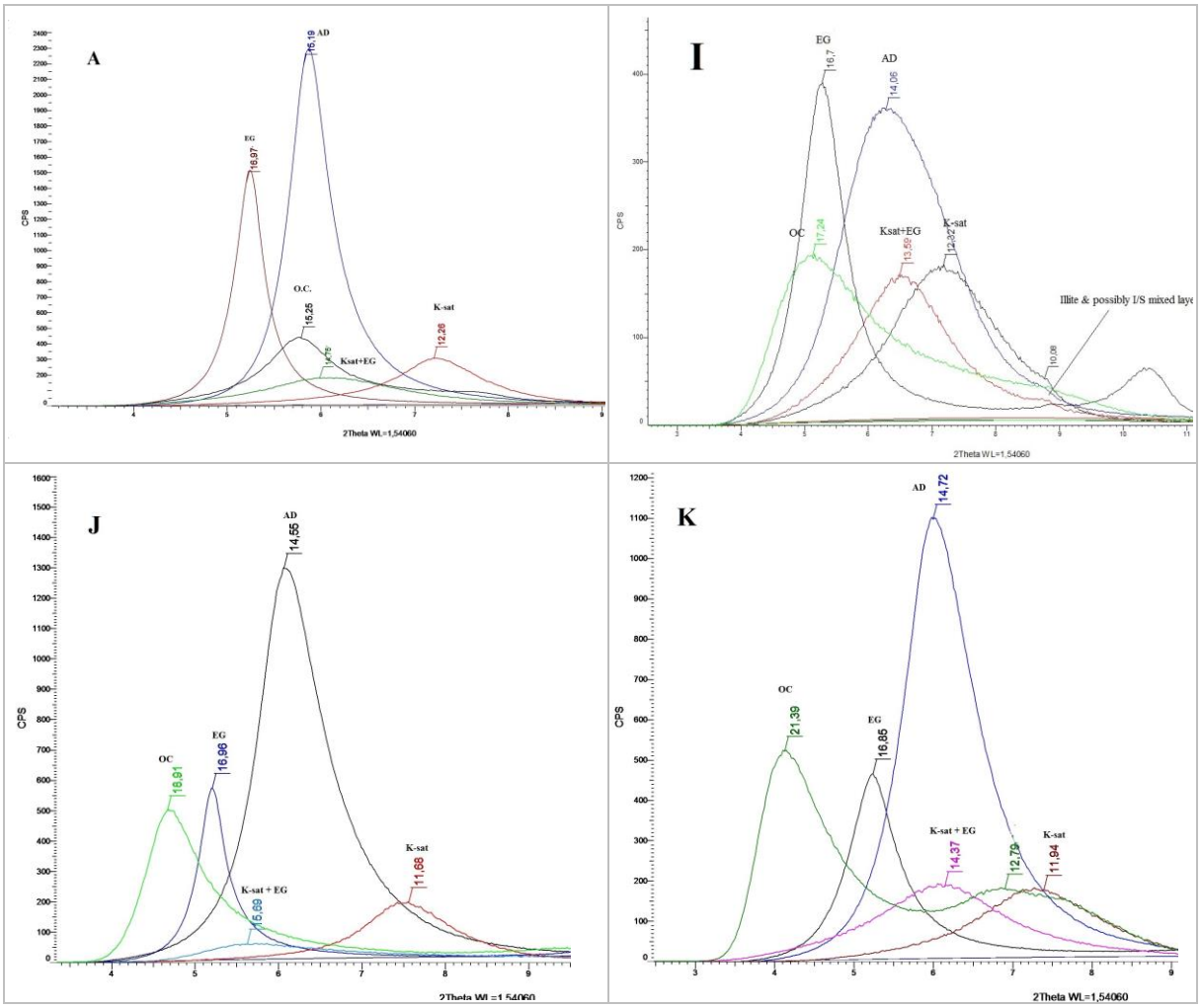

Saple A (top Left), I (top right), J (bottom right) and K (bottom left). Peak labels as presented in Table 6, section 3.4.2

Sample “I” (Figure 24 top right) shows a fixed reflection at 10 Å for all XRD traces, belonging to a member of the mica/illite family, as a trace mineral present only at the <1 μm size fraction, a slight grade of illitization observed.

3.11 Chemical analysis by XRF

Results from XRF chemical analysis on whole rock samples (Table 8) were used to crosscheck by molar sum the semi-quantitative analysis, also to define clay species and to verify chemical composition of mineral phases present in each sample, it provides a chemical filter necessary in order to improve the quality of mineral phases quantitative approach. On the other hand, bulk chemical composition of bentonites can provide valuable information regarding parent rock, geological context, processability issues and applications restrictions/advantages.

Table 8 - Whole rock chemical analysis obtained by XRF (Wt%)

Sample	SiO_2	Al_2O_3	Fe_2O_3	MnO	MgO	CaO	Na_2O	K_2O	TiO_2	P_2O_5	LOI	∑*(Sum)*
A	64.04	16.37	2.55	0.27	4.68	2.27	0.16	0.29	0.13	0.02	9.09	99.85
B	66.07	16.08	5.74	0.05	1.67	0.51	0.68	2.02	0.86	0.05	6.26	99.97
C	66.30	15.88	5.60	0.06	1.61	0.49	0.66	2.11	0.83	0.05	6.02	99.62
D	46.91	20.62	16.95	0.19	2.94	0.51	0.01	0.97	1.72	0.03	10.02	100.86
E	56.69	19.72	9.21	0.11	3.47	0.38	0.08	0.04	0.40	0.05	10.20	100.35
F	59.22	18.52	4.42	0.04	2.89	2.56	2.89	0.35	0.23	0.08	8.36	99.55
G	56.00	21.98	9.55	0.01	2.25	0.06	0.05	0.08	0.52	0.02	9.90	100.41
H	57.76	20.74	5.48	0.02	2.42	1.55	0.29	1.50	0.72	0.03	9.48	100.01
I	62.82	13.94	8.20	0.03	2.53	2.51	0.61	0.22	0.75	0.04	8.16	99.81
J	56.37	21.16	8.09	0.01	3.70	0.13	0.08	0.04	0.39	0.01	10.10	100.08
K	62.25	18.50	3.50	0.02	3.25	1.97	0.26	0.67	0.63	0.03	8.76	99.83
L	62.40	15.70	4.82	0.10	1.82	3.09	2.71	0.63	0.92	0.24	8.74	101.17

3.11.1 XRF chemical analysis of the clay size fraction

The study of chemical composition on the clay size fraction, provides valuable information regarding crystal chemistry of present clay species, in fact the structural formula is traditionally extracted from this data, although there are several considerations to take into account:

1. The presence of various clay species coexisting at that size fraction
2. The presence of oxides and amorphous silica (generally but not always amorphous)
3. Many variables regarding sample preparation explained beforehand in this document
4. The detection limit of the technique, especially for light elements such as Na and K, crucial for the calculations of interlayer dominating cations.

Table 9 shows the chemical composition of the <1μm size fraction for all bentonites.

Table 9 - XRF chemical analysis results on fused beads over the < 1µm size fraction, arranged by geological area from south (top) to North (bottom).

Sample	Wt.(%)											∑+/- *1%*	Area
	SiO_2	Al_2O_3	Fe_2O_3	MnO	MgO	CaO	Na_2O	K_2O	TiO_2	P_2O_5	LOI		
F < 1 µm	56.70	18.50	4.26	0.10	3.08	1.87	0.98	0.10	0.18	0.10	14.50	100.4	1
L < 1 µm	61.5	14.3	5.92	0.10	2.50	1.44	1.59	0.28	0.79	0.12	10.9	99.4	2
A < 1 µm	54.10	16.50	2.45	0.23	4.74	2.31	0.17	0.17	0.10	0.10	18.10	99.0	3
B < 1 µm	50.50	19.90	7.83	0.10	2.45	0.64	0.10	1.28	0.65	0.10	15.80	99.4	3
C < 1 µm	50.30	19.80	8.01	0.10	2.48	0.65	0.10	1.28	0.69	0.10	15.90	99.4	3
E < 1 µm	52.70	19.80	6.36	0.07	3.21	0.37	0.23	0.05	0.15	0.03	17.10	100.1	4
G < 1 µm	50.30	25.90	6.09	0.01	1.96	0.12	0.08	0.06	0.16	0.01	15.80	100.5	4
J < 1 µm	51.00	24.90	4.99	0.01	2.54	0.16	0.15	0.05	0.09	0.00	16.60	100.5	4
H < 1 µm	49.10	22.40	5.46	0.10	3.07	1.11	0.10	0.66	0.76	0.10	16.60	99.5	5
I < 1 µm	51.70	16.90	9.00	0.01	3.08	1.58	1.95	0.27	0.93	0.04	15.20	100.7	5
K < 1 µm	53.00	20.10	3.41	0.01	3.78	1.64	0.31	0.17	0.72	0.03	16.10	99.3	5
D < 1 µm	48.10	21.60	10.90	0.10	2.52	0.48	0.10	0.78	0.47	0.10	15.20	100.4	6

I -The sum is presented as resulted within an error bar +/-1%.
II-No correction for Si values were undertaken, despite the possible presence of amorphous silica and oxides at the clay size fraction.

3.12 XRD vs XRF crosschecking stage

Table 8 shows chemical data from all bulk samples plus a few replicas, outstanding “B” sample that has been chosen for illustrative purposes, subsequently, due to its challenging and diverse mineral composition. Table 10 shows a dynamic Excel table used to simulate chemical sum base on phase ID from the XRD traces, in comparison to bulk XRF analysis and in likewise, complemented by additional stardardless chemical data. It is relevant to outstand that some phase present below the detection limit of XRD techniques may be identified thanks to this multiple technique approach, even more enriched when incorporating SEM/EDX, TGA or FTIR. Therefore, a crosschecking stage is always recommended before and after performing quantitative mineral analysis, by means of integrated information as presented in Table 10.

Table 10 - Crosschecking mineral phase quantitative analysis by molar sum.

Mineralogy								Chemical analysis				
Mineral	**Formule**	**+20µm**	**-20+2µm**	**-2µm**	**Total calc (Wt.%)**	**Bulk (Wt.%)**	**FINAL**	**Oxide**	**Sieve (%)**	**Bulk (%)**	**FINAL**	**XRF (%)**
Mass (%)		*59.8*	*29.1*	*11.1*	*100.0*	*100.0*	*0.7*					
Quartz, low	Alpha-SiO2 (lo	37.5	17.2	9.3	28	40.94		SiO2	53.3	66.07	0.0	49.9
	CaF2	0.4	5.4	3.4	2.2			Al2O3	17.3	16.08	0.0	22.1
Plagioclase	(Na,Ca)Al(Al,S	8.8	1.9	3.8	6.2	11.73		Fe2O3	5.0	5.74	0.0	10.7
					0.0			MnO	0.0	0.05	0.0	0.31
Hematite	Alpha-Fe2O3	1.9	3.5	3.2	2.5	2.60		MgO	3.5	1.67	0.0	0.76
					0.0			CaO	3.1	0.51	0.2	2.58
Anatase	TiO2	2.6	1.9	9.9	3.2			Na2O	0.7	0.68	0.0	0.44
Calcite	CaCO3 (trigon	0.4	0.4	4.7	0.9			K2O	2.2	2.02	0.0	3.52
Dolomite	CaMg(CO3)2	3.0	4.1	1.6	3.2			TiO2	3.2	0.86	0.0	1.50
					0.0			P2O5	0.0	0.05	0.1	0.75
Topaz	Al2Si4(F,OH)2	17.8	10.4	4.4	14							
					0.0			PF	5.8	6.26	0.0	
Sn metalic	Sn				0.0		**0.39**					5.67
Apatite					0.0		**0.32**	LOI TGA				
Grafite					0.0			Mid		100.0		
					0.0							
Kaolinite	Al2Si2O5(OH)	0.0	23.9	39.3	11	6.90		Standardless				0.39
Di- Smectite	K(Mg,Fe)3(Al,I	17.2	27.0	20.4	20			correction				
					0.0							
		10.3	4.5	0.0	7.5							
					0.0							
					0.0							
Smectite (montm)					0.0							
					0.0							
					0.0							
SUM		**99.9**	**100.2**	**100.0**	**100.0**	**62.2**	**0.7**		**94.1**	**92.9**	**0.3**	**98.6**

Note: sample B is presented as example only. It is a free format that shall be built according to the characterization information available. In this case, we are using FTIR, TGA, Loi, XRF (10 major elements and Stardardless on bulk samples), only to illustrate.

3.13 Layer charge determination

One of the methods used to stablish is the evaluation of swelling after K-saturation by zooming in the low angle region of the OS XRD trace. In this procedure, is possible to observe the swelling behavior by comparison of the OS d(001) peak at 14.067 Å, and the same peak located at 16.739 Å after ethylene glycol solvation. Layer charge is evaluated from XRD patterns after potassium saturation and ethylene glycol solvation on subsequent comparison with XRD simulated traces calculated from three-component interlayering (CHRISTIDIS; EBERL, 2003).

The profile fitting (Figure 25) is done with a excel sheet that was an output of this investigation and offers at the same time two different ways to compare the measured XRD values to the data base of the layer charge program. (1)-whole

profile fitting (2) - peak position fitting. Yet, issues related to the structural formula method based on the clay size fraction XRF chemical analysis; do not allow having conclusive results at this point. It will be explained later on when presenting <1µm XRF chemical data.

Figure 25 - Layer charge determination by whole pattern method for "A" sample.

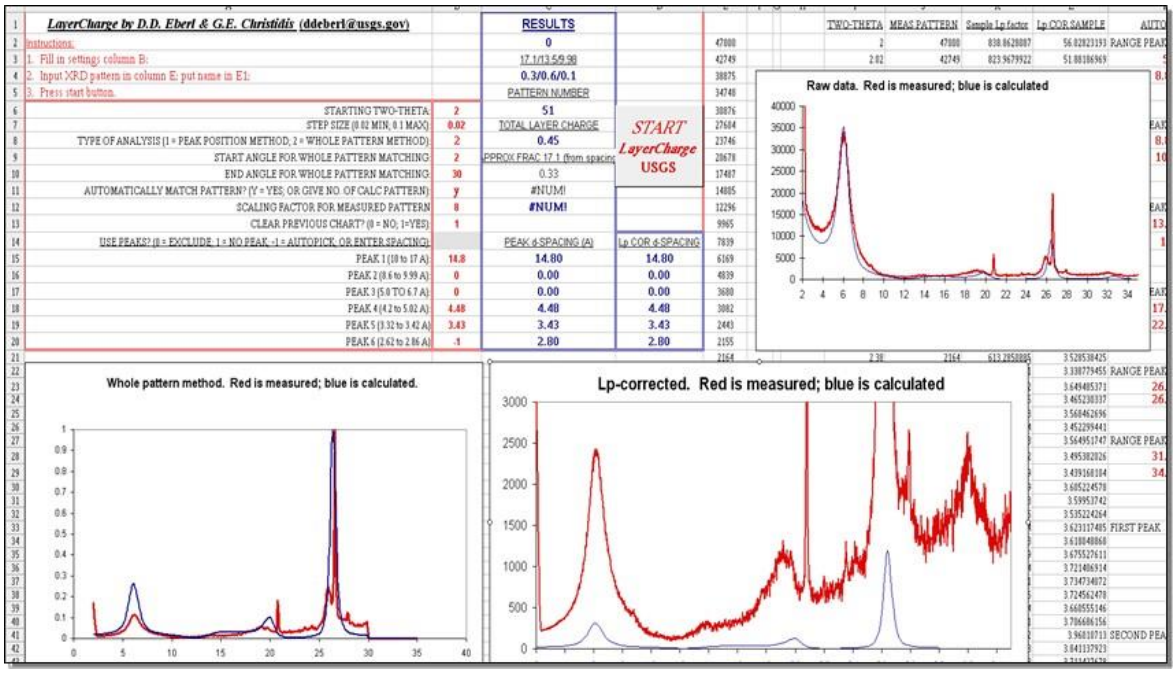

The influence of layer charge over the sorption characteristics of organoclays has been widely described on many related investigations, for the purpose of this research we use the bases proposed by Mermut et al., (1994) regarding "layer charge characteristics of 2:1 silicate clay minerals". Next figure shows a set of two samples in a multi XRD patterns graph, in which is possible to observe a differential organo-interaction when all clay matrix, with no previous activation or d-spacing expansion treatment was performed, interacting under the same experimental conditions as an expression of the relationship between diagenetic features and organophillization.

Using the <1µm and under the same concentrations for all organophillic solutions based on a long (16-C) carbon chain ammonium salt.

Layer charge magnitudes were estimated also, using the formula proposed by Christidis; Eberl, (2003) (Equation 2); as presented in Table 11.

Equation 2

Layer charge *(Y):* 16.118 x (*X)* + 23,033 e^-/half unit cell

Where:

X: positions d 001 in Å

Table 11 - Layer charge magnitudes calculated according to Christidis; Eberl, (2003)

	(001) d-spacing peak position (Å)						Layer charge
Sample	Bulk	Ad	EG	K-sat	Ksat+EG	O.C.	e^-/half unit cell
1-F	11.89	14.088	17.42	11.003	17.98	17.59	0.314
2-L	12.58	12.564	17.967	11.662	13.659	16.328	0.582
3-A	15.235	15.19	16.971	12.26	18.75187	14.556	0.563
3-B	15.01	14.624	16.586	12.177	15.74	15.359	0.452
3-C	15.18	14.159	16.833	12.245	14.759	15.321	0.513
4-E	14.05	14.595	16.934	11.621	17.39	18.0588	0.350
4-G	14.92	15.233	19.93	11.635	16.057	18.04	0.433
4-J	14.5	14.559	16.962	11.691	15.692	18.9	0.455
5-H	15.06	13.665	16.462	11.818	13.776	17.04	0.574
5-I	14.868	14.04	16.739	12.321	13.599	17.247	0.585
5-K	14.879	14.72	16.855	11.947	14.37	21.393	0.537
6-D	14.843	14.57	16.85	12.21	14.79	16.46	0.511

3.14 The structural formula determination

Based on the chemical data over the clay size fraction we estimate the structural formula for all samples, with slight corrections when Si and Fe exceed the theoretical composition on stoichiometric setup and under the assumption that the number of oxygen anions involved in a unit cell must be determined on a dehydrated basis. Table 12 presents proposed structural formulas for all samples, arranged by geological area and chemical distribution as a function of structural sites.

Table 12 - Structural formula calculation

		Tetahedral			Octahedral					Interlayer		
Area	Sample	(Si	Al)	$O_2$10	(Al	Ti	Fe	Mg)	$(OH)_2$	(Na	K	Ca)
1	F < 1 µm	3.34	0.74	10	1.2	0	0.2	0.3	2	0.33	0.03	0.62
2	L < 1 µm	3.62	0.57	10	1	0.1	0.3	0.3	2	1.59	0.28	0.96
3	A < 1 µm	3.18	0.66	10	1.1	0	0.1	0.5	2	0.17	0.17	1.16
3	B < 1 µm	2.97	0.80	10	1.3	0.1	0.4	0.2	2	0.10	1.28	0.64
3	C < 1 µm	2.96	0.79	10	1.3	0.1	0.4	0.2	2	0.10	1.28	0.65
4	E < 1 µm	3.10	0.79	10	1.3	0	0.3	0.3	2	0.23	0.05	0.37
4	G < 1 µm	2.96	1.04	10	1.7	0	0.3	0.2	2	0.08	0.06	0.12
4	J < 1 µm	3.00	1.00	10	1.7	0	0.2	0.3	2	0.15	0.05	0.16
5	H < 1 µm	2.89	0.90	10	1.5	0.1	0.3	0.3	2	0.10	0.66	1.11
5	I < 1 µm	3.04	0.68	10	1.1	0.1	0.5	0.3	2	1.95	0.27	1.58
5	K < 1 µm	3.12	0.80	10	1.3	0.1	0.2	0.4	2	0.31	0.17	1.09
6	D < 1 µm	2.83	0.86	10	1.4	0	0.5	0.3	2	0.10	0.78	0.48

3.15 Trace and rare earth elements by ICP.

Trace elements acquired by ICP-OES for all 33 samples are presented in Table 13 and Table 14, the last one presenting rare earth elements concentrations.

Eventually all data has been treated according to the elemental mobility according to the methodology proposed by Floyd (1977) in order to correlate non-mobile elemental ratios to parent rock type (discussed in section 5.2.1).

Table 13 - Trace elements by ICP-OES for all samples

		Trace elements (ppm)											
Area	Sample	Ba	Co	Cr	Cu	Ga	Nb 3	Ni	Sr	Th	V	Zn 2	Zr
3	A	1970	5	6	6	31	5	5	272	19	25	119	202
3	B	1,023	17	42	24	25	5	16	135	7	73	105	120
6	D	327	57	55	316	35	5	108	31	5	265	199	138
4	E	2,766	67	711	109	19	5	812	37	5	134	188	5
1	F	903	9	9	12	24	5	11	379	5	15	54	84
4	G	232	12	655	87	22	5	124	9	5	107	44	6
5	H	484	15	43	14	26	5	19	100	7	79	67	41
5	I	636	23	127	54	26	5	67	80	10	169	91	31
4	J	457	19	753	87	18	5	190	23	5	93	67	5
5	K	329	16	46	26	24	5	36	111	12	63	66	13
2	L	643	17	6	13	20	5	5	252	6	67	79	201
2	M	659	9	12	5	28	5	9	171	17	16	94	166
2	N	823	9	14	10	25	5	7	191	9	24	84	144
2	O	626	7	8	6	23	5	6	222	11	26	62	203
1	P	891	12	5	9	24	5	10	278	8	13	58	90
1	Q	776	24	6	10	21	5	12	819	5	15	65	69
2	R	134	16	5	50	26	5	16	229	28	67	99	86
2	T	739	6	16	5	21	5	9	511	14	20	62	216
1	W	704	10	5	9	24	5	10	316	2	12	54	77
4	Y	1,178	194	746	135	20	5	668	39	5	108	171	5
7	AA	244	5	5	5	29	10	5	264	40	6	105	141
7	AB	86	5	6	5	35	5	5	170	24	5	96	128
1	AC	803	10	14	14	24	5	13	272	5	21	48	136
7	AE-A	45	11	11	12	22	5	14	191	16	11	111	146
7	AE-B	116	5	5	9	24	5	6	210	9	5	67	160
2	AF	224	20	31	15	30	5	20	116	14	63	108	266
2	AH	395	19	6	5	22	5	5	268	13	13	56	182
2	AJ	229	19	8	9	18	5	5	138	12	95	48	94
2	AL	160	23	31	16	26	5	20	73	5	65	88	270
7	AM	195	5	9	8	23	5	17	198	22	10	77	131
4	AO	335	26	136	40	27	5	62	88	12	109	97	36
5	AP	1,938	144	631	118	21	5	515	104	5	96	139	5

Sample C, have been removed from the list for it is equal to B

Table 14 - All samples rare earths elements, concentration by ICP-OES

		REEs (ppm)										
Area	**Sample**	**Ce**	**Dy**	**Er**	**Eu**	**La**	**Lu**	**Nd**	**Sc**	**Sm**	**Y**	**Yb**
3	A	97	14	8	5	44	5	54	8	16	69	9
3	B	100	6	5	5	54	5	49	12	11	38	5
6	D	36	5	5	5	12	5	24	48	6	25	5
4	E	151	6	5	5	95	5	91	32	20	40	5
1	F	34	5	5	5	16	5	19	6	5	15	5
4	G	23	5	5	5	20	5	23	39	5	17	5
5	H	112	5	5	5	36	5	29	11	7	12	5
5	I	79	5	5	5	35	5	30	14	7	14	5
4	J	51	5	5	5	31	5	28	44	6	25	5
5	K	22	5	5	5	20	5	12	12	3	5	5
2	L	53	5	5	5	25	5	28	13	8	26	5
2	M	101	5	5	5	46	5	45	8	10	27	5
2	N	63	5	5	5	27	5	28	8	6	22	5
2	O	76	5	5	5	36	5	35	6	8	28	5
1	P	31	5	5	5	16	5	17	5	6	13	5
1	Q	24	5	5	5	12	5	12	5	5	12	5
2	R	70	5	5	5	33	5	28	5	6	14	5
2	T	85	5	5	5	39	5	37	6	9	33	5
1	W	32	5	5	5	16	5	16	5	5	13	5
4	Y	199	15	9	5	99	5	93	34	20	85	5
7	AA	112	8	5	5	53	5	52	6	13	41	5
7	AB	66	5	5	5	33	5	33	6	9	18	5
1	AC	46	5	5	5	20	5	23	9	6	19	5
7	AE-A	78	5	3	5	35	5	31	10	9	25	5
7	AE-B	72	5	5	5	26	5	27	10	9	27	5
2	AF	109	9	5	5	57	5	55	12	14	48	5
2	AH	89	6	5	5	43	5	39	6	9	31	5
2	AJ	55	5	5	5	27	5	22	5	6	14	5
2	AL	65	5	5	5	33	5	40	14	9	32	5
7	AM	74	5	5	5	32	5	31	9	9	21	5
4	AO	95	5	5	5	49	5	45	15	9	23	5
5	AP	250	7	5	5	108	5	85	34	18	29	5

Sample C, have been removed from the list for it is equal to B

3.16 Organophillization

The basal spacing for each type of intercalation can be describe as step wise, and for mono-bilayer interactions with samples having layer charge heterogeneity can occur over a range of alkylammonium carbon chain range rather than in a single discrete step size; moreover, It has been reported that hydrophobicity increases with the degree of coverage and the alkyl ammonium

chain length (LAGALY, 1984). Figure 26, illustrates this stepwise sorption behavior, observed in 10 samples, samples “A” and “B”, were withdrawn from the set from further considerations, due to the presence of I/S mixed layers, illite and kaolinite at clay size and other reasons explained before in this same section, in order to avoid comparative distortions.

Figure 26 - Relative organo-sorption behaviour as a function of relative layer charge for 10/12 samples.

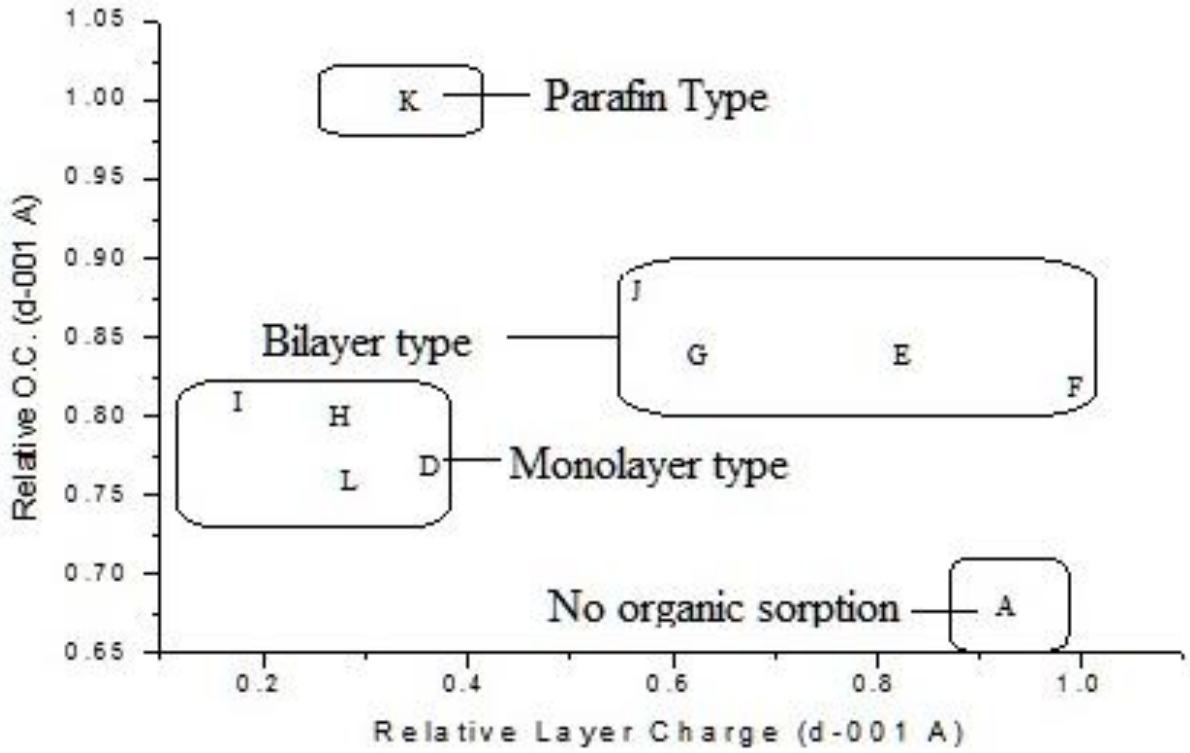

3.17 Organic pollutant sequestration

For tailoring organoclays in order to maximize 17-Beta estradiol removal, 27 experiments have been executed, from those results, six representative high performance liquid chromatography are presented in Figure 27, experimental summary as follows:

A. Top left = blank sample with full 17-Beta estradiol concentration

B. Top right = organophillic X sample organophillic (commercial product) best removal performance for 17-Beta estradiol.

C. Middle left = organophillic Z sample (coming from geological area 2), almost as good as sample X.

D. Middle right = organophillic sample AB

E. Bottom right = WOC2 (special functionalized W sample with a natural organic polymer (chitosan variation)

F. Bottom left = Organophillic Y sample (Low polarity)

Figure 27 - 17-B Estradiol removal evaluated on HPLC

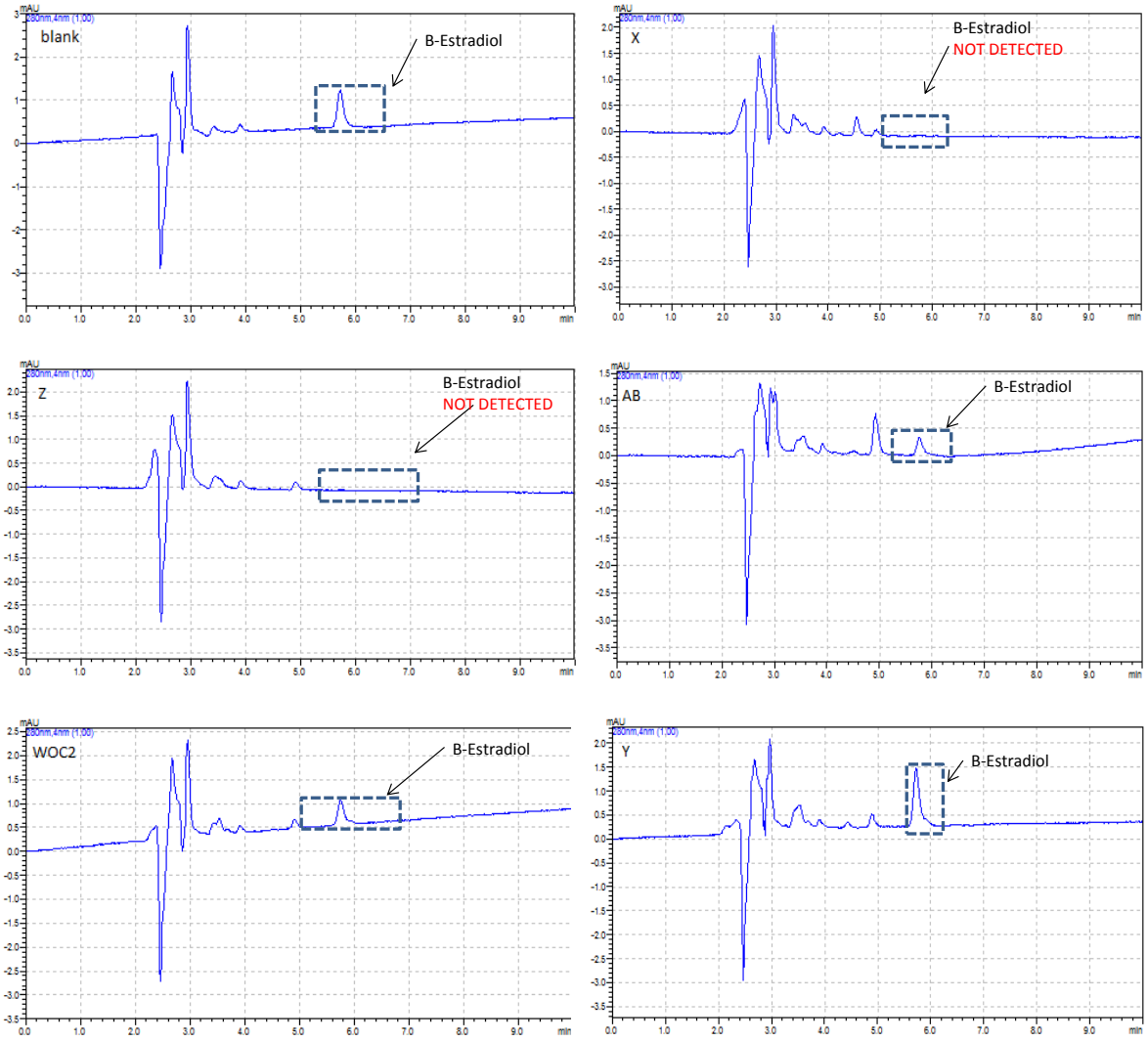

Results indicate that the clay dosage is the most important variable, since higher hormone removals are always obtained with higher clay dosages, independently on the pH value and mixing period. However, for the same clay dosage, a little adsorption enhancement is observed under slightly alkaline medium.

Notwithstanding, one day as mixing time seems to be enough to obtain 99% removal, as long as clay dosages higher than 1.25 gL-1 are applied. Better to work with pH 8. Bentonite "X" stills performing better than any other else tested until now. Comparative results are presented as follows in Table 15.

Table 15 - 17-B Estradiol removal efficiency for 5 different organoclay configurations

batch name	Area (280 nm) - after 3 days	B estradiol% Removal
X	0	100%
Z	0	100%
AB	2895	59%
Y	10798	0%
WOC2	4449	38%
BLANK	7130	0%

Selective sequestration of 17-Beta estradiol by means of a tailor-made organoclay, presented only in relevant, summarized result.

The following table (Table 16), presents a whole summary of the first twelve experimental rounds that corresponds to the none selective stage of 17-B Estradiol removal efficiency by means of organoclay interactions in aqueous media; outstanding the correspondence of the clay matrices used to prepare organoclays with respect to their geological area. In order to grant representative results for such a large set, most abundant samples were used to optimize experimental conditions, until stablishing a best setup as follows:

- 1-ppm 17-B Estradiol solution under free pH at 5.5.
- Sample “W” coming from Area 1, was used as a base setup Na-Bentonite.
- Optimum time 24 hrs. at low agitation and room temperature.
- Clay dosage was set at 1 gr/Lt, although results showed a clear tendency to increase recovery coefficient in growing clay wt%, even at 3 gr/Lt tried during the experiments.
- Samples were purified up to <2 µm size fraction, in order to avoid mineralogical composition interference.

Table 16 Experimental summary, for the none selective stage of 17-B Estradiol removal efficiency by means of organoclay interactions in aqueous media.

Exp. Round	Preparation-Code	exp-no	Time(Hr)	pH	Clay Dosage	**Removal**	Remarks	Area
EXP 2	XBE1	1	72	free	1	**100.00%**	1st experiment was carried out using comercial birth control pills, it didnt work out due to organic interfearence when meassuring hormone concentration on HPLC	7
	ZBE1	2	72	free	1	**100.00%**		4
	ABBE1	3	72	free	1	**59.40%**		7
	YBE1	4	72	free	1	**0.00%**		4
	WOC2BE1	5	72	free	1	**37.60%**		1
	BLANK							
EXP 3	XBE2	7	24	4.5	0.875	**97.40%**		7
	XBE3	9	24	4.331986143	1.625	**98.49%**		7
	XBE4	11	24	6.8	1.25	**98.59%**		7
	WOC2S2BE1	13	24	4.5	1	**98.68%**	NOT CONSISTENT IN EXP10	1
	VBE1	14	24	4.5	1	**97.68%**		2
	WOC3S1BE1	15	24	4.5	1	**66.42%**		1
	BLANK 1*	LANK EXP 3						
EXP 4	XBE5	4	62	5.5	1.63	**98.60%**		7
	XBE6	12	62	6.5	1.63	**98.61%**		7
	XBE7	13	62	4	1.25	**98.37%**		7
	WOK3BE2	16	62	5.5	1.00	**68.94%**		1
	ANBE1	17	62	5.5	1.00	**0.00%**	lost	1
	BLANK *	LANK EXP 4						
EXP 5	XBE8	1	48	5	1.25	**98.41%**		7
	XBE9	1 rep1	48	5	1.25	**98.21%**		7
	XBE10	1 rep2	48	5	1.25	**98.01%**		7
	XBE11	2	48	5.5	2.00	**98.60%**		7
	XBE12	5	48	4.5	0.50	**95.92%**	low clay dosage=low performance	7
	BLANK 3	LANK EXP 5						
EXP 6	XBE13	3	48	9	1.63	**98.74%**		7
	XBE9	6	48	2	0.88	**96.48%**		7
	XBE10	8	48	2	1.63	**98.18%**		7
	XBE11	10	48	9	0.88	**98.34%**		7
	BLANK 3	blank-exp 6						
EXP 7	XBE14	18	24	5.5	1.25	**97.73%**	ph 5.5 considered free	7
	WOC4BE1	19	24	5.5	1.25	**91.44%**		1
	WOC5BE1	20	24	5.5	1.25	**46.90%**		1
	WOC52A-BE2	21	24	5.5	1.25	**34.09%**		1
	WOC55A-BE3	22	24	5.5	1.25	**39.60%**		1
	7th Blank	blank 7						
EXP 8	XBE15	23	24	5.5	1.25	**97.80%**		7
	AROCBE1	24	24	5.5	1.25	**24.09%**		5
	ANOCBE1	25	24	5.5	1.25	**0.00%**	lost	1
	WOC52B-BE4	26	24	5.5	1.25	**46.44%**		1
	WOC54B-BE5	27	24	5.5	1.25	**45.17%**		1
	8th Blank	blank 7						
EXP 9	XBE16	28	24	5.5	1.25	**98.06%**		7
	WOC55ABE6	29	24	5.5	1.25	**24.75%**		1
	ANOCBE2	30	24	5.5	1.25	**97.87%**		1
	WOC7BE1	31	24	5.5	1.25	**83.79%**		1
	ZMK2BE1	32	24	5.5	1.25	**5.95%**	Synthetic zeolite	none
	9th Blank	blank 7						
EXP 10	XBE17	33	24	5.5	1.25	**97.76%**		
	WOC2BE2	34	24	5.5	1.25	**53.30%**		1
	WOC4BE2	35	24	5.5	1.25	**86.91%**		1
	WOC6BE1	36	24	5.5	1.25	**74.59%**		1
	WOC8BE1	37	24	5.5	1.25	**89.85%**	WORTHY TO TRY WOC 9 & 10	1
	9th Blank	LANK EXP 8						
EXP 11	XBE17	Extra 1	24	Free	1.25	**99.23%**		7
	WOC9BE1	Extra 2	24	Free	1.25	**88.06%**		1
	WOC10BE1	Extra 3	24	Free	1.25	**99.23%**		1
	ANOCBE3	Extra 4	24	Free	1.25	**99.23%**		1
	VOCBE2	Extra 5	24	Free	1.25	**99.23%**		4
	ZOCBE2	Extra 6	24	Free	1.25	**99.23%**		2
	10th Blank	0.209272						

Free pH= 5.5

4 DISCUSSION

4.1 Regarding mineral characterization

In terms of particle size distribution, it appears to be that the major influential factor is mineralogical composition as presented in section 4.3, in the sense that greater smectite content can be correlated to smaller mean size values, with the exceptions of samples A and E, containing roughly 80% smectites although they were also rich in relatively larger size mineral phases such as quartz, K-feldspar and kaolinite.

Figure 28 outlines the relevance of Fe_2O_3 and SiO_2 content, for it stablishes geochemical affinity with respect to parent rock, and therefore crystal chemistry characteristics of smectite species. According to Christidis; Huff (2009), smectites derived from basic rocks may have roughly three times the iron content forming than those of intermediate to basic volcanic source, and they tend to alter into Fe-montmorillonites and Fe-beidellites. Silica levels in a lesser extent may also indicate the acid to basic parent rock, tending towards intermediate to acidic in higher SiO_2 contents, and lower contends derived from basic composition extrusive rocks. Although, these trends shall be verified over data collected on the clay size fraction, therefore, Figure 28 also plots yield values for all samples over the < 1 μm size fraction (see Table 9 for full chemical composition), further considerations regarding crystal chemistry are discussed in section 5.1.2.

Figure 28 - Fe_2O_3 & SiO_2 (Wt.% by XRF) from whole rock and <1 µm size fraction chemical analysis for all samples, arranged by geological area from South to North.

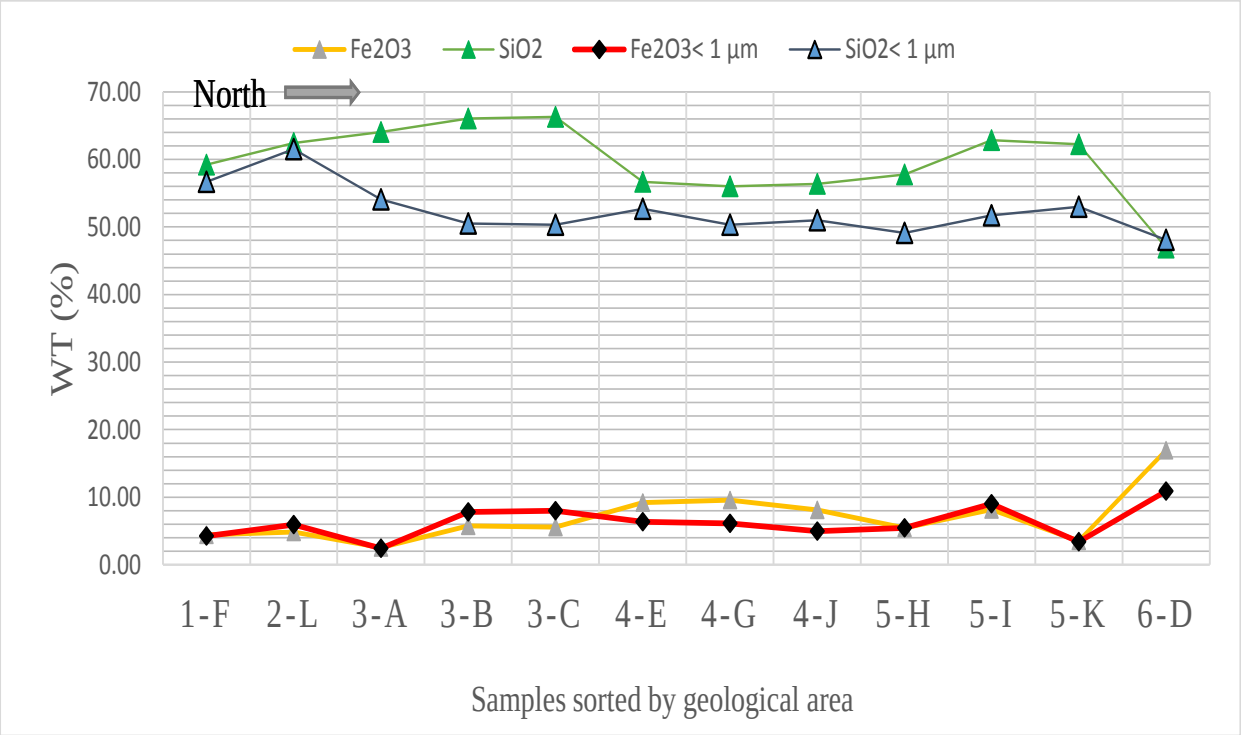

Sample label is preceded by the geological area number, eg: 1-F.

Samples coming from areas 4 and 6 consistently showed higher Fe_2O_3 values (Figure 28) and relatively lower SiO_2, and they seem to be agreement with their basaltic precursors (Table 4). Sample "L" belongs to geological area 2 (parent rock: andesite) showed similar results, particularly in the in the < 1 µm size fraction, possibly due to the interference from hematite (for Fe_2O_3) and quartz, opal-CT and cristobalite (for SiO_2). Slight spread values on samples coming from area 5 was observed, particularly sample K showed a more acidic profile than samples "I" and "H" (see Figure 37) although geochemical variability seems to be a constant in the Paraiba area (SOUZA; SANTOS, 1992; AMORIM et al., 2006), possibly associated to a variations on parent rock composition or alteration environments shifting to lacustrine to deltaic or transitional with higher Na^+ content in interlayer position, that could also explain the Na^+ fluctuations in the < 1 µm chemical data, presumably occupying interlayer position as electrically compensating cations.

Samples "1-F" and "3-A" are both reported as diagenetic from rhyodacidic source, coherently, highest SiO_2 values and lowest Fe_2O_3 were observed, the former sample also presented the highest Mg content in both bulk and clay size

fraction (bulk wt(%):4,68%, < 1 µm Wt%: 4,74%), and provides a good bulk parameter for a bentonite consisting in the montmorillonite end member of the beidellite to montmorillonite series as proposed by Meunier (2005), although samples “A” and “B”, belonging to the same geological area, did not show similar chemical composition, likewise mineralogical composition and structural features, further considerations regarding this apparent inconsistency are discussed in next section when stablishing grade.

4.1.1 Bentonite grade

Figure 21 - Reitveld refinement fit for B sample on Topas V5.1

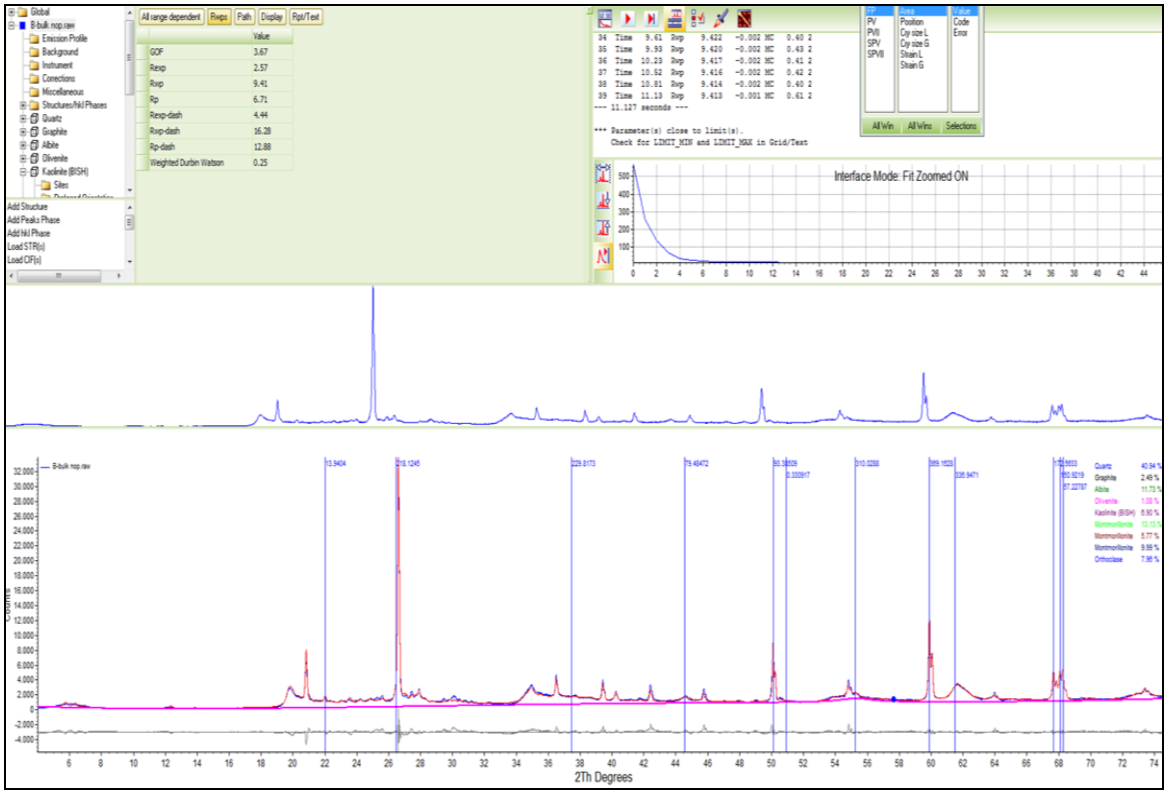

Table 7, presents a summary of all mineral assemblies within all bulk samples after crosschecking Rietveld refinement against XRF chemical data and even phase discrimination by means of SEM coupled with EDS. As stated before, with the information available at this stage, is possible to establish grade and a few observations regarding mineral processing and applications.

1. Other clay minerals present in a specific deposit, may be impossible or too expensive to separate by means of available dry mineral processing

methods; such is the case for samples “D”, “E”, “G”,”H” and “J”, containing more than 10% of kaolinite, pyrophyllite or illite.

2. Samples containing more than 3% of hematite (samples “L” and “D”) could affect color and textural properties for specific advanced clay applications,
3. The presence of cristobalite, when morphologically appears as “flakes”, often interacts in the less than 2µm size fraction affecting negatively rheological properties of bentonites (CHRISTIDIS, 1998), as it is the case of sample “L”. basin after considerable transport and deposition .
5. Based on mineralogical and geochemical information of samples “B” and “C”, they appear to be out of bentonite range by definition, mainly due to the low smectite content, more than 40% quartz and considerable amounts of kaolinite, olivine and other accessory phases. Moreover, the illitization observed having K-feldspar as potassium source in the process (ALTANER, 1986), may be a sign that this smectite containing rocks, are the consequence of transported and deposited particles in an sedimentary environment. Although, the illite and mixed layer contents for samples “B” and “C”, are way below the detection limit, on the ROP bulk XRD traces; they were only evident in the OS slides XRD´s and therefore, they are not considered in the quantification summary chart (Figure 21 and Table 7), but they may be observed in Figure 29, were a especial treatment was carried out, comparing the <10µm and <1µm , both air dried, against the >1µm OS-EG treated to evaluate both the mineralogical composition of clay minerals as a function of particle size but also expandability behavior of those mineral phases, the reflection peak located near 10.1 Å typically belonging to the illite-mica species, shows a non-expandable population after EG, as well as the smectitic component shifting towards 16.003 Å (d(001) located in 14.2 Å in AD), a what appears to be a shoulder composed of mixed layers.

Figure 29 - Natural, air dried and EG OS XRD traces for sample "C".

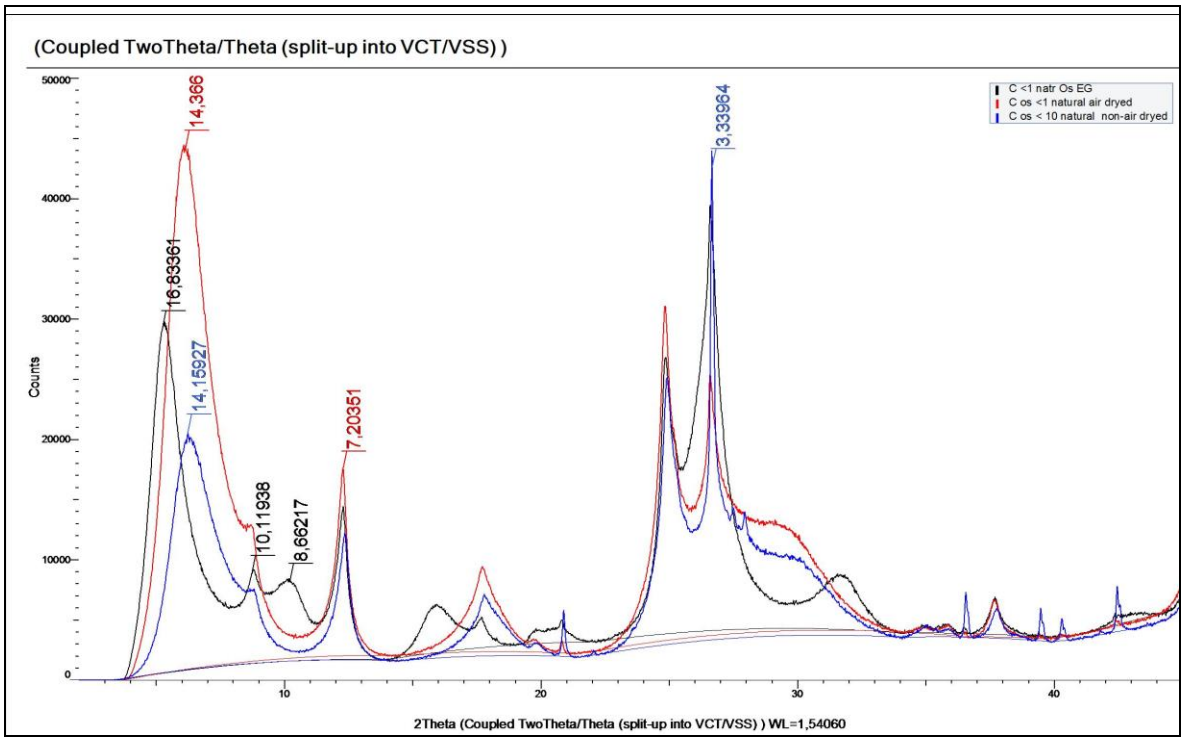

4.1.2 Bentonite quality

A swelling behavior comparison parameter may be established by comparison of the air dried (AD) d (001) at 14.067 Å, and the same peak located at 16.739 Å after ethylene glycol solvation (EG) according to Equation 3.

Equation 3

Swelling comparative value (SW): EG d001 in Å (EG) - EG d001 in Å (AD)

Layer charge is evaluated from XRD OS patterns after K-saturation and subsequent EG treatment, as proposed by Christidis; Eberl, (2003) with the only goal to achieve a comparative value among treated samples, hence a relative Layer charge value may be estimated from Equation 4,

Equation 4

Layer charge comparative value (SW): EG d001 in Å (EG) - EG d001 in Å (AD)

A broad variety organophilic XRD patterns indicates diversity of organic sorption capabilities among samples, measured in terms of their 001 (CTAC)-

montmorillonite d(001) basal reflection position, ranging from 15.2 Å (sample “A”) to 21.68 Å (sample “K”). As a function of sorbed organo-compound according size of the 19 carbon chain ammonium salt used, and the known sorption isotherm (JAYNES; BOYD, 1991), almost all sorption where observed, from the lateral monolayer type (from 0 to 1.75 nm), to the paraffin-type monolayer (from 3.5 to 5.25 nm).

Figure 30, is a graphical representation of this observed effect, based upon experimental observations and extracted from (YARIV; CROSS, 2002) after G. Machado.

Figure 30 - Arrangement of alkyl ammonium ions in mica-type silicates with different layer charges. A) Lateral monolayer, B) Lateral bilayer, C) Paraffin-type monolayer and D) Paraffin type bilayer.

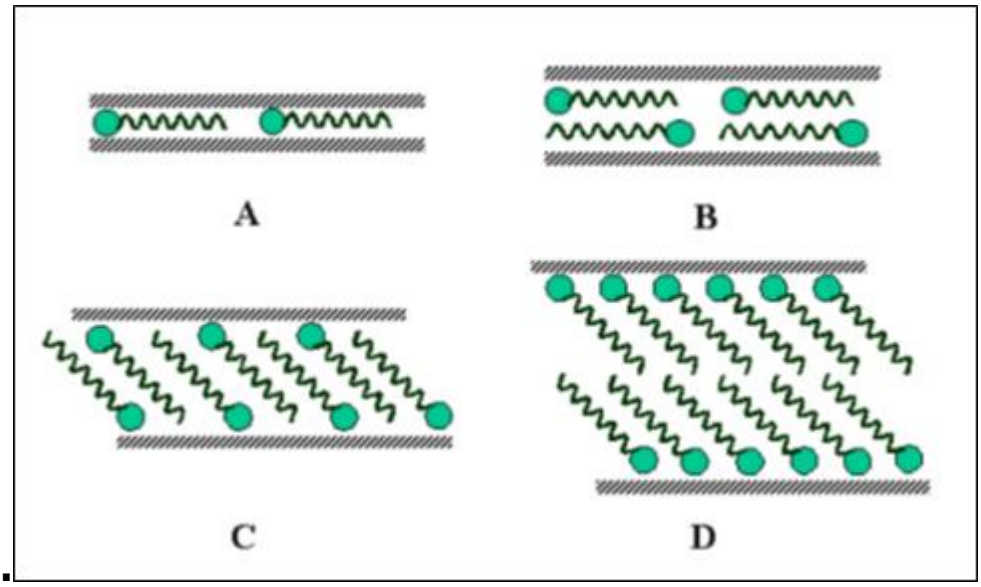

The basal spacing for each type of intercalation can be describe as step wise, and for mono-bilayer interactions with samples having layer charge heterogeneity can occur over a range of alkylammonium carbon chain range rather than in a single discrete step size to the previous figure shows, It has been reported that hydrophobicity increases with the degree of coverage and the alkyl ammonium chain length (LAGALY; 1987).

XRF chemical analysis on the <1µm size fraction is a key technique to gather conclusions regarding crystal chemistry of smectites from the unit formula (SCHULTZ, 1969; EBERL et al., 1986; NEWMAN; BROWN 1987; ONAL, 2006), without them handily in within an acceptable error bar ranging ±1% with respect to 100%, any attempt to validate a research work base upon smectite quality would be heavily argued for lacking information regarding charge location and nature. Nevertheless, and for practical objectives of this research, the conclusions

obtained thus far are more than enough to have a complete perspective regarding to industrial applications.

4.1.3 Observed trends in terms of grade & quality.

The summary chart for mineral phase quantification (Figure 21 and Table 7), within all bulk samples after crosschecking Rietveld refinement against XRF chemical data. As stated before, this information offers a set of fundamental parameters to filter candidates to be taking into consideration for the pilot scale processing, filtering criteria is explained as follows, in terms of samples regardless of geological areas (this point is developed in conclusions):

1. Other clay minerals present in a specific deposit, may be impossible or too expensive to separate by means of available mineral processing methods. Therefore, samples containing more than 10% of kaolinite, pyrophyllite or illite are disregarded for further use; it is the case for samples “D”, “E”, “G”, “H” and “J”.
2. Samples containing more than 3% of hematite could affect color and textural properties in applications related to specific PCN, eventually that is an issue that could be emphasize in the case of sample “L” but levels in sample “D” are way over the limit.
3. The presence of cristobalite, when morphologically appears as “flakes”, often interacts in the less than 2μm size fraction affecting negatively rheological properties of bentonites. Eventually, and only at sight of remarkable properties attached to sample “L”, SEM evaluation at a morphological scale could be considered.
4. Low grade of di-octahedral smectite also translates in unbearable processing costs, consequently samples “B” and “C” will not be considered furthermore, and “G” and “H” will be left in a secondary plane for further evaluation if required.
5. The presence of mixed layering if often far from quantification but will have implications on the OS evaluation. Already samples “B” and “C” have shown signs of illitization, giving another reason to be discarded.

As a consequence, and from the perspective of whole rock analysis base on grade, only samples “A”, “I”, and “K” stand foot as high-quality material thus far, although samples “I” and “K”, contain only 55% and 54% smectite content respectively, they are considered high quality materials for having only smectites in the clay size fraction and no penalty mineral phase. In addition, samples “F” and “L” can still be considered with a question mark over them. (Å)

Summarized data from XRD traces is presented in Table 17 based on structural data extracted from all XRD patters and summarized in Table 17, and in order to reach further observations related to the clay matrix quality apply Equation 3 and Equation 4.

Table 17 - Key data derived from all XRD patterns

	(001)d-spacing Peak position (Å)						
Sample	Bulk	Ad	EG	K-sat	Ksat+EG	O.C.	060 pos
A	15.24	15.19	16.97	12.26	14.75	15.26	Di
B	15.01	14.62	16.59	12.18	15.74	15.36	Di
C	15.18	14.16	16.83	12.25	14.76	15.32	Di
D	14.84	14.57	16.85	12.21	14.79	16.46	Di
E	14.05	14.60	16.93	11.62	17.39	18.06	Di
F	11.89	14.09	17.42	11.00	17.98	17.59	Di
G	14.92	15.23	19.93	11.64	16.06	18.04	Di
H	15.06	13.67	16.46	11.82	13.78	17.04	Di
I	14.87	14.04	16.74	12.32	13.60	17.25	Di
J	14.50	14.56	16.96	11.69	15.69	18.90	Di
K	14.88	14.72	16.86	11.95	14.37	21.39	Di
L	12.58	12.56	17.97	11.66	13.66	16.33	Di

To stablish a correlation of all data presented in Table 17, some premises are stablished as selective criteria:

1. Swelling behavior is measured in terms of expansion after EG treatment, has to be in agreement within certain thresholds (10% +/-) with respect to theoretical AD 001 peak position, extracted from (MOORE; REYNOLDS, 1997). In this document calculated as presented in Equation 3.
2. Layer charge, is not only more accurate measurement for bentonite grade, but also a fingerprint for bentonite occurrences from a geological perspective. For the purpose of this work, the methodological approach has

simplified its calculations and the relative (12 sample framework) magnitude of each sample, will be estimated from Equation 4.

3. As for organophillization comparative index, or organic sorption relative behavior (in the context of the 12 samples framework) there is simple ratio to measure for what we are trying access here is how this clay matrices tend to incorporate organo compounds without previous Na-treatment.

4. But we can define the nature of organo interactions in terms of what is described in Figure 30, giving birth to another evaluation parameter resulting from the natural d(001) oriented slide peak against the organoclay d(001) peak position. In other words, OC-AD will not drop a value but a distinctive sorption isotherm, considering that d-spacing increment is always stepwise as a function of the carbon chain size incorporated, and that all these values are positives regardless of the magnitude, as Table 18 shows. Then we will have four well defined groups:

    I. Lateral monolayer: going from 0 to 1.75 (nm)

    II. Lateral bilayer: going from 1,75 to 3.5 (nm.)

    III. Paraffin-type monolayer: going from 3.5 to 5.25 (nm.)

    IV. Paraffin type bilayer: going from 5.25 to 7 (nm.)

Table 18 - Smectite quality features from all samples derived from XRD traces.

	(001)d-spacing	Peak position (Å)		
Sample	**Swelling**	**LyCh (Å)**	**O.C**	**O.C. Type**
3-A	1.781	6.49	-0.634	I
3-B	1.962	3.56	0.735	I
3-C	2.674	2.51	1.162	I
6-D	2.28	2.58	1.89	II
4-E	2.339	5.77	3.4638	II
1-F	3.332	6.98	3.502	III
4-G	4.697	4.42	2.807	II
5-H	2.797	1.96	3.375	II
5-I	2.699	1.28	3.207	II
4-J	2.403	4.00	4.341	III
5-K	2.135	2.42	6.673	IV
2-L	5.403	2.00	3.764	III

Note: the number preceding sample names, corresponds to the geological area

XRF chemical analysis on the <1μm size fraction is a key technique to gather information regarding crystal chemistry of smectites by modeling the unit formula (SCHULTZ, 1969; EBERL et al., 1986; BROWN; NEWMAN, 1987; ONAL, 2006). It is not the intention of the present study to propose a detailed site elemental distribution at the crystal scale, but to observe possible tendencies as a function of geological track and possible applications for each sample and geological area. Table 8, presents XRF enabling correlations with respect to XRD observed behaviour.

Figure 31, shows the relation between layer charge and organic sorption for this set of samples, which also explains the observed results with the general tendency to layer charge be inversely proportional to organic sorption, although some exceptions applied.

Figure 31 - All sample swelling Index vs relative layer charge derived from OS XRD patterns.

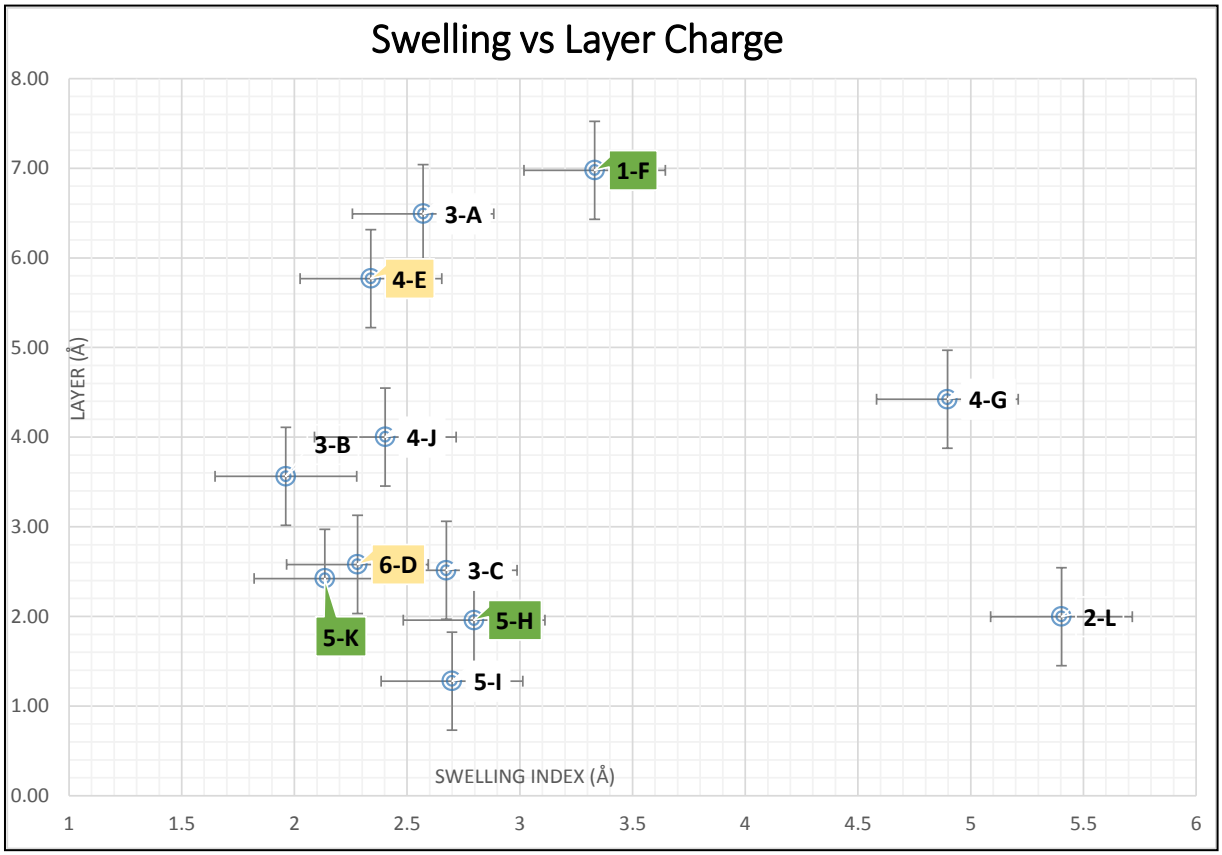

Figure 31 shows structural features that could be used for high added value applications selection criteria for smectites; nevertheless, it is based upon a single peak data unlike the mineral quantification criteria. Then again, the former is related to grade and not quality. Ideally, a second methodology base upon whole patter profile fitting would leave no place for doubt.

From joint observations XRD-OS and XRF <1µm size fraction, is possible to stablish bentonite quality. In other words, information regarding the crystal chemistry and physical properties of smectite species present in each sample. In overall, a broad variety of the dioctahedral smectite species and no tri-octahedral smectites were found. Certain assumptions apply, aluminum substitutions in the tetrahedral never exceed 15% (GRIM, 1968), although the existence of tetrahedral Fe is highly arguable; the Fe oxidation state (Fe^{2+} to Fe^{3+}), was not specifically accessed in this study, thus it is know that typically di-octahedral smectites contain mostly Fe^{3+} in the octahedral sheet substituting Al (GOODMAN,1988), and there is not enough information regarding genesis conditions in order

extrapolated the tendency of Fe^{2+} to oxidize into Fe^{3+} closer to the surface at the presence of oxygen (CHRISTIDIS, 2008; WILLIAMS; ELSEY; WEINTRITT, 1953). On the other hand, it was also considered the fact that tetrahedral Fe substitutions, do tend to favour the context of acidic parent rock (KAUFHOLD et al., 2017), such is the case for samples “F”, “L”, “A”, and possibly “K”. In any case, certain grade of uncertainty still remains regarding charge location.

Accordingly, best examples for both end members of the montmorillonite to beidellite series were sample “A” as a typical montmorillonite electrically compensated by Ca and Mg, and sample “J” for beidellite containing Na and Ca in interlayer position. F sample also appears to be a Ca/Na montmorillonite, while “I” and “K” samples tends more to a Fe rich montmorillonite (being “K” calcic and “I” abnormally sodic: 1.95% Na_2O Wt.%).

Intermediate member of the series were found as regularly interstratified di-octahedral smectites in samples “H” and “L” (“H”: Ca>Na and “L”: Na, interlayering), and two Fe rich di-octahedral smectites randomly ordered, in samples “E” and “D” (“E”: Ca>Na and “D”: Mg>Ca, interlayering). Samples “J” and “G”, yield very similar characteristics tending towards the beidellite end member of the series, only that “G” is Fe richer and both of them polyatomic having mostly by Ca and secondly by Na in the interlayer.

In terms of the geographical context and different geological backgrounds, upcoming Figure 32 and Figure 33, present a comparative graphical perspective of chemical and physical properties for all samples.

Figure 32 - Comparative geochemical ternary plot for all samples.

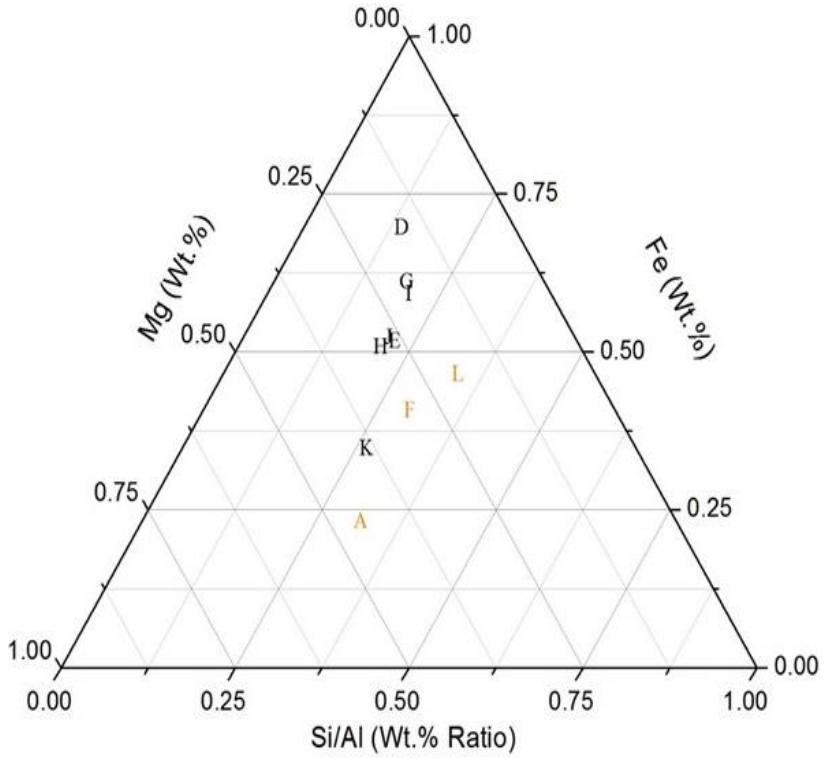

Note: Relative values were obtained from Table 9, normalized to one and scaled to minimum and maximum values.

The geochemical fingerprint based on the elemental composition, seems to be grouping samples as a function of parent rock pH, samples coming from acidic to intermediate precursors (“A”, “F” and ‘L”) are colored in red (Figure 33) yielded higher Si/Al relative values as expected, “K” sample associated to area 5, has been reported typically in associations to basaltic parent rocks, nevertheless it showed all geochemical characteristic of acidic to intermediate associated samples, perhaps corroborating ambiguity in the literature and the need for further geological research in that area, not only in terms of parental rock acidity, but also regarding genesis mode, age and preservation conditions.

Figure 33 - Comparative ternary plot of physical properties for all samples, based on XRD patterns.

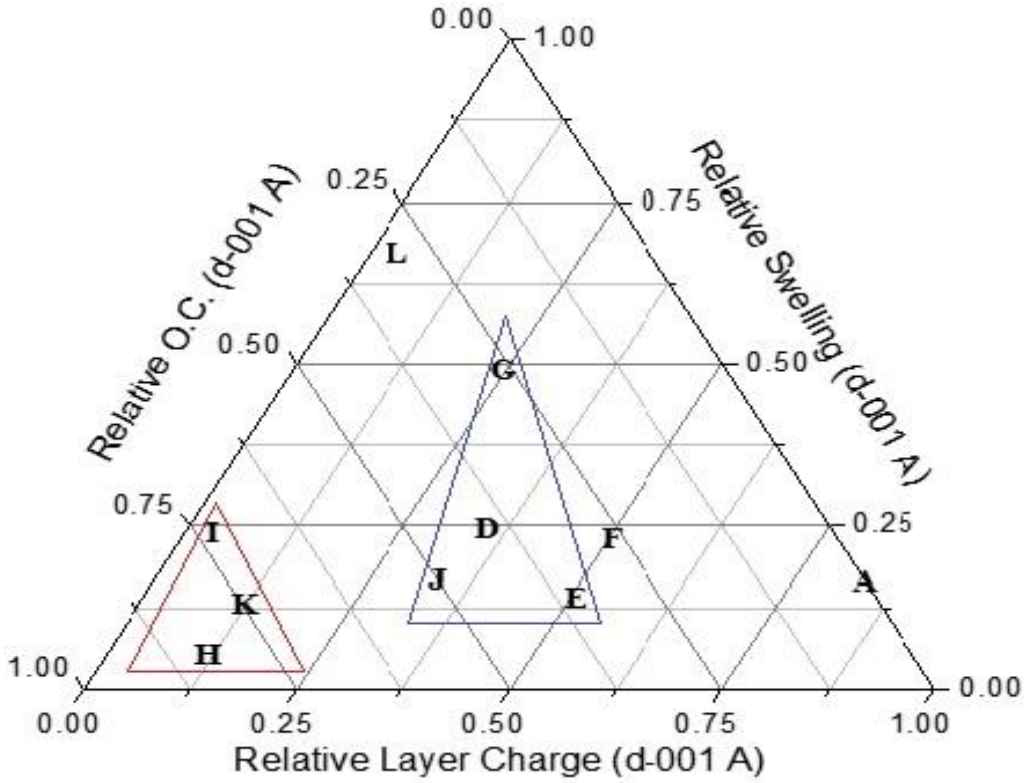

Note: Relative values for Swelling and layer charge, were obtained from equations 2 and 3, and organophilic d-001 reflection position in Angstroms, all values normalized to one and scaled to minimum and maximum values.

Physical properties evaluated mainly by XRD-OS is presented in Figure 33 once again samples showed relative behaviour by grouping in agreement to they're geological area. The red triangle encloses samples coming from area 5 and the blue one encloses groups 4 and 6 (all of them coming from acidic parent rocks). As general trends, it was observed that lower layer charge combined with higher crystalline swelling behaviour and high Na content in interlayer position, tend to favour organic sorption.

The exceptional case of "L" sample, having the highest swelling relative value, low layer charge and yet, discrete organic sorption, may be explained by the presence of silica phases present at the clay size fraction, mineralogical composition indicated the presence of cristobalite in 13% (see Figure 21 and Table 7) and no Si depletion was observed in chemical composition of the < 1µ size fraction (Table 9) indicating that even most cristobalite still remains and It could also influence rheological behaviour negatively.

4.1.4 The cluster analysis

Performing cluster analysis to XRD data, when supported by a robust XRD trace database and backed-up with chemical information, is with no doubt, a very powerful tool. However, at the same time it can be a dangerous misleading artefact if proper selective criteria is not along.

In this study, we used EVA (Bruker™) software and the polySNAP tools to compare results; Figure 34 shows the dendogram alone for the ROP bulk XRD patterns for all 12 samples, it is possible to observe four clusters and three singularly grouped samples.

Figure 34 - Dendrogram derived from the cluster analysis of all ROP XRD traces.

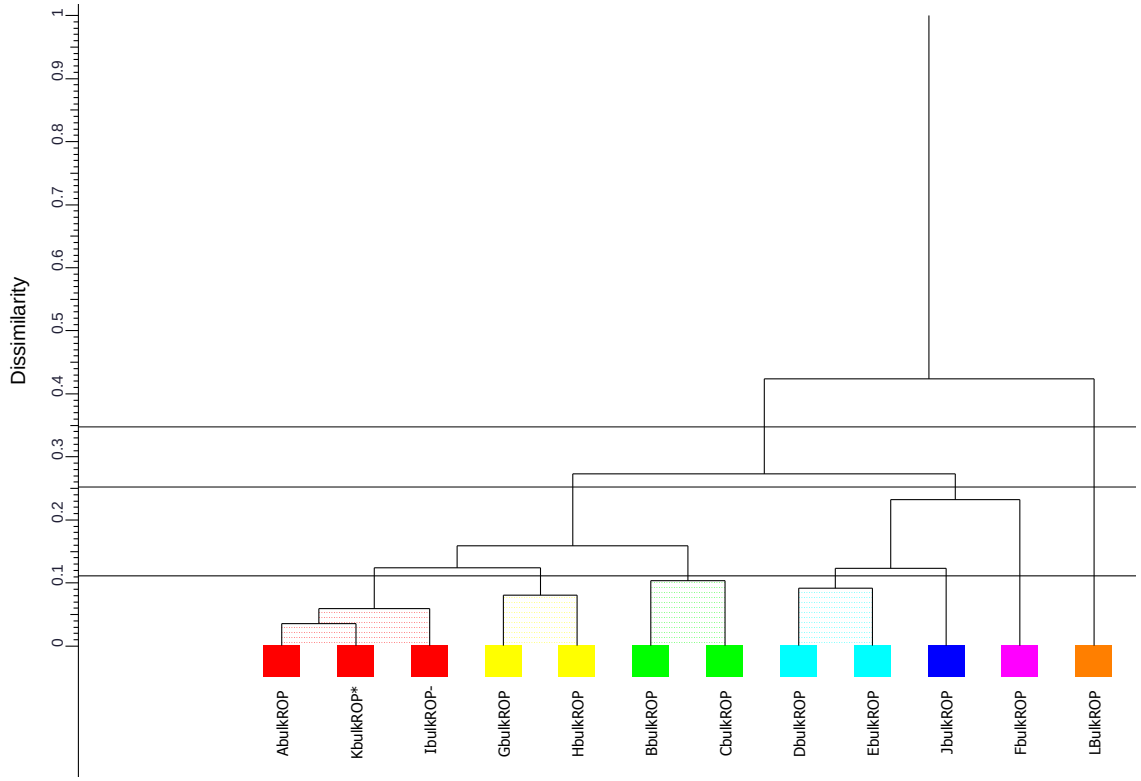

There is a straight correlation for the red cluster containing samples “A”, “K” and “I” (in red), with respect to mineralogical composition, having all predominant montmorillonite and relatively large amounts of quartz and K-feldspar, also none of them presented accessory clay mineral phases, as it can be observe in Figure 35 showing the cluster analysis overlapping the XRD patters beneath the dendrogram.

Figure 35 - Cluster analysis combining XRD traces and dendrogram view.

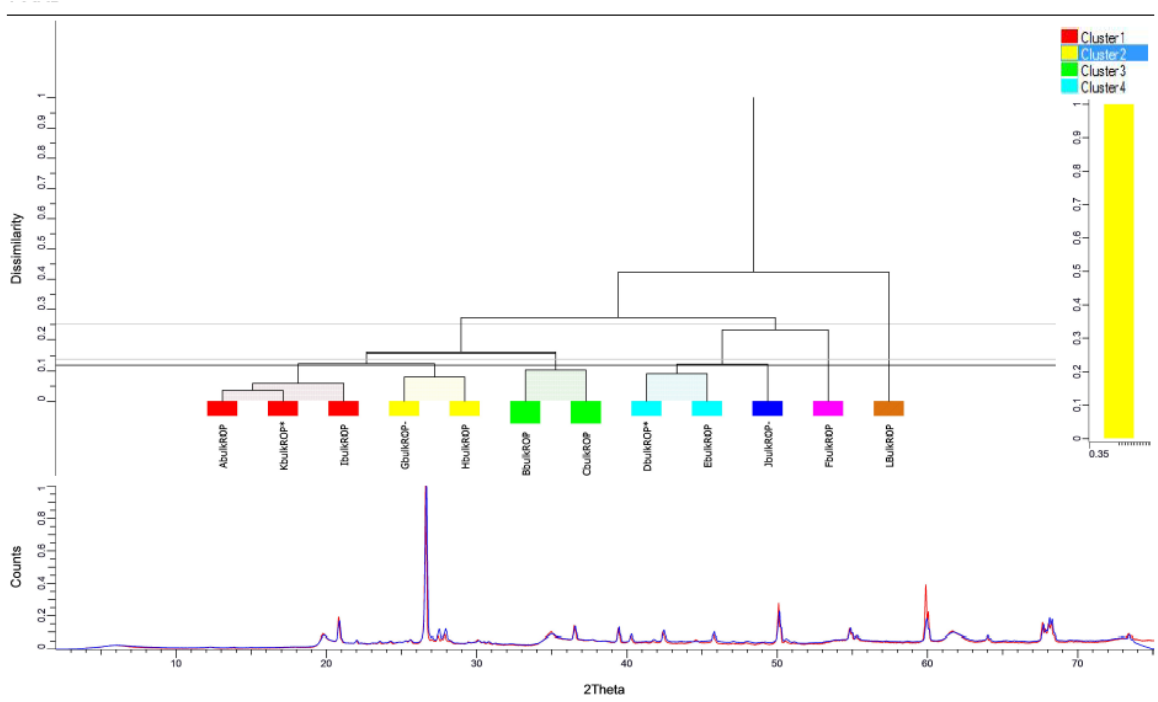

The yellow (“G” and “H”) and cyan (“D” and “E”) clusters contain similar mineral phases present, although the one containing samples “G” and “H” (yellow cluster) has lower grade in terms of smectite content and more kaolinite, in comparison to the cyan group containing samples “D” and “E”.

“L” sample separates from the rest for having the major d(001) reflection at 12.564 Å as it may be expected from this Na-bentonite, and also an abnormal (relative to this set of samples) content of cristobalite, and therefore it groups alone in the orange cluster.

The green cluster groups samples “B” and “C” that showed to be identical in mineralogical composition and are not considered bentonite in terms of grade neither quality; “J” sample is solely clustered in blue for having the same mineralogical composition with respect to the red cluster mainly composed of montmorillonite and quartz but considerable amounts of kaolinite, and differs from the cyan cluster for a greater quartz content.

Finally, the magenta cluster contains F sample alone, presumably for being a clear Na-bentonite but differing from sample L due to the presence of pyrophyllite and anortite and the absence of hematite and zeolites.

The Figure 36 outlines the correlation between mineralogical composition of samples and clustering tendency by outstanding the green cluster, belonging to samples B and C, which are probably the most atypical mineral assembly from the group (being them both almost identical).

Figure 36 - The cluster analysis of ROP XRD patters by PCA.

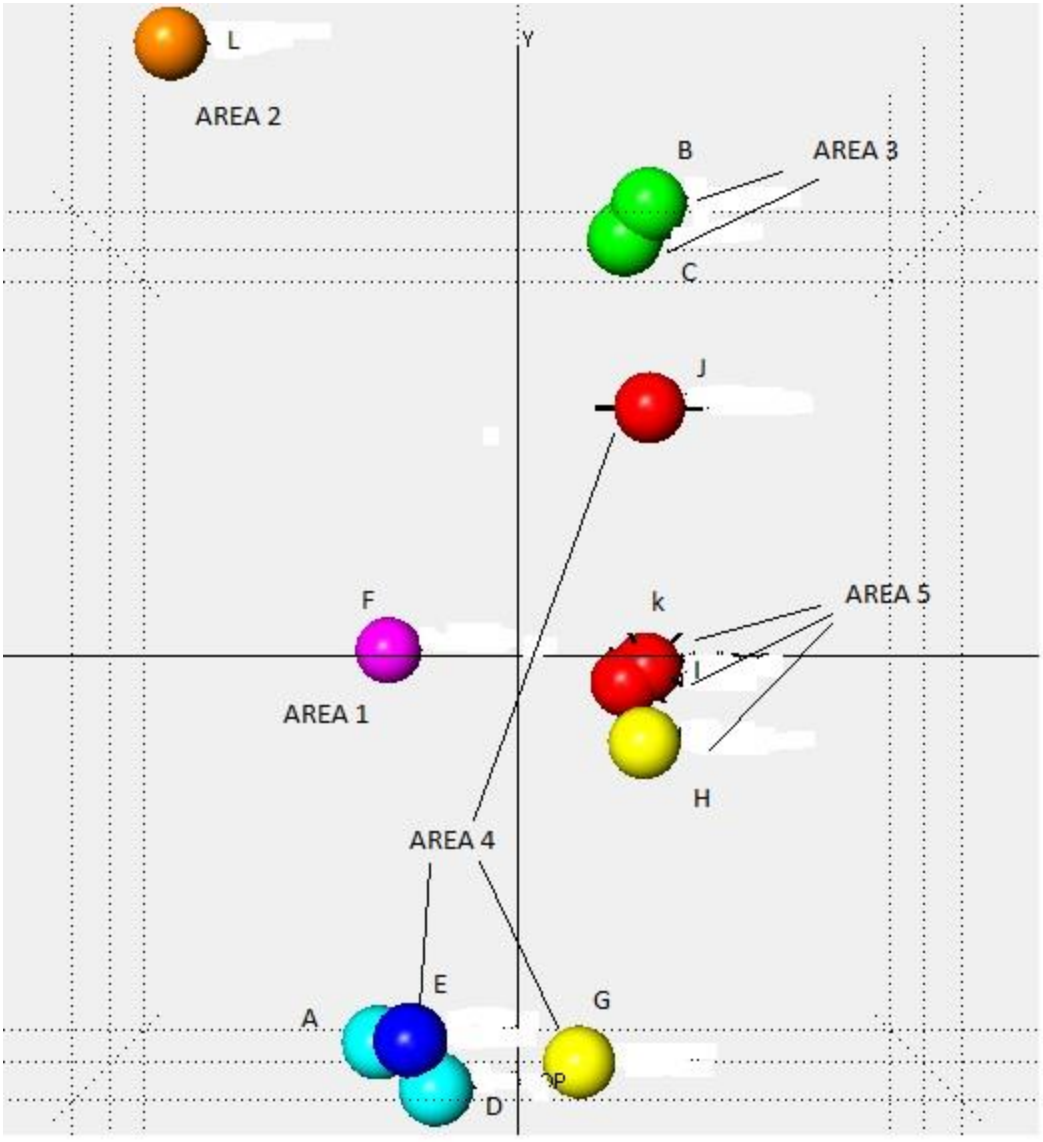

The principal component analysis (PCA), offers a 3D view of relative location for all clusters, the specific angle was selected in order to point specifics regarding sample “F”; giving the fact that the reasons for them being sole clustered is not so evident. Sample “F”, appears close to a set of three samples containing similar mineralogy, but it defers from having cristobalite, as does L

sample, representing the extreme –X to +Y axial plane, towards which sample F seems to be approaching.

4.2 Observations for all samples & applications

As explained before in the previous chapter, results thus attended mostly a set of 12 samples covering all areas of interest, in order to stablish a comparative framework, hereafter, considerations regarding all 33 samples be presented

4.2.1 Geochemical fingerprint

From Table 19, derived from treated values presented on Table 13 and Table 14, is possible to plot the parent rock type for the first 12 samples (framework), based on immobile elemental composition of trace and RREs.

Table 19 - Treated REEs and trace elements, according to Winchester; Floyd, (1977)

		(ppm)			Wt(%)			(ppm)		Ratios		
Sample	**Area**	**Nb 3**	**Zr**	**Y**	**SiO_2**	**Al_2O_3**	**TiO_2**	**TiO2(ppm)**	**Nb/Y**	**Zr/Tio2**	**log(Nb/Y)**	**log (Zr/Tio2)**
A bulk	3	5.0	201.7	69.3	64.0	16.4	0.1	1250.00	0.07	0.16	-1.14	-0.79
B bulk	3	5.0	119.6	38.3	66.1	16.1	0.9	8550.00	0.13	0.01	-0.88	-1.85
D bulk	6	5.0	138.0	24.8	46.9	20.6	1.7	17160.00	0.20	0.01	-0.70	-2.09
E bulk	4	5.0	**15***	40.1	56.7	19.7	0.4	4020.00	0.12	0.00	-0.90	-2.43
F bulk	1	5.0	84.2	15.1	59.2	18.5	0.2	2330.00	0.33	0.04	-0.48	-1.44
G bulk	4	5.0	**25***	17.1	56.0	22.0	0.5	5150.00	0.29	0.00	-0.53	-2.31
H bulk	5	5.0	41.1	11.6	57.8	20.7	0.7	7230.00	0.43	0.01	-0.36	-2.25
I bulk	5	5.0	30.8	13.6	62.8	13.9	0.7	7460.00	0.37	0.00	-0.43	-2.38
J bulk	4	5.0	**15***	24.7	56.4	21.2	0.4	3860.00	0.20	0.00	-0.69	-2.41
K bulk	5	5.0	**22***	15.0	62.2	18.5	0.6	6270.00	0.33	0.00	-0.48	-2.45
L bulk	2	5.0	201.5	25.7	62.4	15.7	0.9	9200.00	0.19	0.02	-0.71	-1.66

Note: * values have been adjusted to fit the plot scale corresponding to Figure 34. Only Zr was modified under the thresholds offered by standard deviation

.

After REEs and trace elements are treated, is possible to represent in a graphical manner, the rock type as a function of log Zr/TiO_2 vs Lofg Nb/Y; on the same plot (Figure 37), some published references are contrasted of known bentonite deposits having proofed diagenetic origins with well know volcanic source ph. In fact, samples plotted in green, come from the same bentonite bearing area than Area 3, as described in this document, and they seem to be in agreement with respect to their acid origin (SILVA et al., 2017).

Figure 37 - Rock type as a function of log Zr/TiO_2 vs Lofg Nb/Y (ppm)

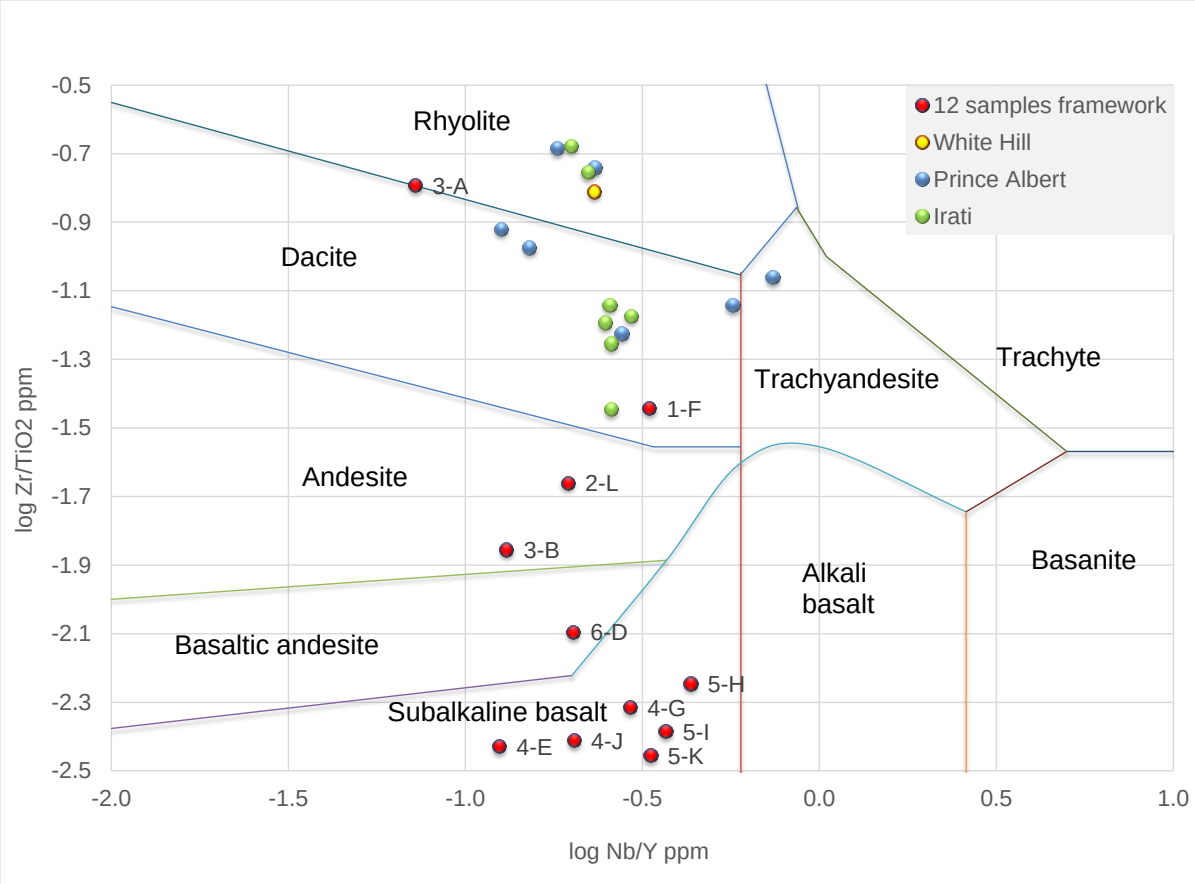

All samples from Paraiba, Bahia and Maranhão, have place themselves among the area corresponding to sub-alkaline basalt, as reported in the literature (see section 2.1.2). Moreover, all samples are within the area of rock type, according to information given in section 3.3 with respect to parent rock.

5 CONCLUSIONS

Bentonite formation processes and the inherent structural features present in smectites species is still poorly understood, even after decades of applied clay research. Moreover, the six bentonite bearing geological areas considered for the scope of the present study are not the exception with respect to geological uncertainty. In fact, the ambiguity reported in literature (see section 2.1.2) could be an expression of the diversity of unknown variables ruling bentonite grade and quality, particularly for areas 4 and 5 (Bahia and Paraiba, respectively). Yet, observed trends appear to correlate physical and chemical properties found in most samples as a function of parent rock composition firstly, and secondly genesis mode (probably due to lack of information in this aspect).

Age, on the other hand, could on the contrary, be a misleading parameter; in the sense that preservation is not necessarily time dependent, perhaps the best example for such a statement is present in the Parana Basin, where sample “A” (Mid Permian), after 250 million years still remains as a highly crystalline, almost monomirerallic Mg rich montmorillonite of high grade and quality, implicating that it may constitute one of the oldest bentonite deposits actively mined due to extraordinary preservation conditions, while other two samples coming from the same geological area (“B” and “C”), showed signs of illitization, considerable amounts of kaolinite and illite, and a whole mineralogical and geochemical constitution far away from bentonite ranges by definition.

Sample “L” from Neuquen, alike sample “A”, shows typical characteristics of a rhyolitic ash source altered in situ to a montmorillonite rich bentonite deposit, containing higher Fe and Al in octahedral position with respect to sample “A” (Mg richer). Samples coming from Bahia (Area 4, samples “E”, “G” and “J”) and Maranhao (sample “D”), showed similar geochemical fingerprint, as well as physical properties (swelling, layer charge and organic sorption), due to the presence of considerable amounts of kaolinite as a secondary phase in all samples and could point into the hydrothermal alteration hypothesis rather than In situ alteration, although, sample “D” from Maranhão, yielded considerably higher Fe content even at the < 1μm size fraction; presumably located mostly in

octahedral position (oxidation state and tetrahedral Fe fraction, are beyond the scope of the present study).

Great deal of variations in chemical composition, was observed in samples from Paraiba (“H”, “I” and “K”), they all had similar mineral composition tending towards low grade and similar predominant smectite polytype (Fe rich dioctahedral smectite, Ca>Na compensated). Based on randomly oriented powder diffraction patterns, interlayer Na content and the relative location among samples coming from different outcrops within the area, the doubt arises regarding the possibility of alteration occurring (at list partially) in a transitional to marine environment. “L” sample coming from Mendoza-San Juan area, showed high swelling and low layer, being a Na compensated Fe rich dioctahedral smectite (tending towards beidellite).

A general tendency was observed, for acid volcanic source to alter into the montmorillonite end member of the series; and accordingly, basic to intermediary parent rocks alter into transitional up to beidellite end members respectively.

The information contained in Figures 8 and 9, could be used to withdraw predictions regarding compared expected performance for specific applications, of course, taking into account processing limitations; for the graphs are based upon the smectitic rich powder response in highly diluted media. Therefore, and in order to have a realistic application threshold in perspective as a function of physical properties, is necessarily to keep grade in mind.

The fact that apparently there is a general trend from south to north in terms of both: grade and quality (with certain exceptions), may be just coincidence or due to geological aspects beyond the scope of the present study. Although, they seem to be related to genesis type expressed in higher smectite content and no kaolinite, and parent rock pH.

5.1 Suggestios for further and complementary work

The complete characterization to stablish a comparative framework for 12 samples is presented in this final version of the research project; nevertheless the same protocols are being followed for the whole set of 33 samples and a continuously growing number of bentonite deposits and prospect is being added

to the set within the six geological areas studied and others contained in the Mercosur region. The research team intends to keep on enriching this data set and future publications will contribute to build a more sadistically robust framework.

An ongoing research line is presented in Annex F related to bentonite purification by wet classification by means of hydrocyclones and several pre-treatment stages, finding interesting features in association to the predominating interlayer cation and the optimum solid ration as a function of beneficiation grade, this topic is not included among the main features of the thesis but it constitutes an ongoing.

The issue of genesis mode with respect to the broad geological setup covered in these pages, still presents several aspects outlined along this document that required substantial research work, particularly in the case of northern Brazilian deposits. Although, it is the intention of the author to keep on working in the field, these are large project that would require the interaction and collaboration with other researchers in the geological aspects of bentonite genesis, therefore we are open to join efforts in other to obtain a better comprehension of the topic.

Water treatment technologies and especially organic pollutant selective sequestration is an ongoing research line for the members of the research team, having been able to achieve very interesting results thus far in a bench scale; the next step is to try in a larger and more realistic experimental conditions in order to probe efficiency and feasibility in actual environmental conditions. For that purpose, the author is in carrying out conversations with local water quality authorities to move forward and any contribution from readers is welcome.

6 REFERENCES

MERMUT, A and LAGALY, G. Baseline studies of the clay minerals society source, layer-charge determination and characteristics of those minerals containing 2:1 layers Clays and Clay Minerals, Vol. 49, No. 5, 381–386 and Vol. 49, No. 5, 393–397, 2001.

ALLO, W. and MURRAY, H. H. Mineralogy, chemistry and potential applications of a white bentonite in San Juan Province, Argentina. **Appl. Clay Sci.,** n. 25, p. 237–243, 2004.

ALTANER, S. P. C O M P A R I S O N OF RATES OF SMECTITE ILLITIZATION. v. 34, n. 5, p. 608–611, 1986.

AMORIM, L. V. et al. Estudo Comparativo entre Variedades de Argilas Bentoníticas de Boa Vista, Paraíba. **Revista Matéria**, v. 11, n. 1, p. 30 – 40, 2006.

ANADÃO, P.; WIEBECK, H.; VALENZUELA-DÍAZ, F. R. Panorama da Pesquisa Acadêmica Brasileira em Nanocompósitos Polímero/Argila e Tendências para o Futuro. **Polímeros**, v. 21, n. 5, p. 443–452, 2011.

AQUINO, S. F. DE; BRANDT, E. M. F.; CHERNICHARO, C. A. DE L. Remoção de fármacos e desreguladores endócrinos em estações de tratamento de esgoto: revisão da literatura. **Revista Engenharia Sanitária e Ambiental**, p. 187–204, 2013.

AXELROD, D. et al. Mobility measurement by analysis of fluorescence photobleaching recovery kinetics. **Biophysical Journal**, v. 16, n. 9, p. 1055–1069, set. 1976.

BARBOSA R. E., et al., Ceramica 52 (2006) pp264-268, Efeito de sais quaternários de amônio na organofilização de uma argila bentonita nacional.

BARKER, J. M. & K. S. T. K. J. E. T. N. **Industrial minerals and rocks: commodities, markets, and uses**. 7th editio ed. [s.l.] Society for Mining, Metallurgy and Exploration Inc, 2006. v. 4BERGAYA, F.; LAGALY, G. Chapter 1

General Introduction: Clays, Clay Minerals, and Clay Science. In: **Handbook of Clay Science**. [s.l.] Elsevier Ltd., 2006. v. 1p. 1-18.

BERGAYA, F.; LAGALY, G.; BENEKE, K. Chapter 15 History of clay science: a young discipline. In: [s.l: s.n.]. p. 1163–1181.

BEURLEN, H. The mineral resources of the Borborema Province in Northeastern Brazil and its sedimentary cover: a review. Journal of South American Earth Sciences, v. 8, n. 3–4, p. 365–376, 1995.

BLACHIER C., L. MICHOT, I. BIHANNIC, O. BARRÈS, A. JACQUET, M. MOSQUET , Adsorption of polyamine on clay minerals Journal of Colloid and Interface Science 336 (2009) 599–606

BLUMSTEIN, A. Polymerization of adsorbed monolayers. I. Preparation of the clay–polymer complex. **Journal of Polymer Science Part A: General Papers**, v. 3, n. 7, p. 2653–2664, jul. 1965.

BOHOR, B. F.; HUGHES, R. E. Scanning electron microscopy of clays and clay minerals. **Clays and Clay Minerals**, v. 19, n. 1, p. 49–54, 1971.

BORDAS, A. F. Contribution to the knowledge of bentonites in Argentina. **Serv. Geol. Min., Estud. Espec.**, v. 15, p. 60, 1943.

BOSSI, J. **Geología del Uruguay. Montevideo**. [s.l.] Universidad de la República, 1966.

BRAXOLEY, G. W. IDENTIFICATION OF CLAY MINERALS BY X-RAY DIFFRACTION ANALYSIS. [s.d.].

BROWN; NEWMAN. The chemical constitution of clays and Clay minerals. **Clay Minerals**, v. 31, n. 2, p. 163–167, 1987.

CABRAL; COELHO. **ESTUDO PROSPECTIVO DA BENTONITA : TENDÊNCIAS DE**. II SIMPÓSIO DE MINERAIS INDUSTRIAIS DO NORDESTE. **Anais**...2013

CAI, K. et al. Removal of androgens and estrogens from water by reactive materials. **2010 4th International Conference on Bioinformatics and Biomedical Engineering, iCBBE 2010**, v. 2010, n. November, p. 990–993, 2010.

CALARGE, L. et al. The smectitic minerals in a bentonite deposit from Melo (Uruguay). **Clay Minerals**, v. 38, p. 25–34, 2003.

CALARGE, L. M.; MEUNIER, A.; FORMOSO, M. L. L. A bentonite bed in the Aceguá (RS, Brazil) and Melo (Uruguay) areas: A highly crystallized montmorillonite. **Journal of South American Earth Sciences**, v. 16, n. 2, p. 187–198, 2003.

CALDASSO, A. L. **Novas consideracoes sobre a Genese e a idade dos depositos de argilas montmorilloniticas da Paraiba**. Atlas do IX Simposio de Geologia do Nordeste. **Anais**...1979

CARVALHO, I. DE M. **ESTUDO GEOLÓGICO COMPARATIVO ENTRE AS BENTONITAS DE REGIÃO DE MELO (URUGUAI) E DA REGIÃO DE VITÓRIA DA CONQUISTA (BAHIA)**. [s.l: s.n.].

CBPN. **PROGRAMA DE EXPLORAÇÃO MINERAL 40 ANOS DESENVOLVENDO O SETOR MINERAL BAIANO**. [s.l: s.n.].

CHIPERA, S. J.; BISH, D. L. Baseline studies of the clay minerals society source clays: Powder X-ray diffraction analyses. **Clays and Clay Minerals**, v. 49, n. 5, p. 398–409, 2001.

CHRISTIDIS, G. E. Physical and chemical properties of some bentonite deposits of Kimolos Island , Greece. **Applied Clay Science**, v. 13, n. October, p. 79–98, 1998.

CHRISTIDIS, G.E. Comparative study of the mobility of major and trace elements during alteration of an andesite and a rhyolite to bentonite, in the islands of Milos and Kimolos, Aegean, Greece. Clays and Clay Minerals 46: 379-399, 1998

CHRISTIDIS, G. E. Do bentonites have contradictory characteristics ? An attempt to answer unanswered questions. **Clay Minerals**, n. 43, p. 515–529, 2008.

CHRISTIDIS, G. E.; EBERL, D. D. Determination of layer-charge characteristics of smectites. **Clays and Clay Minerals**, v. 51, n. 6, p. 644–655, 2003.

CHRISTIDIS, G. E.; HUFF, W. D. Geological aspects and genesis of bentonites. **Elements**, v. 5, n. 2, p. 93–98, 2009.

CHURCHMAN, G. J. et al. **Chapter 11.1 Clays and Clay Minerals for Pollution Control**. [s.l: s.n.]. v. 1

CLAY MINERALS SOCIETY., J. et al. **Clays and clay minerals : proceedings of the ... National Conference on Clays and Clay Minerals.** [s.l.] National Academy of Sciences--National Research Council, 1954. v. 49

CLEM, A. G. Industrial Applications of Bentonite. **Clays and Clay Minerals**, v. 10, n. 1, p. 272–283, 1961.

COELHO, J. M. **DESENVOLVIMENTO DE ESTUDOS PARA ELABORAÇÃO DO PLANO DUODECENAL (2010 - 2030) DE GEOLOGIA, MINERAÇÃO E TRANSFORMAÇÃO MINERAL,Outras Rochas e Minerais Industriais Relatório**. Brasilia: [s.n.].

CUTRIM, A. A.; MARTÍN-CORTÉS, G. R.; VALENZUELA-DÍAS, F. R. **Bentonitas da Paraíba**. [s.l: s.n.].

CZÍMEROVÁ, A.; BUJDÁK, J.; DOHRMANN, R. Traditional and novel methods for estimating the layer charge of smectites. **Applied Clay Science**, v. 34, n. 1–4, p. 2–13, 2006.

DA PAZ, S. P. A.; ANGÉLICA, R. S.; DE FREITAS NEVES, R. Mg-bentonite in the Parnaíba paleozoic Basin, northern Brazil. **Clays and Clay Minerals**, v. 60, n. 3, p. 265–277, 2012.

DAZAS, B. et al. Influence of tetrahedral layer charge on the organization of interlayer water and ions in synthetic Na-saturated smectites. **Journal of Physical Chemistry C**, v. 119, n. 8, p. 4158–4172, 2015.

Deligiann L., A. Ekonomakou Uses of Organo Clays, Bentonite Division- Silver &

Barite Group. (2010).

DE PAIVA, L. B.; MORALES, A. R.; VALENZUELA DÍAZ, F. R. Organoclays: Properties, preparation and applications. **Applied Clay Science**, v. 42, n. 1–2, p. 8–24, 2008.

DERMATAS, D. et al. Influence of X-Ray Diffraction Sample Preparation on Quantitative Mineralogy. **Journal of Environment Quality**, v. 36, n. 2, p. 487, 2007.

DNPM. **SUMÁRIO MINERAL 2015 Departamento Nacional de Produção Mineral**. [s.l: s.n.].

EBERL, D. D. et al. Chemistry of Illite/Smectite and End-Member Illite. **Clays and Clay Minerals**, v. 34, n. 4, p. 368–378, 1986.

ELZEA, J. M.; ODOM, I. E.; MILES, W. J. Distinguishing well ordered opal-CT and opal-C from high temperature cristobalite by x-ray diffraction. **Analytica Chimica Acta**, v. 286, n. 1, p. 107–116, 1994.

Elements magazine, Bentonites versatil clays. Vol 5 number 2, April 2009 issue.

Encyclopedia of Nanotechnology by Springer,2012 and Rubber Clay nanocomposites by Maurizio Galimberti,2011

FANNING, C. M. et al. K-bentonites in the Argentine Precordillera contemporaneous with rhyolite volcanism in the Famatinian Arc. **Journal of the Geological Society**, v. 161, n. 5, p. 747–756, 2004.

FORMOSO, M. L. L.; CALARGE, L. M.; GARCIA, A. J. V. . A.; D. B.; GOMES, M. B. MISUSAKI, A. M. Permian tonsteins from the Paraná Basin, Rio Grande do Sul, Brazil. **11th Clay Conference**, p. 613–621. Ottawa, 1997.

FORMOSO, M. L. L.; CALERGE, L. M.; MISUSAKI, A. M.; MEUNIER; A., ALVES, A. D.; ZALBA, P. **Occurrences of bentonites in southern South America**. 1st Latin American Clay Conference. **Anais**...2000

GARRELS, R. M. MONTMORILLONITE/ILLITE STABILITY DIAGRAMS. **Clays and Clay Minerals**, v. 32, n. 3, p. 161–166, 1984.

GOODMAN, B. A.; P.H., N.; J., C. E V I D E N C E F O R T H E M U L T I P H A S E N A T U R E OF BENTONITES FROM MOSSBAUERAND. **Clay Minerals**, n. 23, p. 147–159, 1988.

GOPINATH, R. G. **Analise ambiental dos arenitos associados com bentonita da Boa Vista, Paraiba**. IX Simposio de Geologia do Nordeste. **Anais**...Campina Grande: 1979

GOPINATH, T. R.; SCHUSTER, H. D.; SCHUCKMANN, W. K. Modelo de ocorrencia e genese da argila bentonitica de Boa Vista, Campina Grande. Paraiba. **Revista Brasileira de Geociencias**, p. 185–192, 1981.

GOPINATH, T. R.; SCHUSTER, H. D.; SCHUCKMANN, W. K. Clay mineralogy and geochemistry of continental bentonite and their geologic implications, Boa Vista, Campina Grande, PB. **Revista Brasileira de Geociencias**, v. 18, n. 3, p. 345–352, 1988.

GRIM, R. E. **Applied Clay Mineralogy**. New York: [s.n.].

GRIM, R. E. **Clay Mineralogy**. 2nd Editio ed. New York: McGraw-Hill, 1968.

HARVEY, C. C.; LAGALY, G. Chapter 10.1 Conventional Applications. **Developments in Clay Science**, v. 1, n. C, p. 501–540, 2006.

HARVEY, C. C.; MURRAY, H. H. Industrial clays in the 21st century: A perspective of exploration, technology and utilization. **Applied Clay Science**, v. 11, n. 5–6, p. 285–310, 1997.

HOWER, J.; MOWATT, T. C. THE MINERALOGY OF ILLITES AND MIXED-LAYERS ILLITE/MONTMORILLONITES. **The american mineralogist**, v. 51, n. May-June, 1966.

HUFF, W. D. et al. Ordovician K-bentonites in the Argentine Precordillera: relations to Gondwana margin evolution. **Geological Society, London, Special Publications**, v. 142, n. 1, p. 107–126, 1998.

IMPICCINI, A.; VALLÉS, J. M. Los depósitos de bentonita de Barda Negra y cerro Bandera, departamento Zapala, provincia del Neuquén, Argentina. **Revista de la Asociacion Geologica Argentina**, v. 57, n. 3, p. 305–314, 2002.

JAYNES, W. F.; BOYD, S. A. Clay Mineral Type and Organic Compound Sorption by Hexadecyltrimethlyammonium-Exchanged Clays. **Soil Science Society of America Journal**, v. 55, n. 1, p. 43, 1991.

KANNGIESSER, B. Quantification procedures in micro X-ray fluorescence analysis. **Spectrochimica Acta - Part B Atomic Spectroscopy**, v. 58, n. 4, p. 609–614, 2003.

KAUFHOLD, S. Comparison of methods for the determination of the layer charge density (LCD) of montmorillonites. **Applied Clay Science**, v. 34, n. 1–4, p. 14–21, 2006.

KAUFHOLD, S. et al. Tetrahedral charge and Fe content in dioctahedral smectites. **Clay Minerals**, n. 52, p. 51–65, 2017.

KLEEBERG, R.; MONECKE, T.; HILLIER, S. Preferred orientation of mineral grains in sample mounts for quantitative XRD measurements: How random are powder samples? **Clays and Clay Minerals**, v. 56, n. 4, p. 404–415, 2008.

KOGEL, J. E. **Industrial Minerals & Rocks**. [s.l: s.n.].KOMADEL, P.; MADEJOVÁ, J. Chapter 7.1 Acid Activation of Clay Minerals. **Developments in Clay Science**, v. 1, n. C, p. 263–287, 2006.

KÖSTER, H. M. et al. Mineralogical and chemical characteristics of five nontronites and Fe-rich smectites. **Clay Minerals**, v. 34, p. 579–599, 1999.

KÖSTER, M. H. et al. **Boron content and boron isotope composition of Na, Ca and Mg bentonites**. European clay meeting. **Anais**...2015

LAGALY, G., FAHN, R. Tone und Tonminerale. fourth ed. Ullmann's. **Encyclopedia of Technical Chemistry**, v. 23, n. vol. 23. Verlag Chemie, Weinheim, p. 311–326, 1983.

LAGALY, G. Clay-organic interactions. **Philos. Trans. R. Soc. Lond.**, n. A311, p. 315–332, 1984.

LAGALY, G.; OGAWA, M.; DÉKÁNY, I. Chapter 7.3 Clay Mineral Organic Interactions. **Developments in Clay Science**, v. 1, n. C, p. 309–377, 2006.

LAIRD, D. A. Layer charge influences on the hydration of expandable 2:1 phyllosilicates. **Clays and Clay Minerals**, v. 47, n. 5, p. 630–636, 1999.

LAIRD, D. A.; SCOTT, A. D.; FEUTON, T. E. Evaluation of the Alkylammonium Method of Determining Layer Charge. **Clays and Clay Minerals**, v. 37, n. 1, p. 41–46, 1989.

LOMBARDI, B., ET AL. Bentonite deposits of Northern Patagonia. **Applied clay science**, v. 22, p. 309–312, 2003.

MALLA P. B. et al., Charge heterogeneity and nanostructure of 2:1 layer silicates by high-resolution transmission electron microscopy. Clays and Clay Minerals, Vol. 41, No. 4, 412-422, 1993

ONAL M., **Determination of Chemical Formula of a SmectiteCommunications, Series B: Chemistry and Chemical Engineering**, 2006.

MACHADO, G. et al., **SPATIAL DISTRIBUTION OF LAYER CHARGE IN A BENTONITE DEPOSIT. A POWERFUL TOOL FOR MINE PLANNING**. XIII Jornadas Argentinas de Tratamiento de Minerales. **Anais**...2016

MACHADO, G. G. **Variação espacial da carga interfoliar de esmectitas do depósto de bentonita de melo (norte do Uruguai): implicações nas propriedades físicas e na organofilização**. [s.l.] Universidade Federal do Rio Grande do Sul, 2012.

MACHADO, G. G. et al. **Spatial Variation of Layer Charge in Melo Bentonite Deposit Northern Uruguay . Implications on Physical Properties and Organophilization**. 15th international clay conference. **Anais**...Rio de Janeiro: 2013

MADEJOV, J. et al. Base Line Studies of the Clay Minerals Society Source Clays: Infrared Methods. **Clay and Clay Minerals**, v. 49, n. 5, p. 410–432, 2001.

MAYNARD, J. B.; GAINES, R. R. Bentonites in the Late Permian (Tartarian) Irati Formation of Brazil : Geochemistry and Potential for Stratigraphic Correlations. n. October, 1996.

MERMUT, A. R.; LAGALY, G. Baseline studies of the clay minerals society source clays: Layer-charge determination and characteristics of those minerals containing 2:1 layers. **Clays and Clay Minerals**, v. 49, n. 5, p. 393–397, 2001.

MEUNIER, A. The Reactivity of Bentonites: A Review. An Application to Clay Barrier Stability for Nuclear Waste Storage. **Clay Minerals**, v. 33, n. 2, p. 187–196, 1998.

MEUNIER, A. **Clays**. New York: [s.n.].

MEUNIER, A. et al. Chemical signature of two Permian volcanic ash deposits within a bentonite bed from Melo, Uruguay. **Anais da Academia Brasileira de Ciencias**, v. 78, n. 3, p. 525–541, 2006.

MEUNIER, A.; VELDE, B. Solid solutions in I/S mixedJayer minerals and illite. **American Mineralogist**, v. 74, p. 1106–1, 1989.

MILLOT, G. **Geology of clays weathering, sedimentology, geochemistry.** [s.l.] Springer-Verlag, 1970.

MIRELLA, D. et al. Caracterização Mineralógica E Tecnológica De Um Depósito Argiloso Na Região De Cubati (Pb). **Geociencias**, v. 33, n. 3, p. 516–534, 2014.

MONTAGNER, C. C.; JARDIM, W. F. Spatial and seasonal variations of pharmaceuticals and endocrine disruptors in the Atibaia River, Sao Paulo State

(Brazil). **Journal of the Brazilian Chemical Society**, v. 22, n. 8, p. 1452–1462, 2011.

MOORE, D. M. & REYNOLDS, R. C., J. **X-Ray Diffraction and the Identification and Analysis of Clay Minerals**. 2nd ed ed. New York: Oxford University Press, 1997.

MORAES, D. S. et al. Mineralogy and chemistry of a new bentonite occurrence in the eastern Amazon region, northern Brazil. **Applied Clay Science**, v. 48, n. 3, p. 475–480, 2010.

MURRAY, H. H. Applied Clay Mineralogy. In: **Developments in Clay Science**. [s.l.] Elsevier, 2007a.

MURRAY, H. H. Applied Clay Mineralogy. In: **Developments in Clay Science**. [s.l: s.n.].

MURRAY, H. H., Clay sorbents: the mineralogy, processing and applications. Acta Geodyn. Geomater., Vol.2, No.2 (138), 131-138, 2005

NANOBUSINESS. **Estudo de viabilidade de uma planta de insumos nanométricos para aperfeiçoamento de embalagens plásticas**. [s.l: s.n.].

O'CONNOR, B. H.; CHANG, W. -J. The amorphous character and particle size distributions of powders produced with the Micronizing Mill for quantitative x-ray powder diffractometry. **X-Ray Spectrometry**, v. 15, n. 4, p. 267–270, 1986.

ODOM, E. Smectite clay minerals: properties and uses. **Philos. Trans. R. Soc. Lond.**, n. A 311, p. 391–409, 1984.

OLPHEN, H. VAN. **Advances in colloid and interface Science.** Amsterdam: [s.n.]. v. 9

PINHEIRO, J. P.; BULHÕES ARANHA, I., Caracterização cristaloquímica preliminar de bentonitas brasileiras. Arquivos do Museu Nacional, Rio de Janeiro, v.65, n.2, p.225-234, abril a Junio de 2007.

PINTO, G. G.; PIMENTEL, E. **Consideracoes geo-economicas sobre os depositos argilosos de Boa Vista, PB.** Campina Grande: [s.n.].

103 PIRES, E. F.; GUERRA-SOMMER, M. Sommerxylon spiralosus from Upper Triassic in southernmost Paran?? Basin (Brazil): A new taxon with taxacean affinity. **Anais da Academia Brasileira de Ciencias**, v. 76, n. 3, p. 595–609, 2004.

PRIDEAUX, J. Brazil takes off. **The Economist**, 2009.

GRIM R. E. & GUVEN. N. **Developments in sedimentology, vol 24 BENTONIES**. ELSEVIER N ed. [s.l: s.n.].

RAUTUREAU, M. et al. **Clays and health: Properties and therapeutic uses**Springer International Publishing AG, , 2017. (Nota técnica).

REZENDE, N. G. **Argilas nobres e zeólitas na bacia do Parnaíba**. Belen: [s.n.].

ROCHA-CAMPOS, A. C. et al. 30million years of Permian volcanism recorded in the Choiyoi igneous province (W Argentina) and their source for younger ash fall deposits in the Paraná Basin: SHRIMP U-Pb zircon geochronology evidence. **Gondwana Research**, v. 19, n. 2, p. 509–523, 2011.

SCHULTZ, L. G. LITHIUM A N D P O T A S S I U M A B S O R P T I O N , DEHYDROXYLATION TEMPERATURE , AND S T R U C T U R A L W A T E R C O N T E N T OF A L U M I N O U S. **Clays and Clay Minerals**, v. 17, p. 115–149, 1969.

SILVA-VALENZUELA, M. DAS G. et al. Enrichment of clay from Vitoria da Conquista (Brazil) for applications in cosmetics. **Applied Clay Science**, v. 155, p. 111–119, 1 abr. 2018.

SILVA, A. F. et al. Bentonitas da formação irati no setor sul da bacia do paraná. **Geologia USP - Serie Cientifica**, v. 17, n. 1, p. 75–88, 2017.

SILVA; H. C. FERREIRA, Desenvolvimento de Estudos para elaboraçao do plano

duicenal 2010/2030-Pefil Bentonita, by the Ministerio de Minas e Energia e the world banc.¨ A. R. V. 2008

SILVA, I.; COSTA, J. Studies of new occurrences of bentonite clays in the State of Paraíba for use in water based drilling fluids. **Rem: Revista Escola …**, p. 485–491, 2013.

SILVA R. V., H. C. Ferreira Argilas bentoníticas: conceitos, estruturas, propriedades, usos, industriais, reservas, produção e produtores/fornecedores nacionais e internacionais Revista Eletrônica de Materiais e Processos, v.3.2 (2008) 26-35 ISSN 1809-8797

SINGER, S.; ARREOLA, D. M. **Global entreprenership monitor**. [s.l: s.n.].

SODRÉ, F. F.; LOCATELLI, M. A. F.; JARDIM, W. F. Occurrence of emerging contaminants in Brazilian drinking waters: A sewage-to-tap issue. **Water, Air, and Soil Pollution**, v. 206, n. 1–4, p. 57–67, 2010.

SOUZA SANTOS, P. **Ciência e Tecnologia de Argilas**. 2. ed. São Paulo: Edgard Blücher Ltda., 1992.

SRODON, J. et al. QUANTITATIVE X-RAY DIFFRACTION ANALYSIS OF CLAY-BEARING ROCKS FROM RANDOM PREPARATIONS. **Clays and Clay Minerals**, v. 49, n. 6, p. 514–528, 2001.

STUMPF, M. et al. Polar drug residues in sewage and natural waters in the state of Rio de Janeiro, Brazil. **The Science of the Total Environment**, v. 225, p. 135–141, 1999.

TAK-KEUN O. H., The effect of shear force on microstructure and mechanical property of epoxy/clay nanocomposites, Master Thesis at the University OF Florida 2004.

The Clay Mineral Society (CMS). “Workshop lecture Layer charge characteristics of 2:1 silicate clay minerals”. 1994, Volume 6.

TOBY, B. H. R factors in Rietveld analysis: How good is good enough? **Powder Diffraction**, v. 21, n. 01, p. 67–70, 2006.

TOMIO, A. **A MINERAÇÃO NO MERCOSUL E O MERCADO DA BENTONITA Dissertação**. [s.l.] UNICAMP, 1999.

TONNESEN, D. A. Bentonitas Dos Novos Depósitos De Cubati-Pb Bentonitas Dos Novos Depósitos De Cubati-Pb. 2010.

UFER, K. et al. Quantitative phase analysis of bentonites by the rietveld method. **Clays and Clay Minerals**, v. 56, n. 2, p. 272–282, 2008.

VALENZUELA DÍAZ, F. R.; DE SOUZA SANTOS, P. Studies on the acid activation of Brazilian smectitic clays. **Quimica Nova**, v. 24, n. 3, p. 345–353, 2001.

VIANA, R. R. et al. Age of pegmatites from eastern Brazil and implications of mica intergrowths on cooling rates and age calculations. **Journal of South American Earth Sciences**, v. 16, n. 6, p. 493–501, 2003.

WANG, L.; ZHANG, M.; REDFERN, S. A. T. Infrared study of CO2 incorporation into pyrophyllite [Al2Si4O10(OH)2] during dehydroxylation. **Clays and Clay Minerals**, v. 51, n. 4, p. 439–444, 2003.

WEAVER, C. E.; POLLARD, L. D. **The chemestry of clay minerals**. New York: Elsevier, 1973.

WILLEMS; WILDENBERG, VAN DEN. **Roadmap Report on Nanoparticles**. [s.l: s.n.].

WILLIAMS, F. J.; ELSEY, B. C.; D. J. WEINTRITT. THE VARIATIONS OF WYOMING BENTONITE. **Clays and Clay Minerals**, n. 2, p. 141–151, 1953.

YAMADA, H. et al. Smecties in the Montmorilonite-Beidllite series. **Clay Minerals**, v. 26, p. 359–369, 1991.

YARIV, S. The role of charcoal on DTA curves of organo-clay complexes: An overview. **Applied Clay Science**, v. 24, n. 3–4, p. 225–236, 2004.

YARIV, S.; CROSS, H. **Organo-clay complexes and interactions.** Jerusalem: Marcel Dekker, Inc., 2002.

ZWELL, L.; DANKO, A. W. Applications of X-ray Diffraction Methods to Quantitative Chemical Analysis. **Applied Spectroscopy Reviews**, v. 9, n. 1, p. 167–221, 24 jan. 1975.

APPENDIXES

APPENDIX A - PLANNING & CHRONOGRAM

APPENDIX B - CALIBRATION CURVE ON HPLC FOR HORMONE DETECTION

APPENDIX C - RANDOMLY ORIENTED POWDER XRD BY SAMPLE

APPENDIX D - REITVELD REFINEMENT FIT ON TOPAS V5.1 FOR STUDIED SAMPLES

APPENDIX E - ORIENTED SLIDES XRD BY SAMPLES

APPENDIX F - BENTONITE PURIFICATION BY WET CLASSIFICATION

APPENDIX A

PLANNING & CHRONOGRAM

In early February 2013, a research project proposal was presented to the evaluation committee as a requirement to be accepted as a PhD candidate at the post-graduation program of Mineral Engineering of the *Escola Politécnica da Universidade de Sao Paulo* (PPGMIN). Even at that early stage, a chronogram alongside showed roughly the same schedule followed until the end. The lost initial year outlined in green, was overcome with intense work and scope reduction along the way.

Followed chronogram

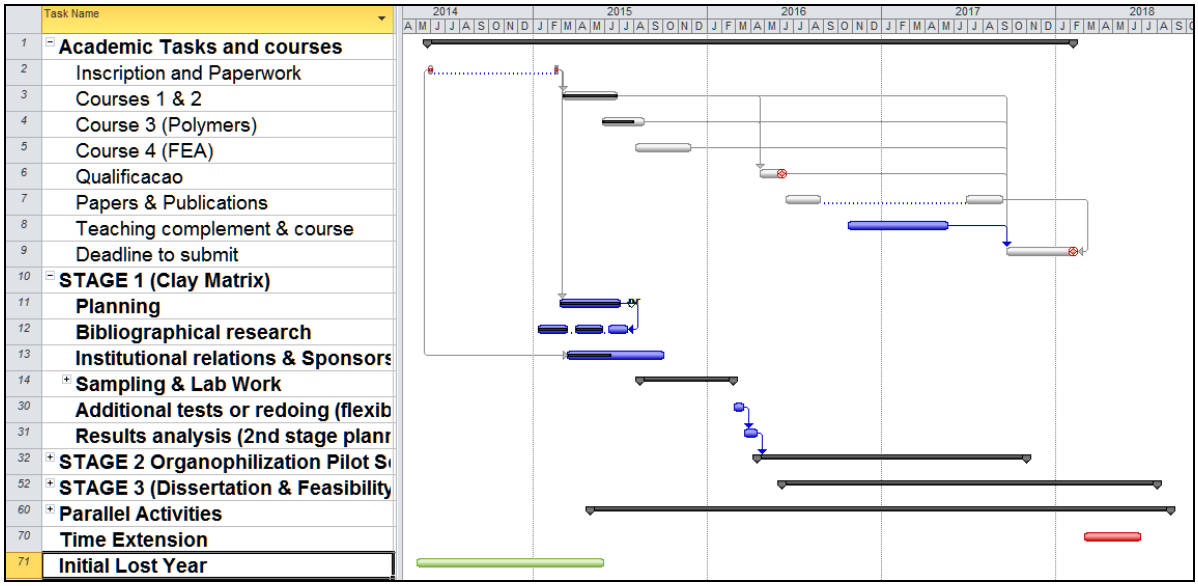

Updated: January 2018

The first planning scheme was presented to the PPGMIN evaluation committee on the 13/11/2013, it features a 3 years planning given a great deal of uncertainties at the initial stages, with the intention to reorganize after a preliminary overview at sight of first characterization results and observed tendencies in terms of applications and local market. Great distances among bentonite sources, was a constant limitation in order to fulfill the chronogram, many of the samples were not handpicked due to budget limitations to travel Northern Brazil. Nevertheless, 20 out of 33 samples analyzed were first handed collected at mine site, and the rest are from known origin.

It may be noted that Stage 1 was fully accomplished somewhere in mid-2016, marking the realizations of fieldwork and mineral characterization, in order to begin with applied aspects of the research project. The red task outlines the period corresponding to an extension request for 6 months at the end of the doctorate.

APPENDIX B

CALIBRATION CURVE ON HPLC FOR HORMONE DETECTION

The Figure bellow illustrates the calibration curve for 17β Estradiol, with a retention time= 9.7 min and a perfect correlation.

Calibration curve with a retention time= 9.7 min

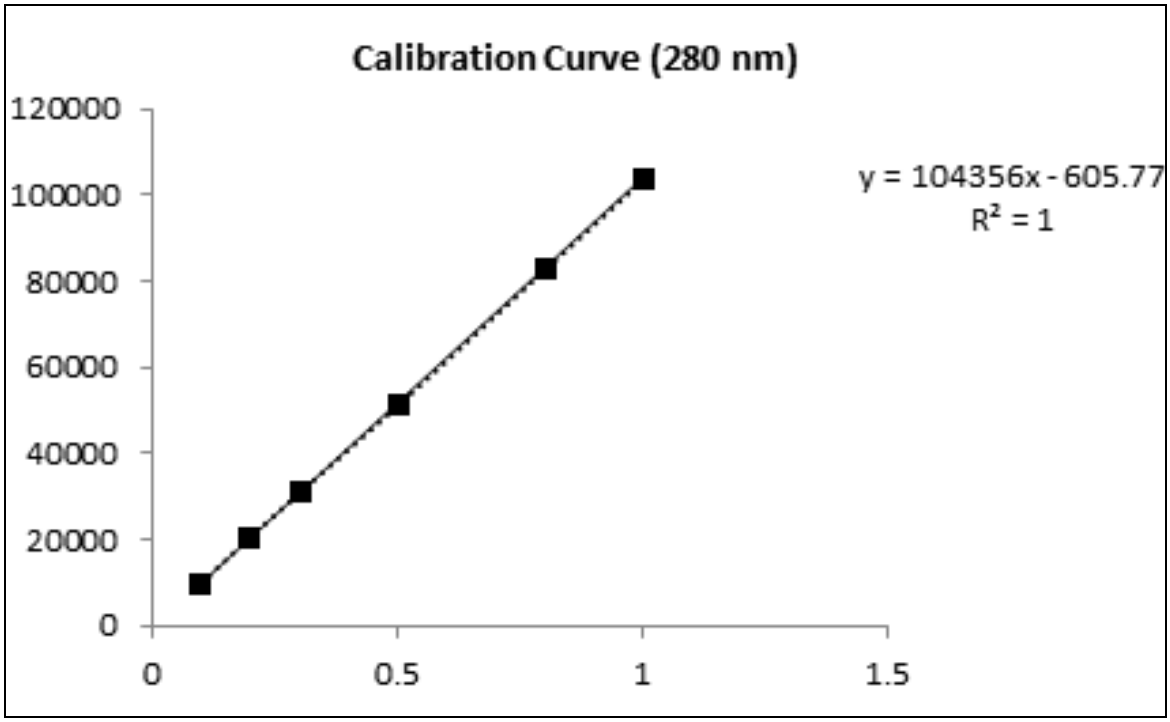

APPENDIX C

RANDOMLY ORIENTED POWDER XRD BY SAMPLE

A

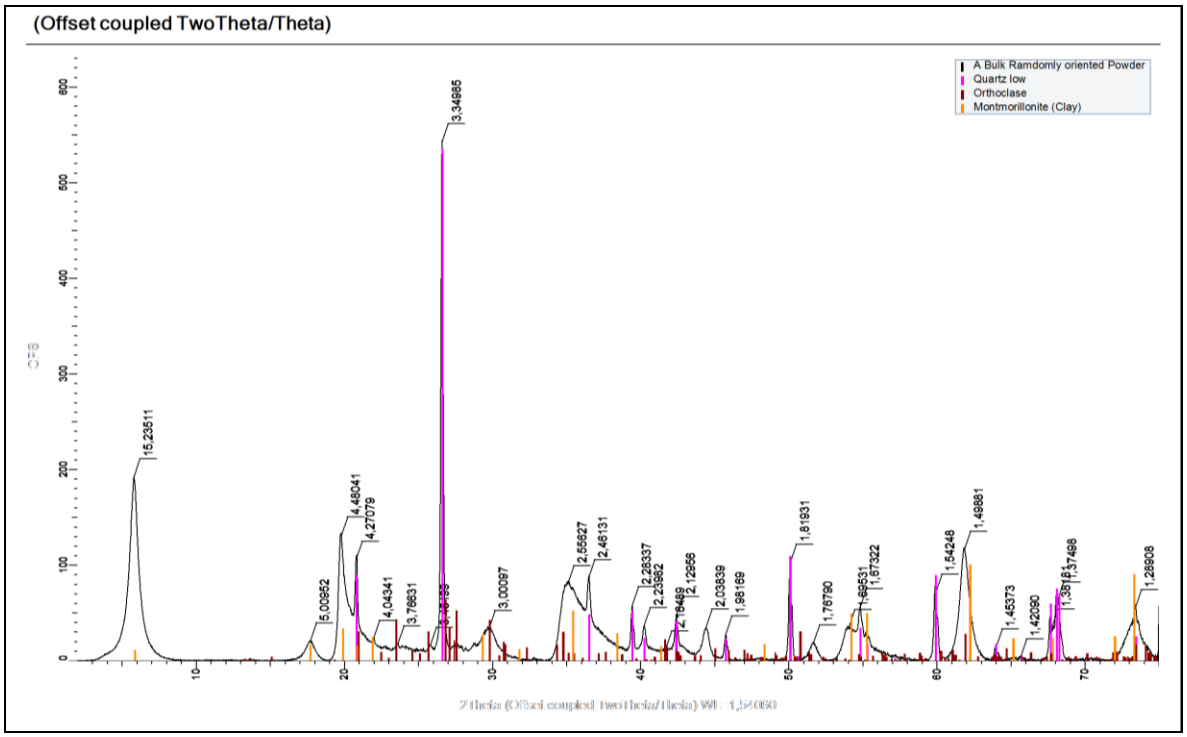

B

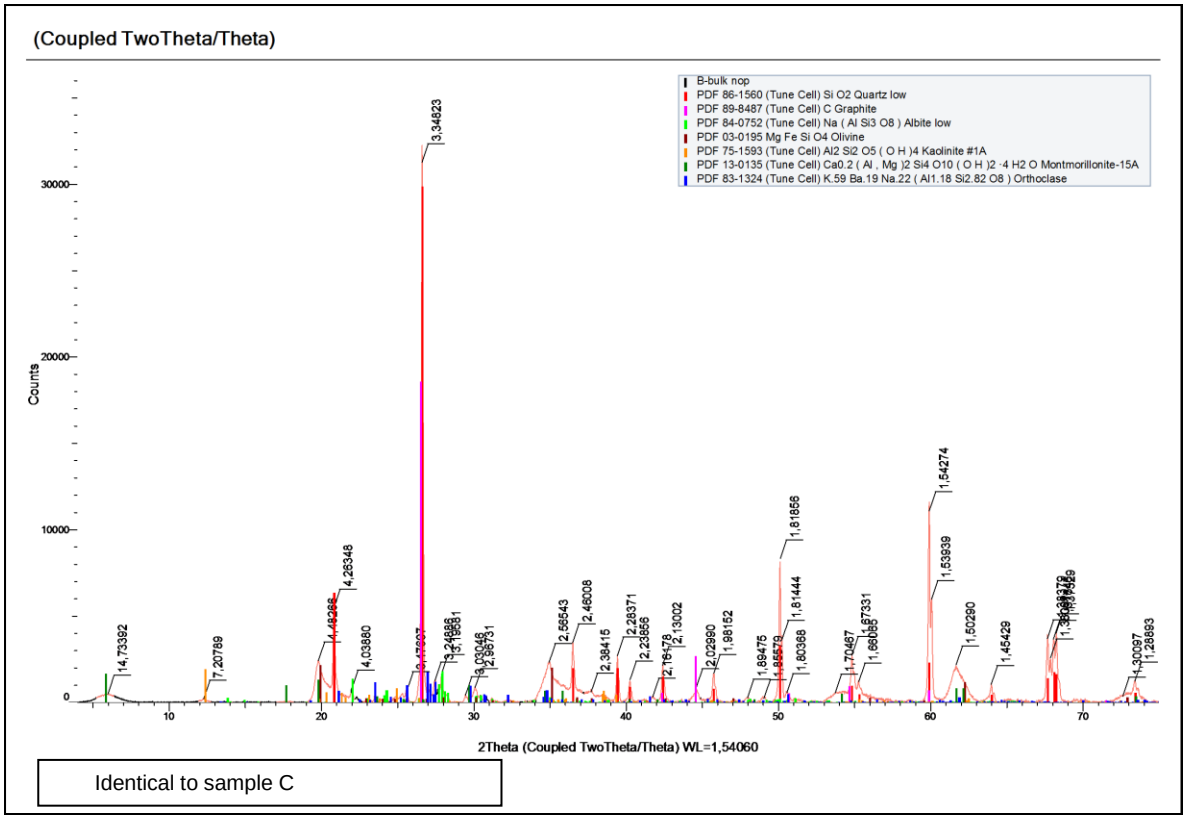

Identical to sample C

D

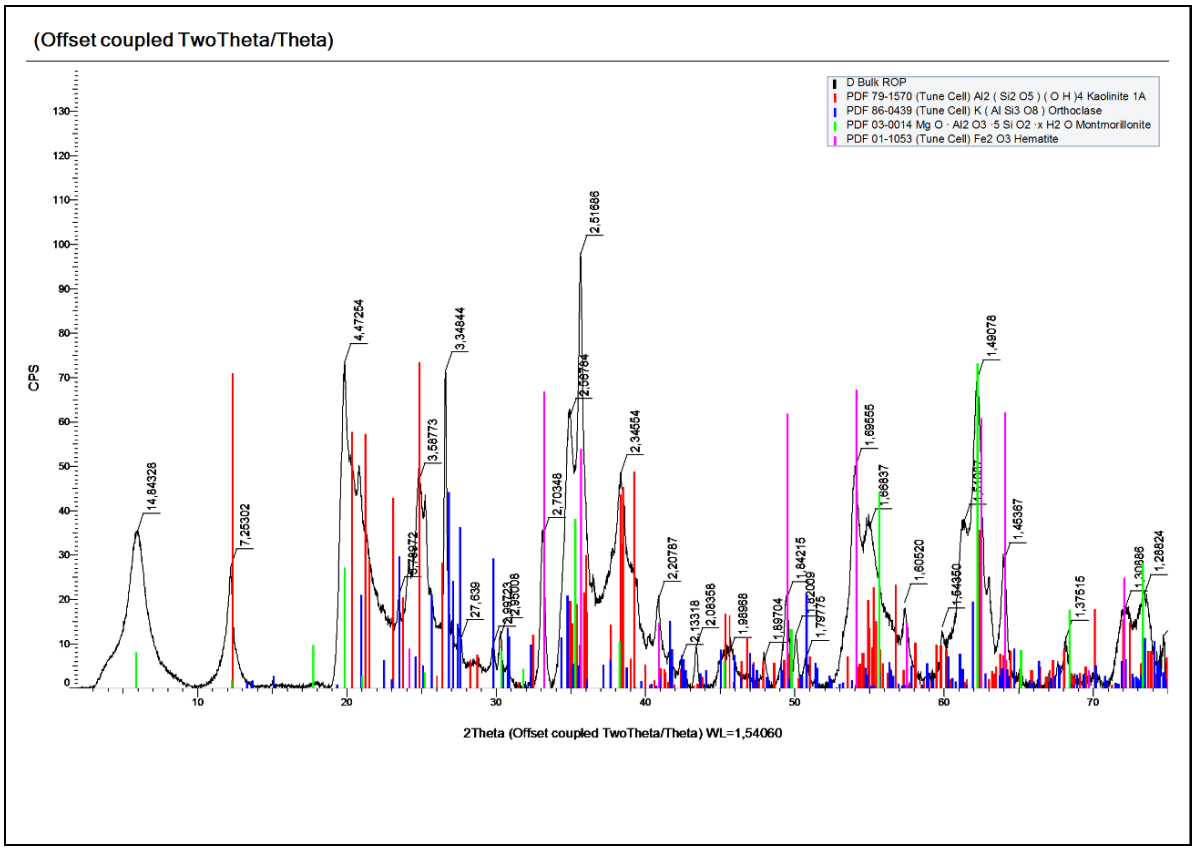
(Offset coupled TwoTheta/Theta)
D Bulk ROP
PDF 79-1570 (Tune Cell) Al2 (Si2 O5) (O H)4 Kaolinite 1A
PDF 86-0439 (Tune Cell) K (Al Si3 O8) Orthoclase
PDF 03-0014 Mg O · Al2 O3 · 5 Si O2 · x H2 O Montmorillonite
PDF 01-1053 (Tune Cell) Fe2 O3 Hematite
CPS
14,84328
7,25302
4,47254
3,58773
3,34844
2,70348
2,51686
2,34654
2,20787
1,98968
1,84215
1,69565
1,68837
1,60520
1,49078
1,45367
1,37515
1,28824
2Theta (Offset coupled TwoTheta/Theta) WL=1,54060

E

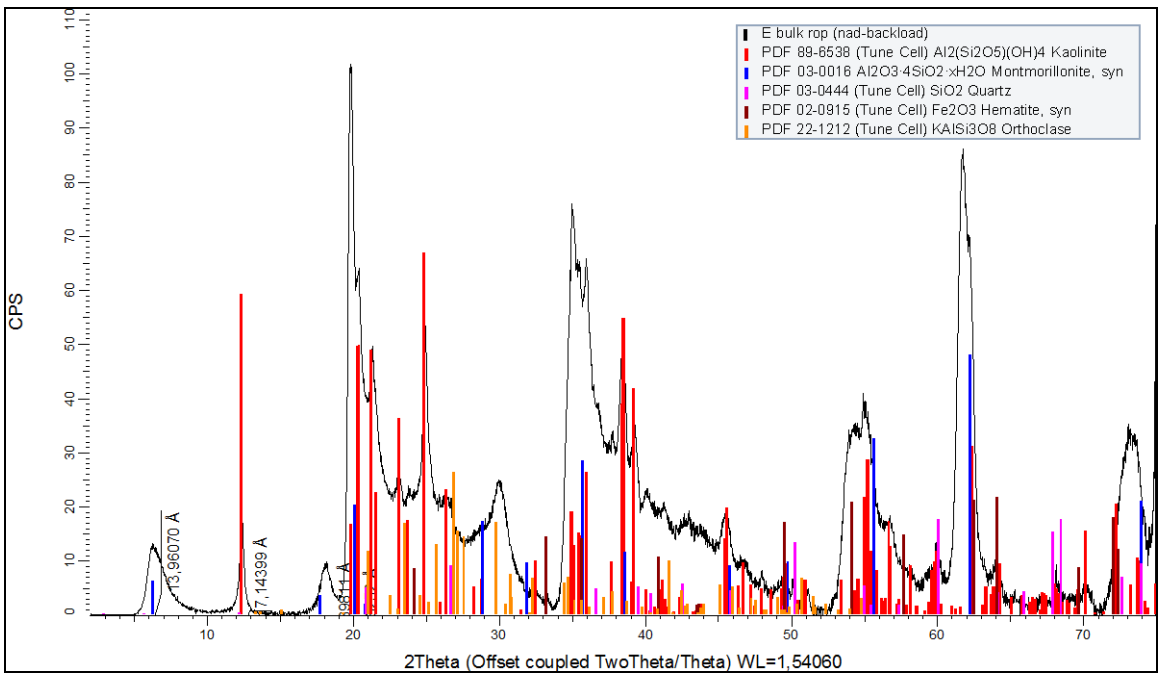
E bulk rop (nad-backload)
PDF 89-6538 (Tune Cell) Al2(Si2O5)(OH)4 Kaolinite
PDF 03-0016 Al2O3·4SiO2·xH2O Montmorillonite, syn
PDF 03-0444 (Tune Cell) SiO2 Quartz
PDF 02-0915 (Tune Cell) Fe2O3 Hematite, syn
PDF 22-1212 (Tune Cell) KAlSi3O8 Orthoclase
CPS
13,96070 Å
7,14399 Å
2Theta (Offset coupled TwoTheta/Theta) WL=1,54060

F

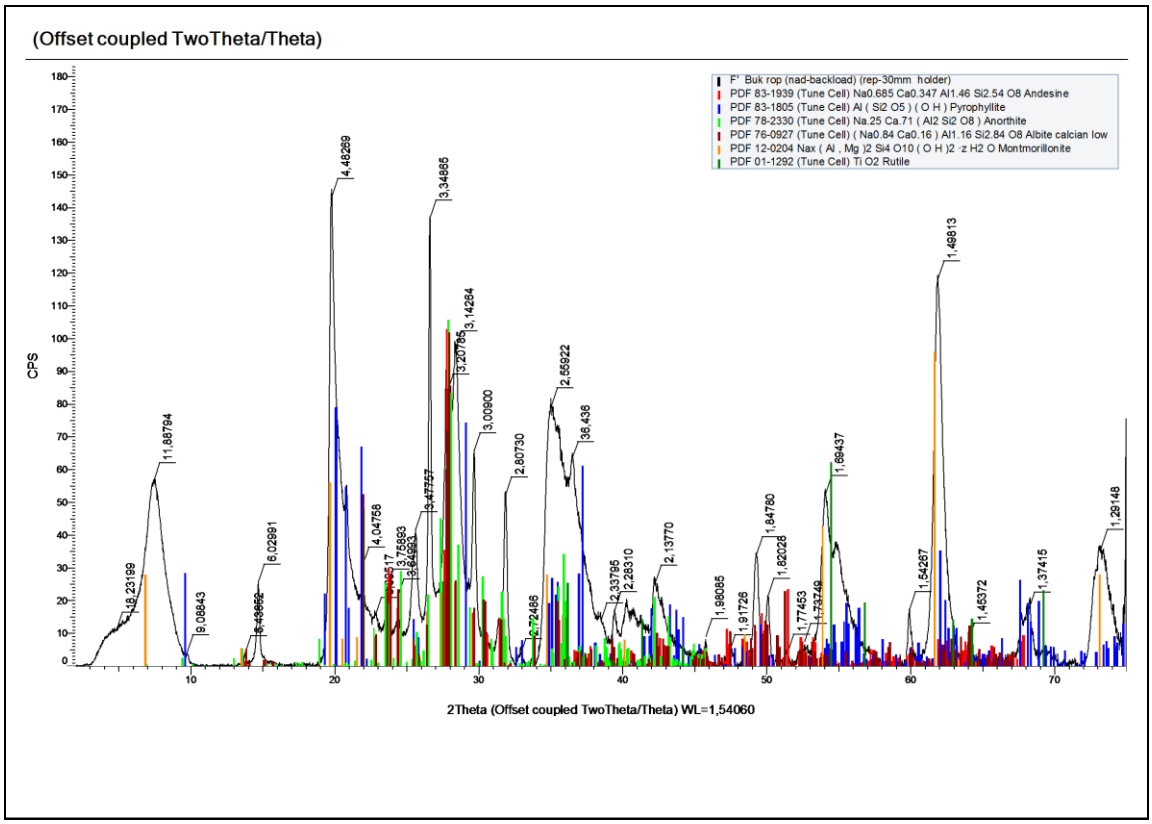
(Offset coupled TwoTheta/Theta)
F' Buk rop (nad-backload) (rep-30mm holder)
PDF 83-1939 (Tune Cell) Na0.685 Ca0.347 Al1.46 Si2.54 O8 Andesine
PDF 83-1805 (Tune Cell) Al (Si2 O5) (O H) Pyrophyllite
PDF 78-2330 (Tune Cell) Na.25 Ca.71 (Al2 Si2 O8) Anorthite
PDF 76-0927 (Tune Cell) (Na0.84 Ca0.16) Al1.16 Si2.84 O8 Albite calcian low
PDF 12-0204 Nax (Al , Mg)2 Si4 O10 (O H)2 ·z H2 O Montmorillonite
PDF 01-1292 (Tune Cell) Ti O2 Rutile
CPS
2Theta (Offset coupled TwoTheta/Theta) WL=1,54060

G

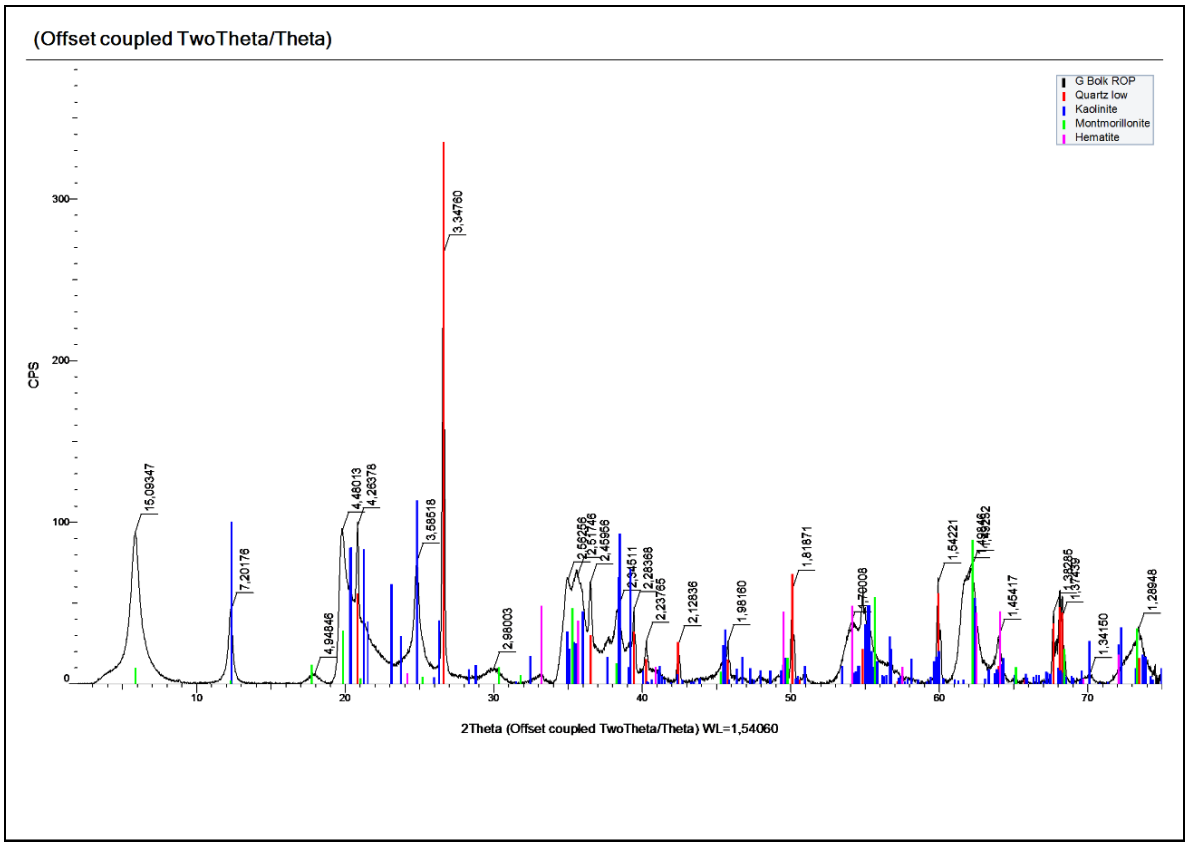
(Offset coupled TwoTheta/Theta)
G Bolk ROP
Quartz low
Kaolinite
Montmorillonite
Hematite
CPS
2Theta (Offset coupled TwoTheta/Theta) WL=1,54060

H

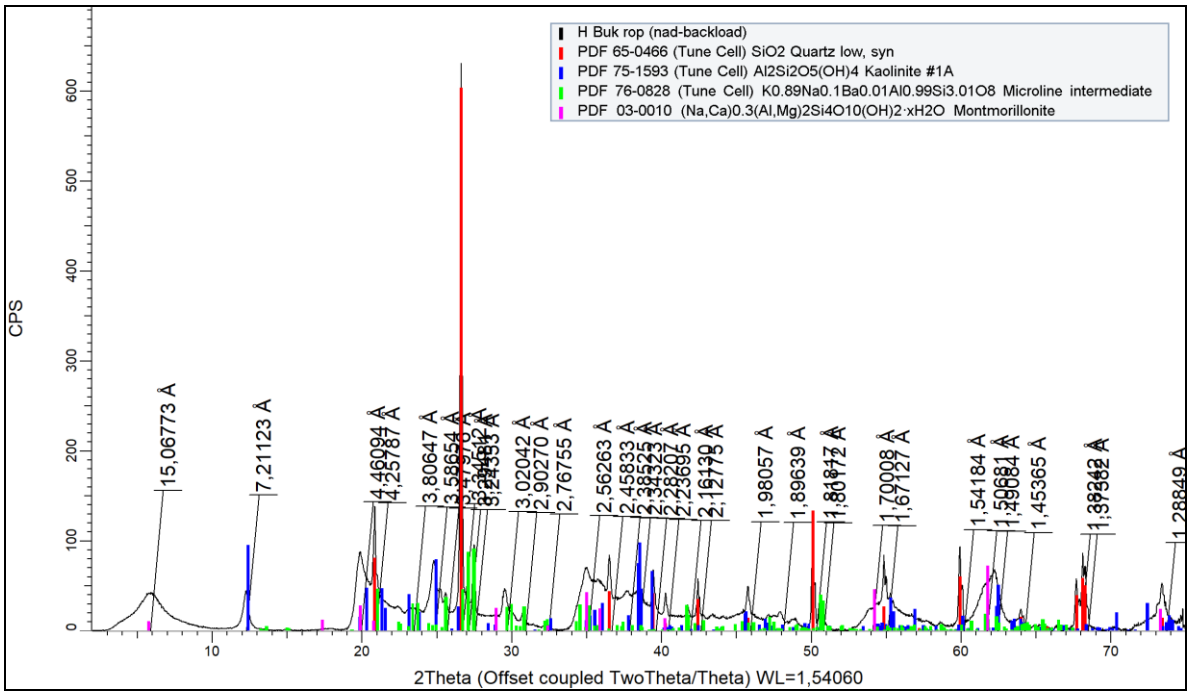
H Buk rop (nad-backload)
PDF 65-0466 (Tune Cell) SiO2 Quartz low, syn
PDF 75-1593 (Tune Cell) Al2Si2O5(OH)4 Kaolinite #1A
PDF 76-0828 (Tune Cell) K0.89Na0.1Ba0.01Al0.99Si3.01O8 Microline intermediate
PDF 03-0010 (Na,Ca)0.3(Al,Mg)2Si4O10(OH)2·xH2O Montmorillonite
CPS
2Theta (Offset coupled TwoTheta/Theta) WL=1,54060

I

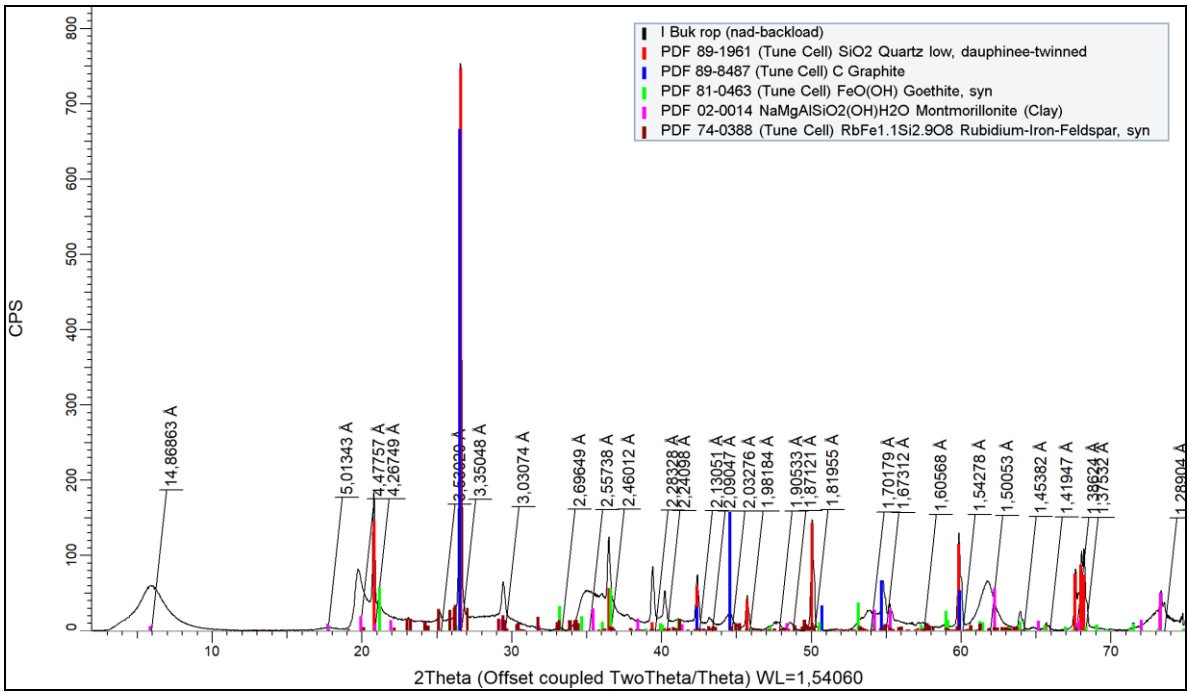
I Buk rop (nad-backload)
PDF 89-1961 (Tune Cell) SiO2 Quartz low, dauphinee-twinned
PDF 89-8487 (Tune Cell) C Graphite
PDF 81-0463 (Tune Cell) FeO(OH) Goethite, syn
PDF 02-0014 NaMgAlSiO2(OH)H2O Montmorillonite (Clay)
PDF 74-0388 (Tune Cell) RbFe1.1Si2.9O8 Rubidium-Iron-Feldspar, syn
CPS
2Theta (Offset coupled TwoTheta/Theta) WL=1,54060

J

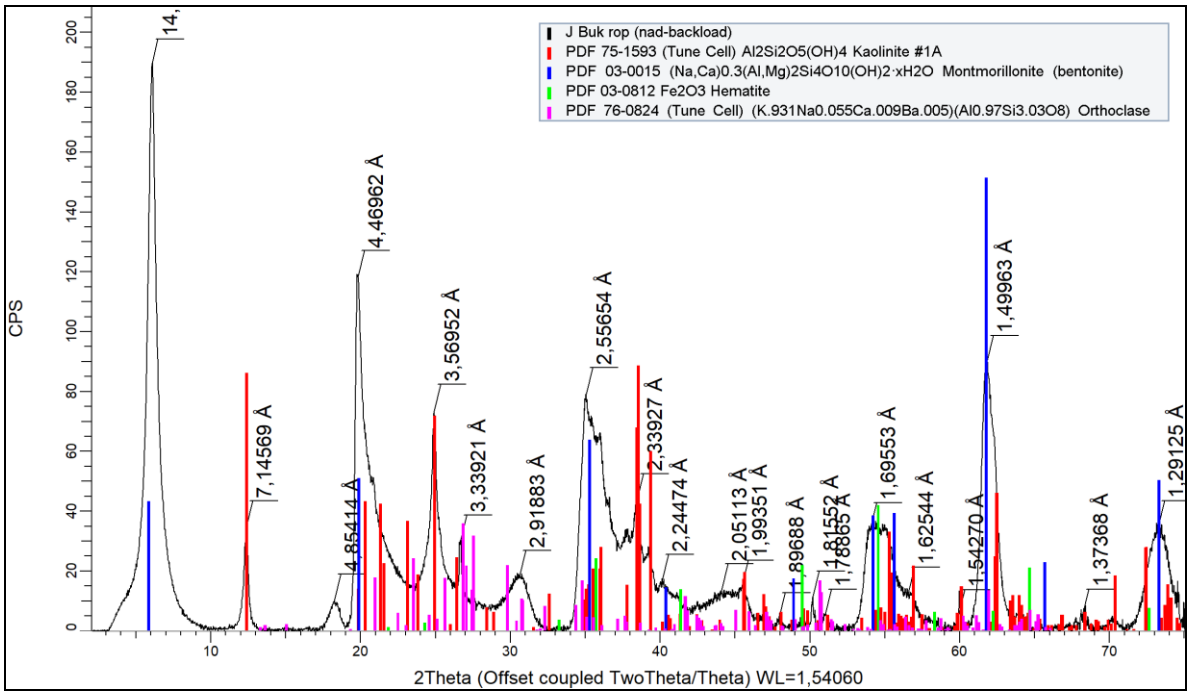
J Buk rop (nad-backload)
PDF 75-1593 (Tune Cell) Al2Si2O5(OH)4 Kaolinite #1A
PDF 03-0015 (Na,Ca)0.3(Al,Mg)2Si4O10(OH)2·xH2O Montmorillonite (bentonite)
PDF 03-0812 Fe2O3 Hematite
PDF 76-0824 (Tune Cell) (K.931Na0.055Ca.009Ba.005)(Al0.97Si3.03O8) Orthoclase
CPS
14,
7,14569 Å
4,46962 Å
4,85414 Å
3,56952 Å
3,33921 Å
2,91883 Å
2,55654 Å
2,33927 Å
2,24474 Å
2,05113 Å
1,99351 Å
1,89688 Å
1,81552 Å
1,78865 Å
1,69553 Å
1,62544 Å
1,54270 Å
1,49963 Å
1,37368 Å
1,29125 Å
2Theta (Offset coupled TwoTheta/Theta) WL=1,54060

K

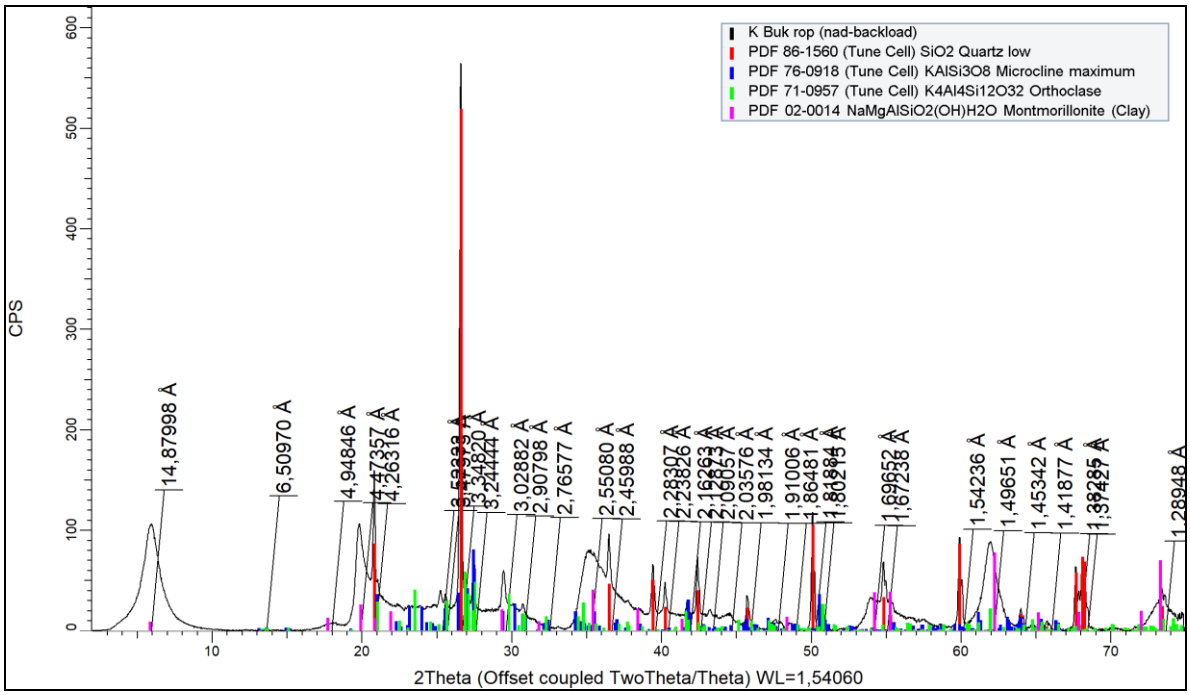
K Buk rop (nad-backload)
PDF 86-1560 (Tune Cell) SiO2 Quartz low
PDF 76-0918 (Tune Cell) KAlSi3O8 Microcline maximum
PDF 71-0957 (Tune Cell) K4Al4Si12O32 Orthoclase
PDF 02-0014 NaMgAlSiO2(OH)H2O Montmorillonite (Clay)
CPS
14,87998 Å
6,50970 Å
4,94846 Å
4,47357 Å
4,26316 Å
3,34820 Å
3,24444 Å
3,02882 Å
2,90798 Å
2,76577 Å
2,55080 Å
2,45988 Å
2,28307 Å
2,23826 Å
2,16263 Å
2,09857 Å
2,03576 Å
1,98134 Å
1,91006 Å
1,86481 Å
1,80215 Å
1,69552 Å
1,67238 Å
1,54236 Å
1,49651 Å
1,45342 Å
1,41877 Å
1,28948 Å
2Theta (Offset coupled TwoTheta/Theta) WL=1,54060

L

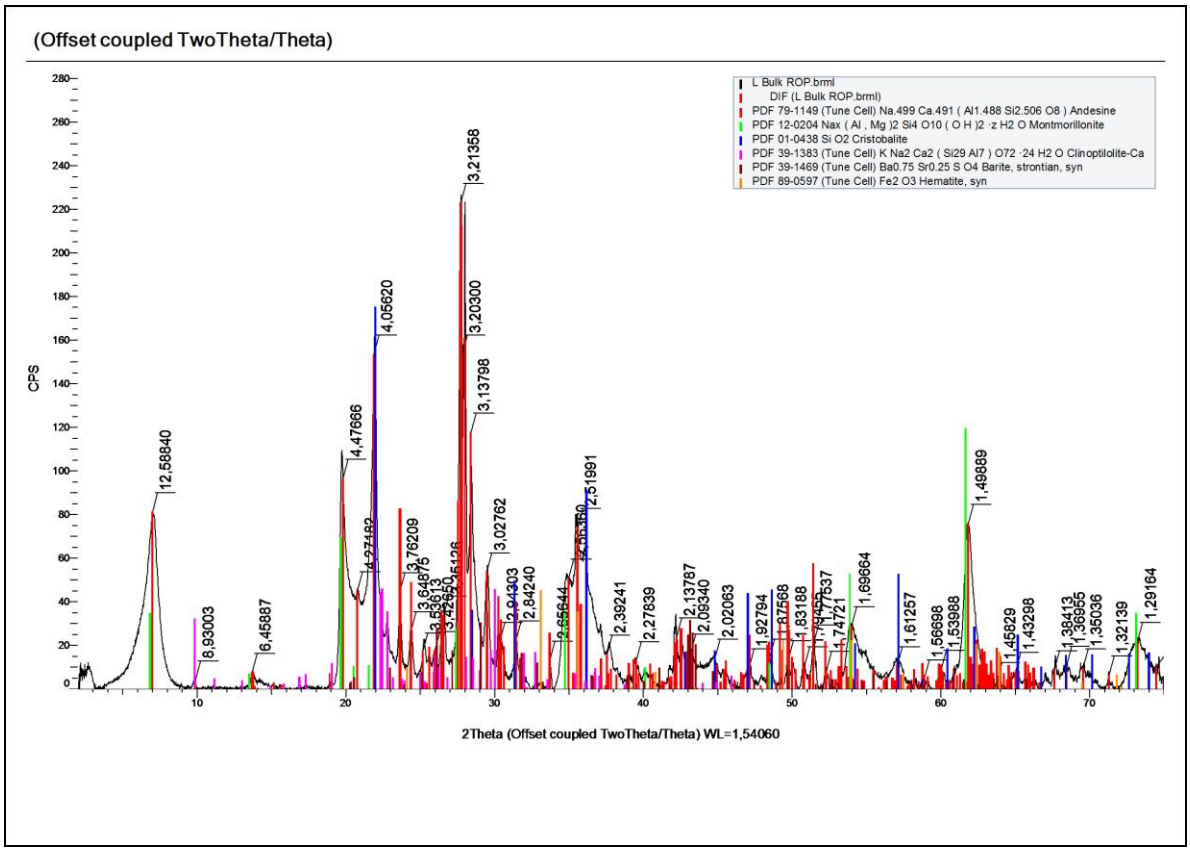
(Offset coupled TwoTheta/Theta)
L Bulk ROP.brml
DIF (L Bulk ROP.brml)
PDF 79-1149 (Tune Cell) Na.499 Ca.491 (Al1.488 Si2.506 O8) Andesine
PDF 12-0204 Nax (Al , Mg)2 Si4 O10 (O H)2 ·z H2 O Montmorillonite
PDF 01-0438 Si O2 Cristobalite
PDF 39-1383 (Tune Cell) K Na2 Ca2 (Si29 Al7) O72 ·24 H2 O Clinoptilolite-Ca
PDF 39-1469 (Tune Cell) Ba0.75 Sr0.25 S O4 Barite, strontian, syn
PDF 89-0597 (Tune Cell) Fe2 O3 Hematite, syn
CPS
2Theta (Offset coupled TwoTheta/Theta) WL=1,54060

APPENDIX D

REITVELD REFINEMENT FIT ON TOPAS V5.1 FOR STUDIED SAMPLES

A

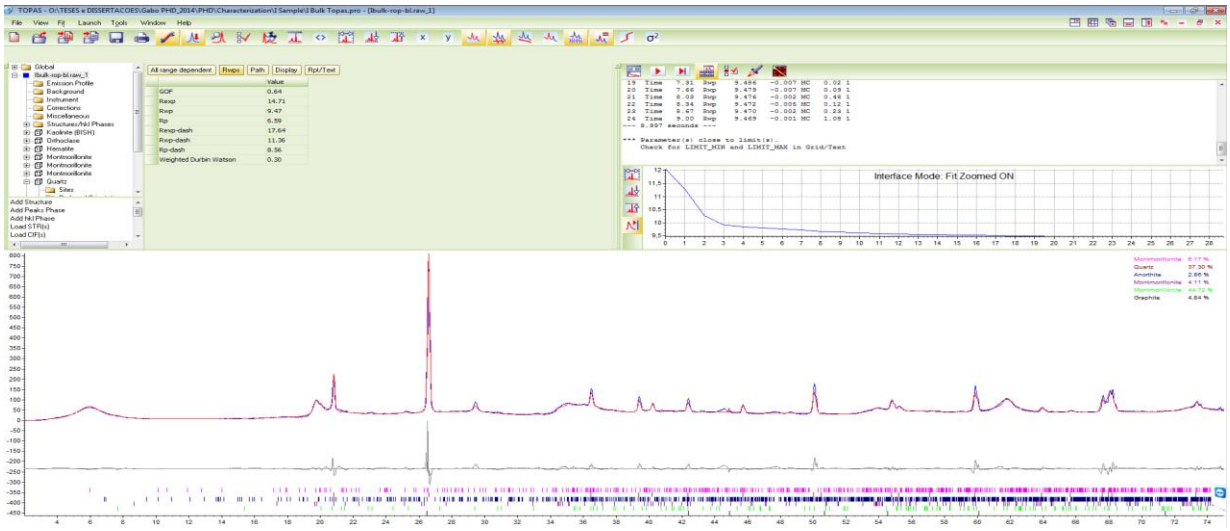

C

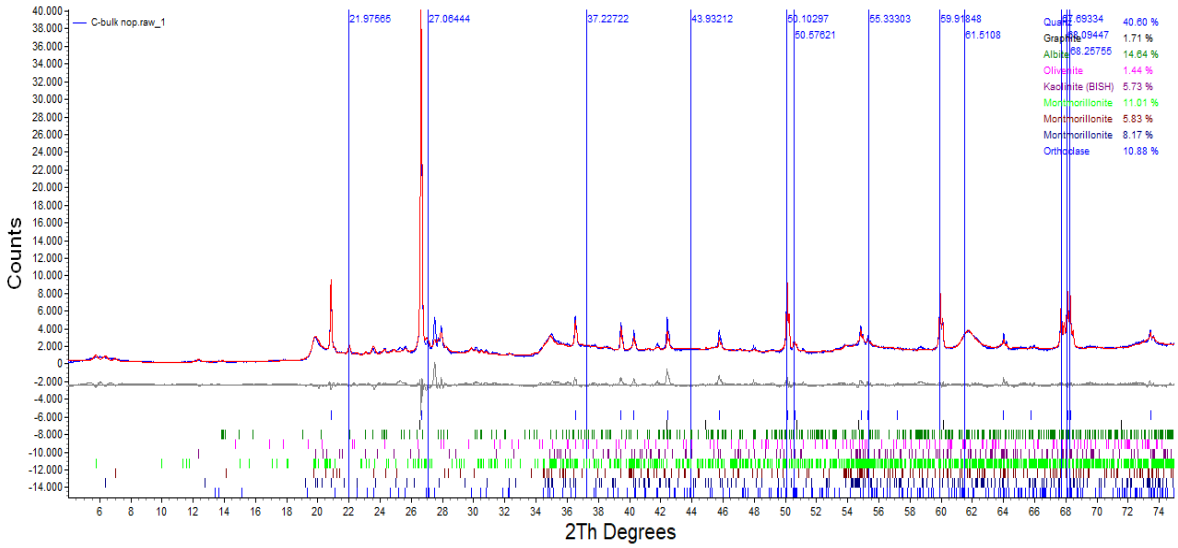

D

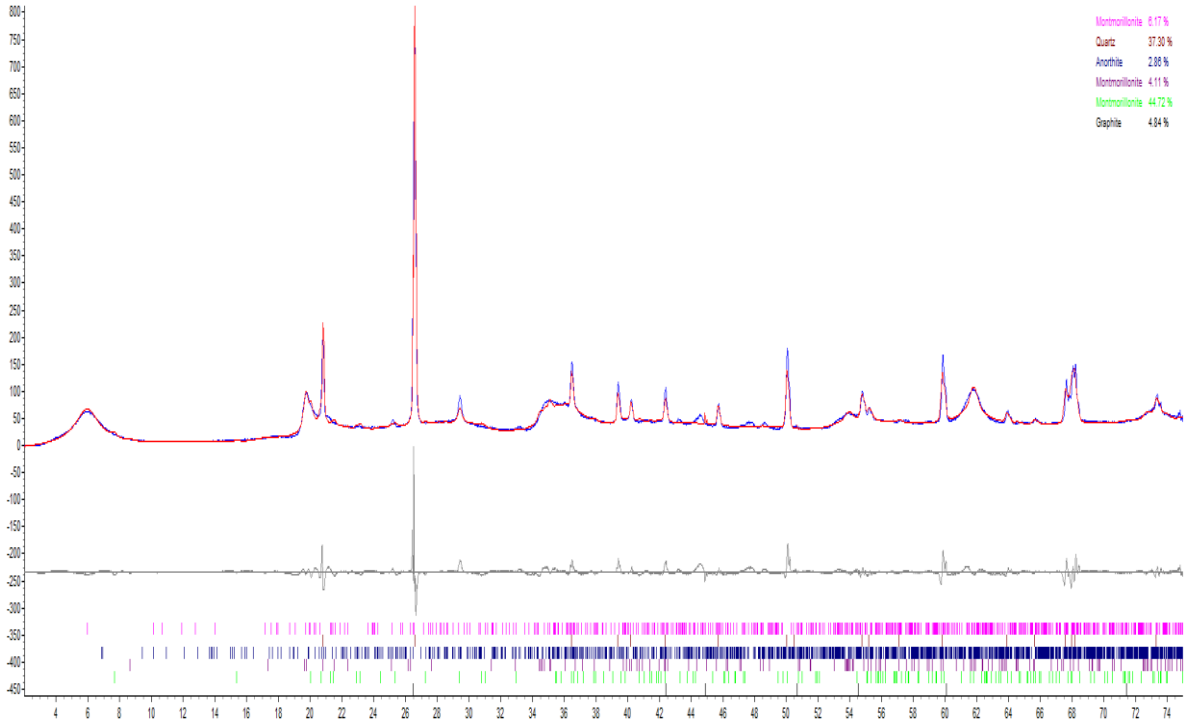
Montmorillonite 8.17 %
Quartz 37.30 %
Anorthite 2.86 %
Montmorillonite 4.11 %
Montmorillonite 44.72 %
Graphite 4.84 %

E

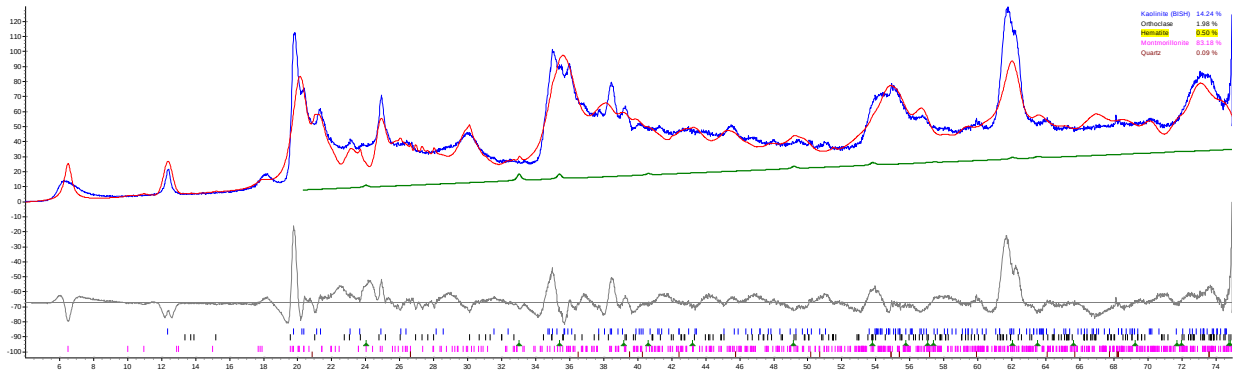
Kaolinite (BISH) 14.24 %
Orthoclase 1.98 %
Hematite 0.50 %
Montmorillonite 83.18 %
Quartz 0.09 %

F

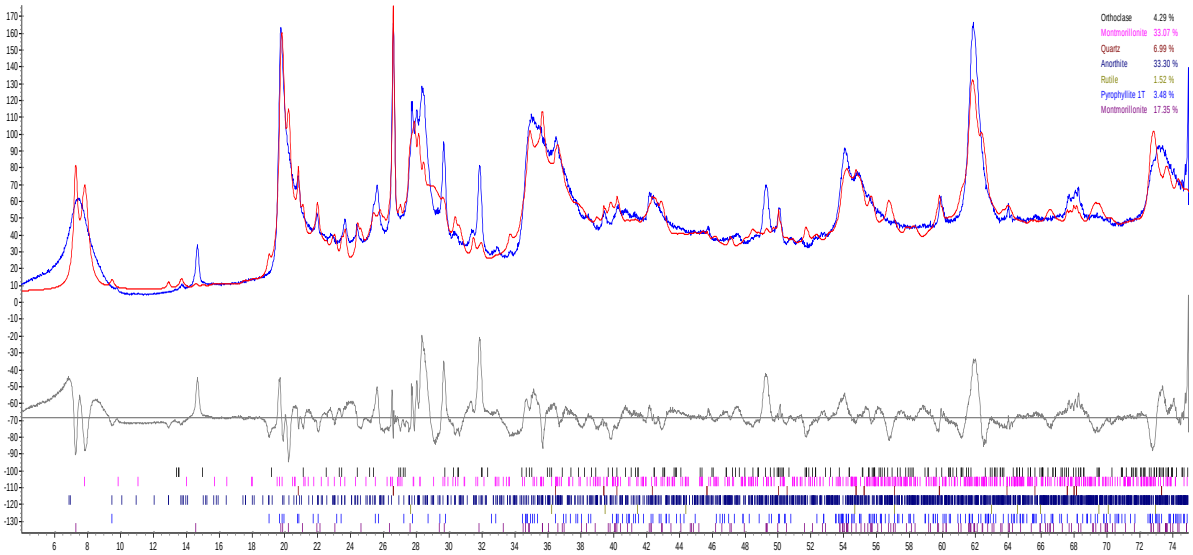
Orthoclase 4.29 %
Montmorillonite 33.07 %
Quartz 6.99 %
Anorthite 33.30 %
Rutile 1.52 %
Pyrophyllite 1T 3.48 %
Montmorillonite 17.35 %

G

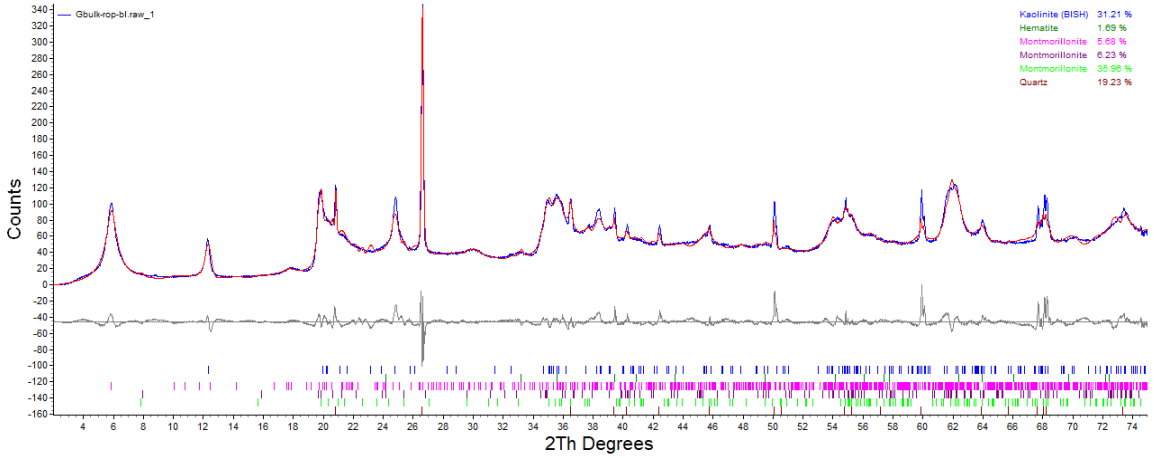
Gbulk-rop-bl.raw_1
Kaolinite (BISH) 31.21 %
Hematite 1.69 %
Montmorillonite 5.68 %
Montmorillonite 6.23 %
Montmorillonite 35.96 %
Quartz 19.23 %
Counts
2Th Degrees

H

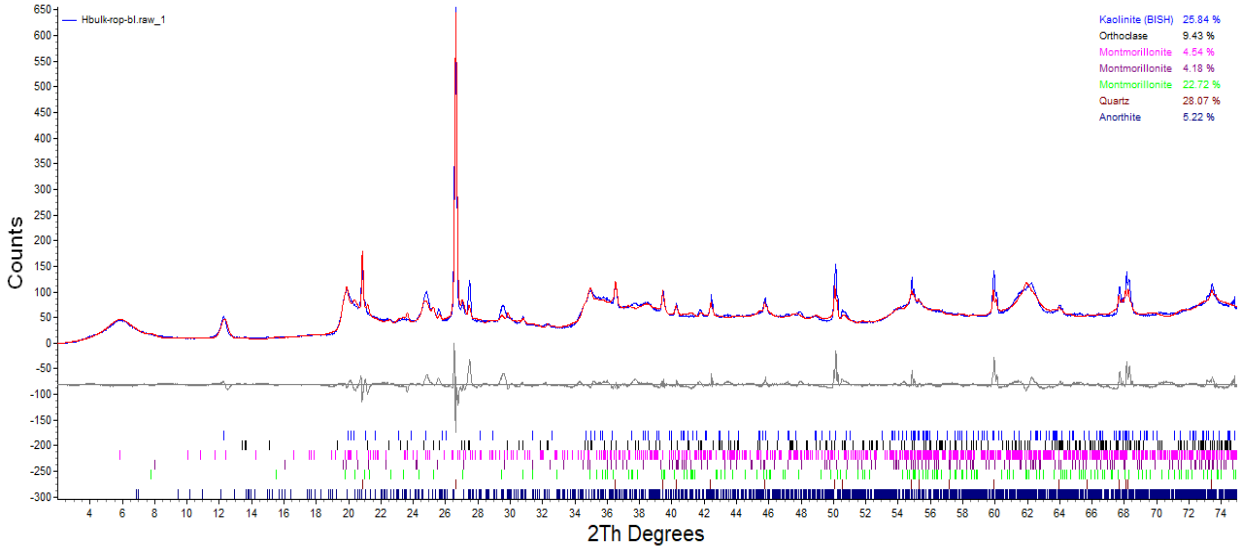
Hbulk-rop-bl.raw_1
Kaolinite (BISH) 25.84 %
Orthoclase 9.43 %
Montmorillonite 4.54 %
Montmorillonite 4.18 %
Montmorillonite 22.72 %
Quartz 28.07 %
Anorthite 5.22 %
Counts
2Th Degrees

I

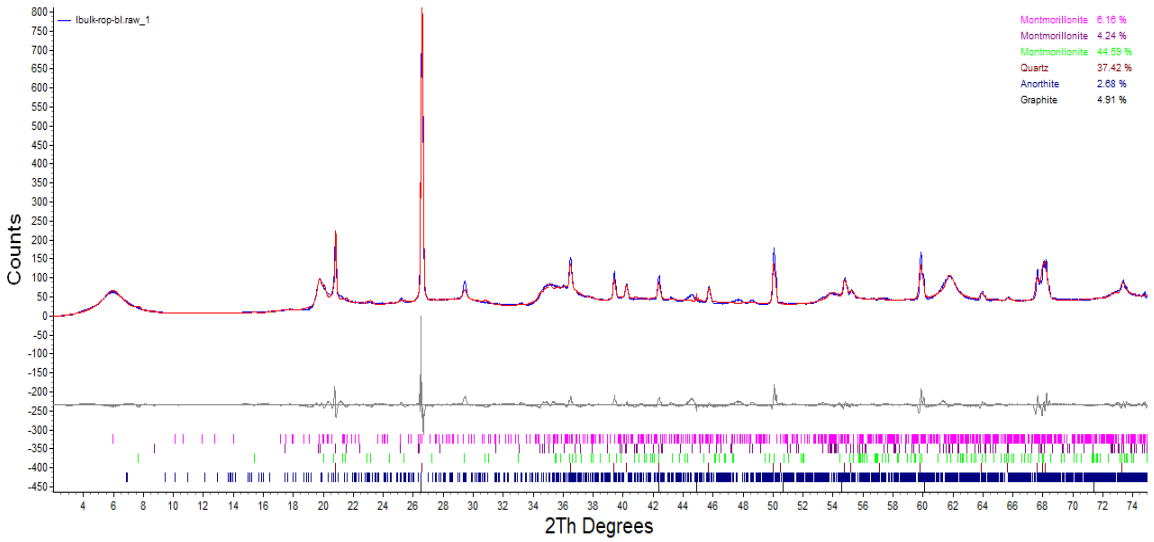
Ibulk-rop-bl.raw_1
Montmorillonite 6.16 %
Montmorillonite 4.24 %
Montmorillonite 44.59 %
Quartz 37.42 %
Anorthite 2.68 %
Graphite 4.91 %
Counts
2Th Degrees

J

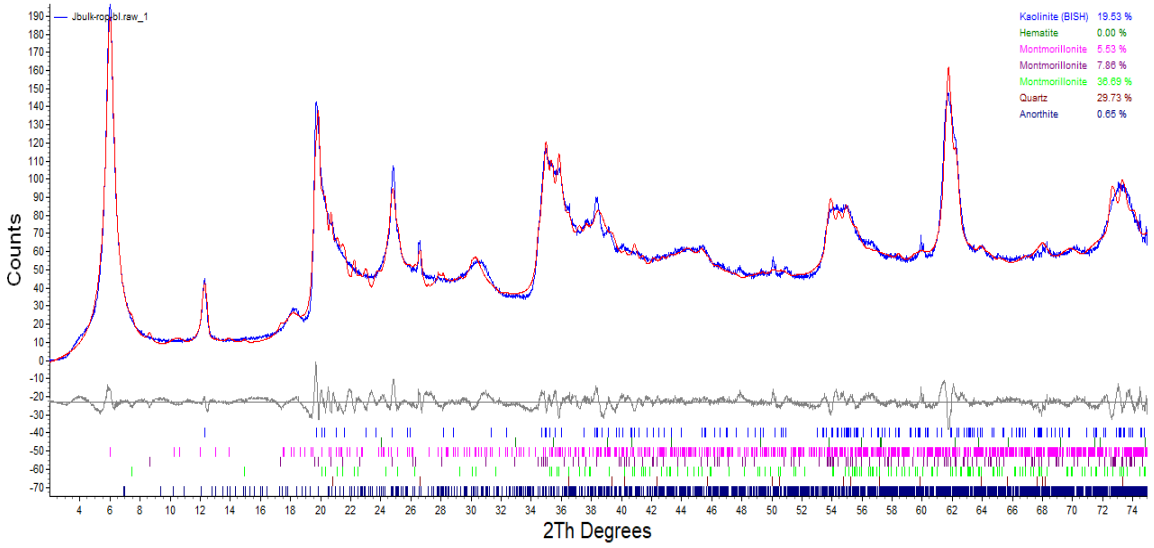
Jbulk-rop-bl.raw_1
Kaolinite (BISH) 19.53 %
Hematite 0.00 %
Montmorillonite 5.53 %
Montmorillonite 7.86 %
Montmorillonite 36.69 %
Quartz 29.73 %
Anorthite 0.65 %
Counts
2Th Degrees

K

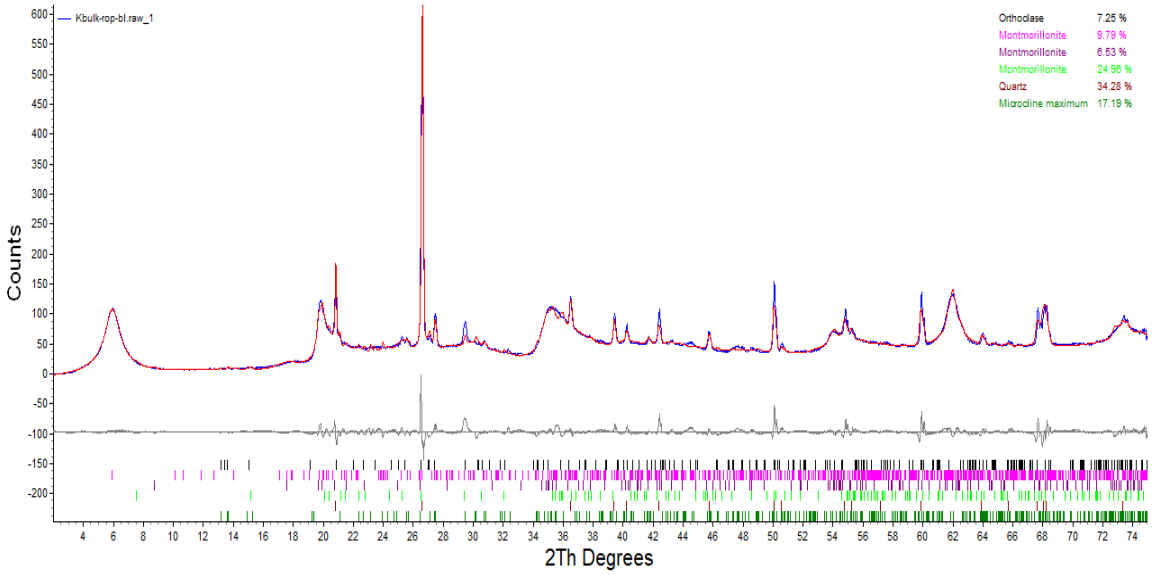
Kbulk-rop-bl.raw_1
Orthoclase 7.25 %
Montmorillonite 9.79 %
Montmorillonite 6.53 %
Montmorillonite 24.96 %
Quartz 34.28 %
Microcline maximum 17.19 %
Counts
2Th Degrees

L

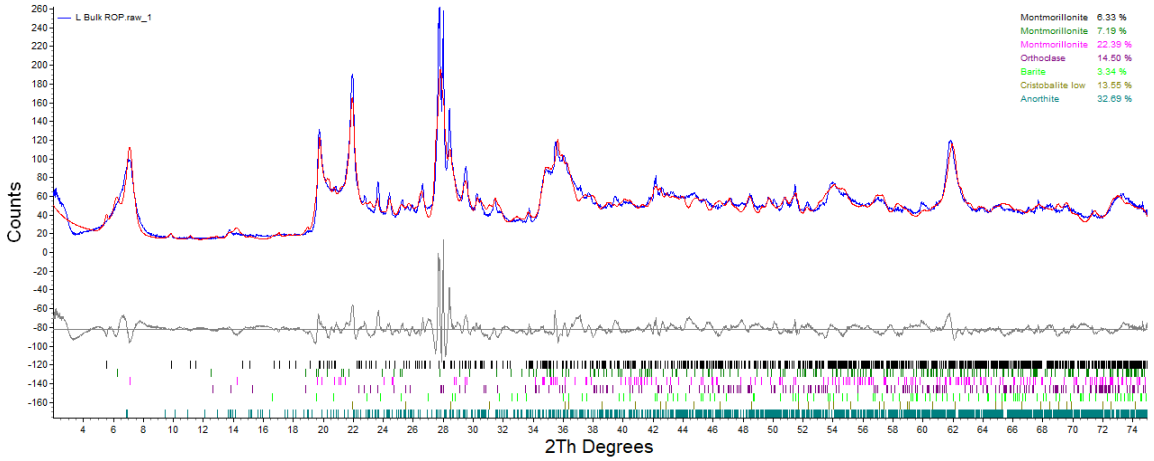
L Bulk ROP.raw_1
Montmorillonite 6.33 %
Montmorillonite 7.19 %
Montmorillonite 22.39 %
Orthoclase 14.50 %
Barite 3.34 %
Cristobalite low 13.55 %
Anorthite 32.69 %
Counts
2Th Degrees

APPENDIX E

ORIENTED SLIDES XRD BY SAMPLES

A

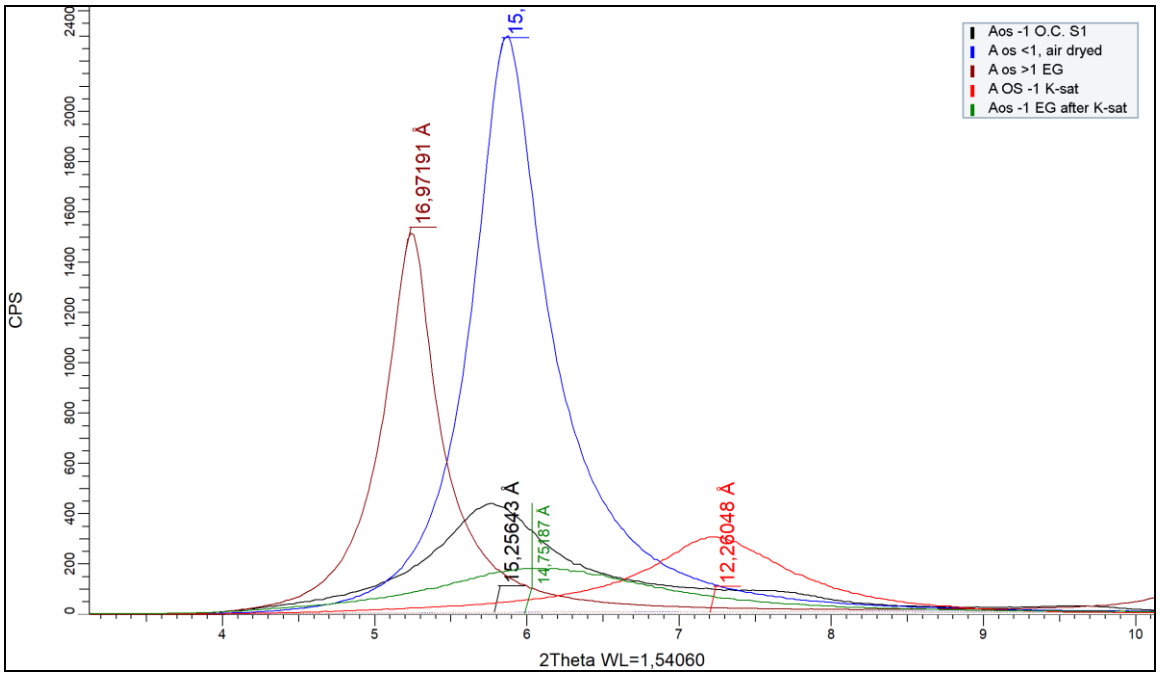

B

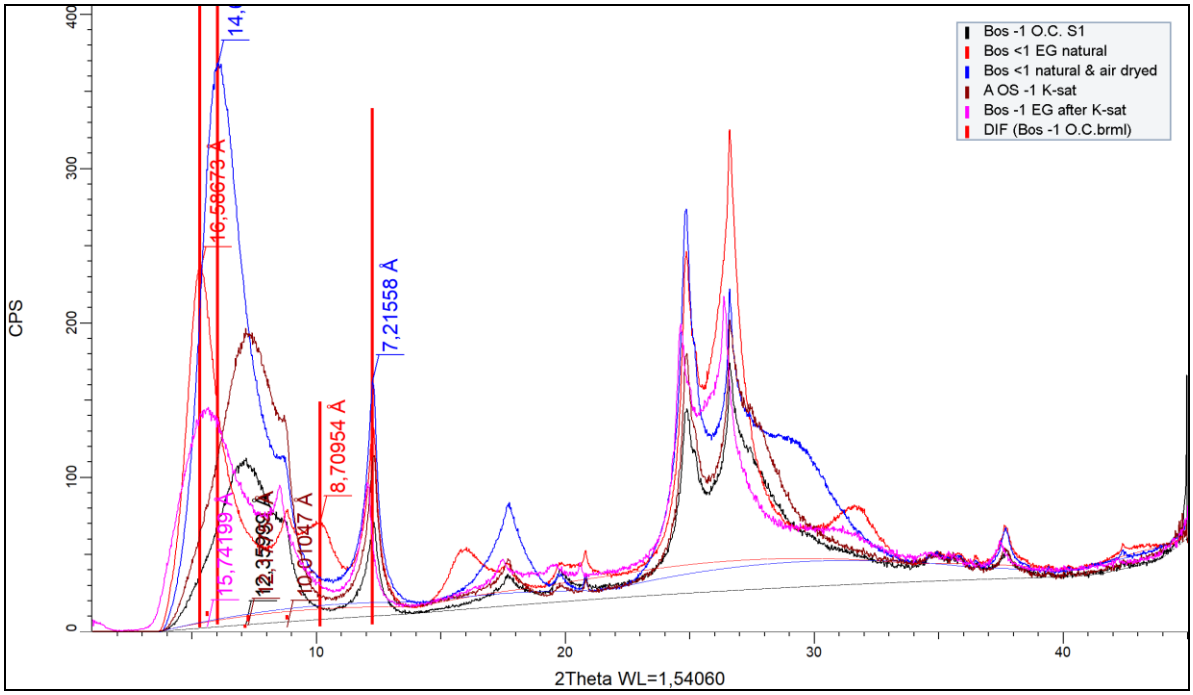
Bos -1 O.C. S1
Bos <1 EG natural
Bos <1 natural & air dryed
A OS -1 K-sat
Bos -1 EG after K-sat
DIF (Bos -1 O.C.brml)
CPS
16,56673 Å
7,21558 Å
8,70954 Å
15,74199 Å
12,35999 Å
10,01047 Å
2Theta WL=1,54060

C

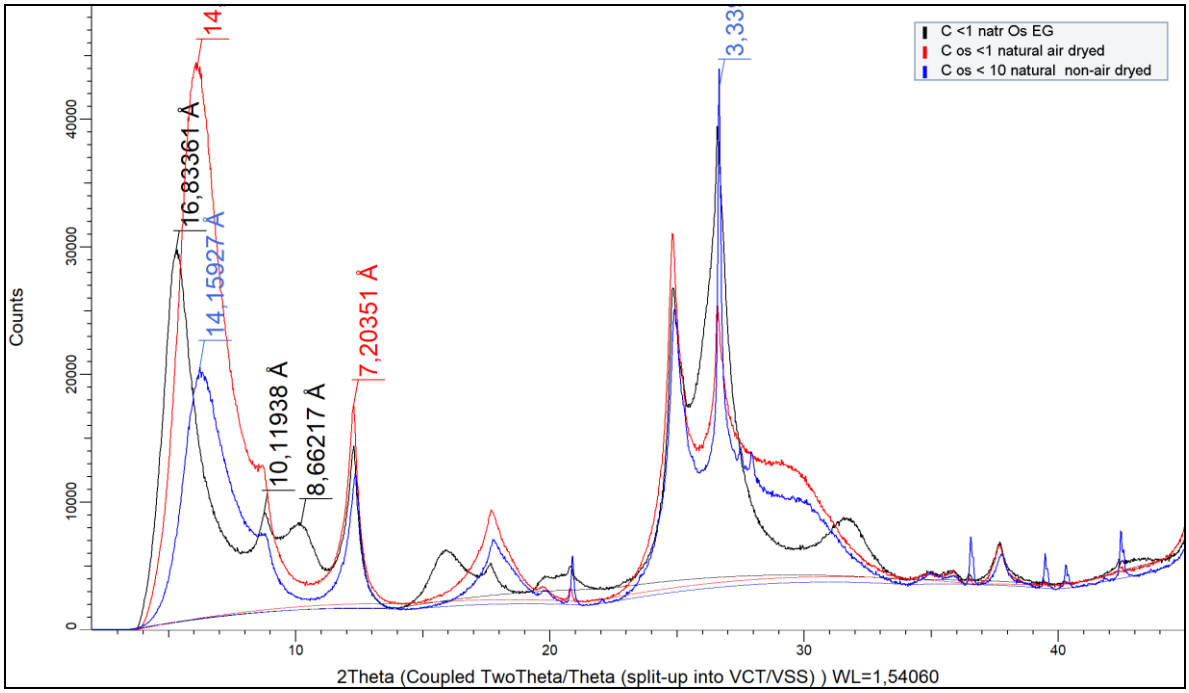
C <1 natr Os EG
C os <1 natural air dryed
C os < 10 natural non-air dryed
Counts
16,83361 Å
14,15927 Å
10,11938 Å
8,66217 Å
7,20351 Å
3,33
2Theta (Coupled TwoTheta/Theta (split-up into VCT/VSS)) WL=1,54060

D

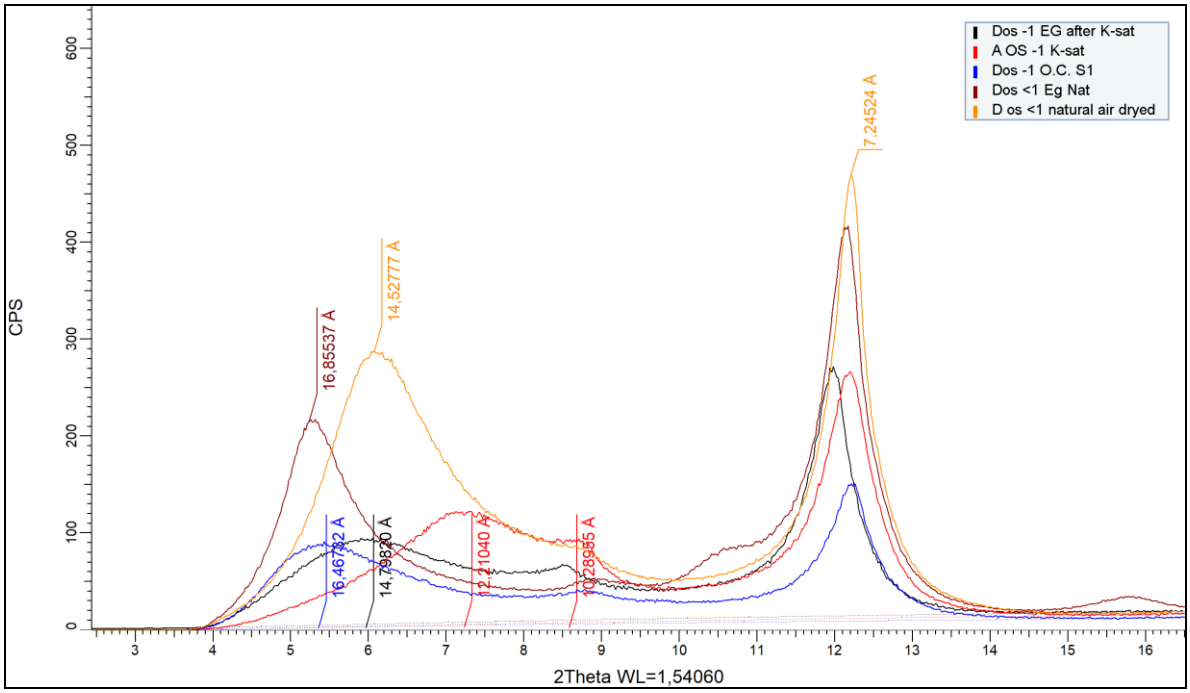
Dos -1 EG after K-sat
A OS -1 K-sat
Dos -1 O.C. S1
Dos <1 Eg Nat
D os <1 natural air dryed
7,24524 Å
14,52777 Å
16,85537 Å
16,46782 Å
14,79820 Å
12,21040 Å
10,28985 Å
CPS
2Theta WL=1,54060

E

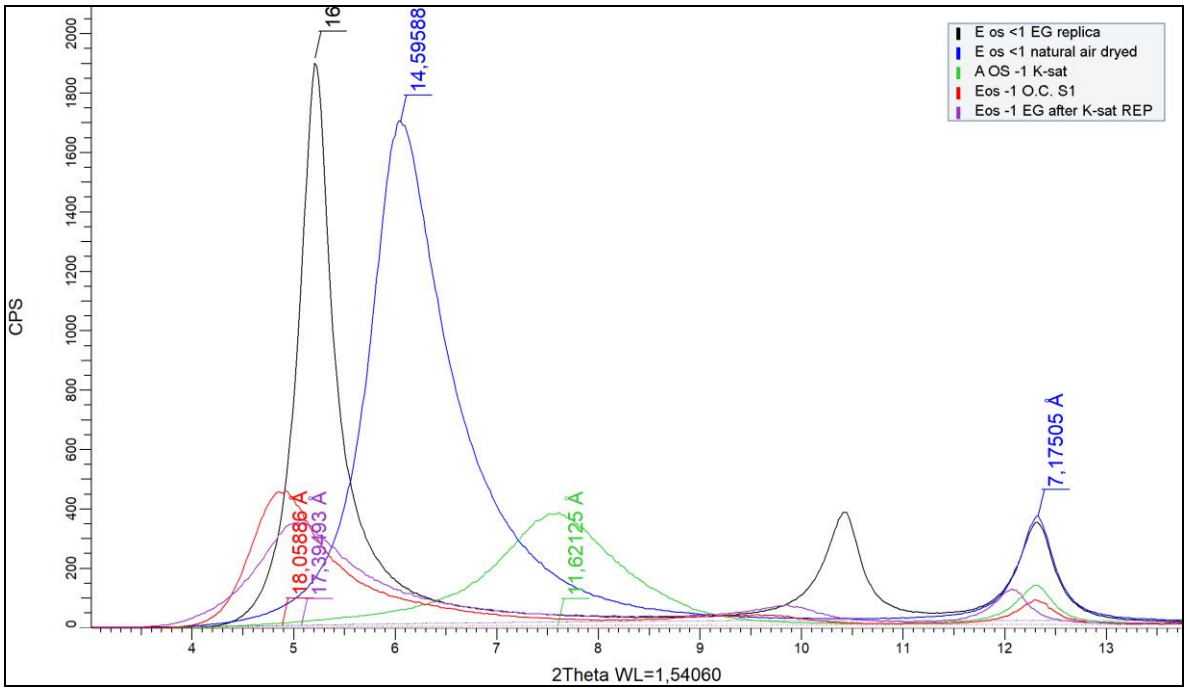
E os <1 EG replica
E os <1 natural air dryed
A OS -1 K-sat
Eos -1 O.C. S1
Eos -1 EG after K-sat REP
16
14,59588
18,05886 Å
17,39493 Å
11,62125 Å
7,17505 Å
CPS
2Theta WL=1,54060

F

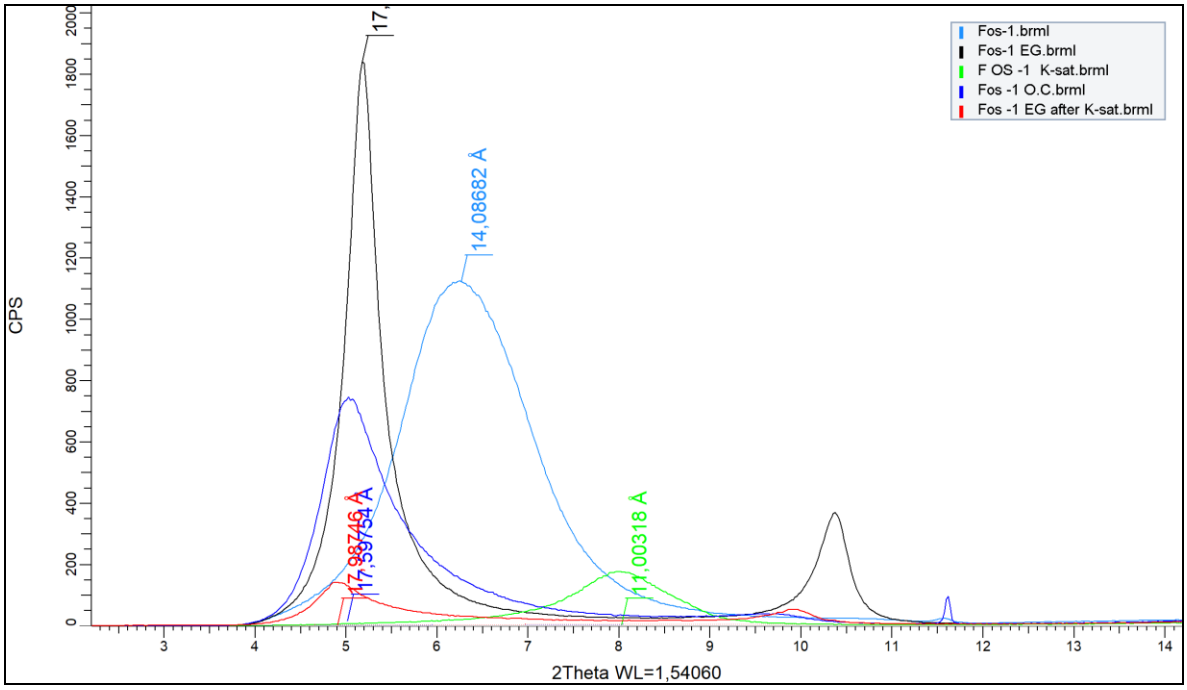
Fos-1.brml
Fos-1 EG.brml
F OS -1 K-sat.brml
Fos -1 O.C.brml
Fos -1 EG after K-sat.brml
14,08682 Å
11,00318 Å
CPS
2Theta WL=1,54060

G

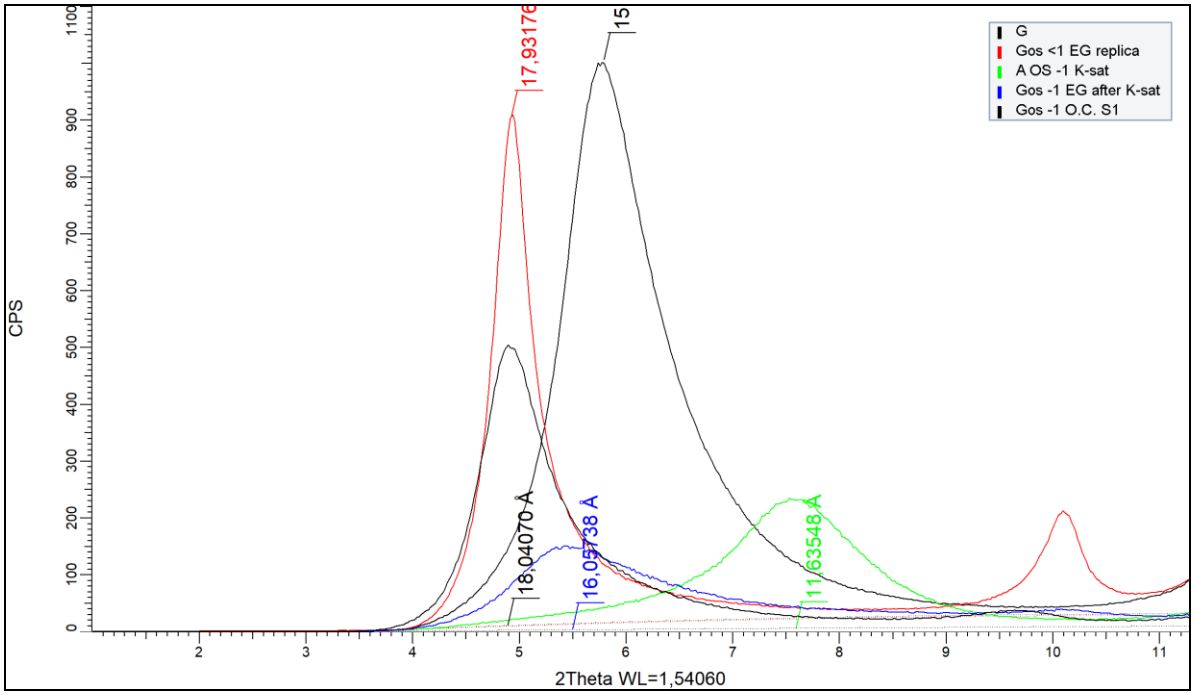
G
Gos <1 EG replica
A OS -1 K-sat
Gos -1 EG after K-sat
Gos -1 O.C. S1
17,93176
18,04070 Å
11,63548 Å
CPS
2Theta WL=1,54060

H

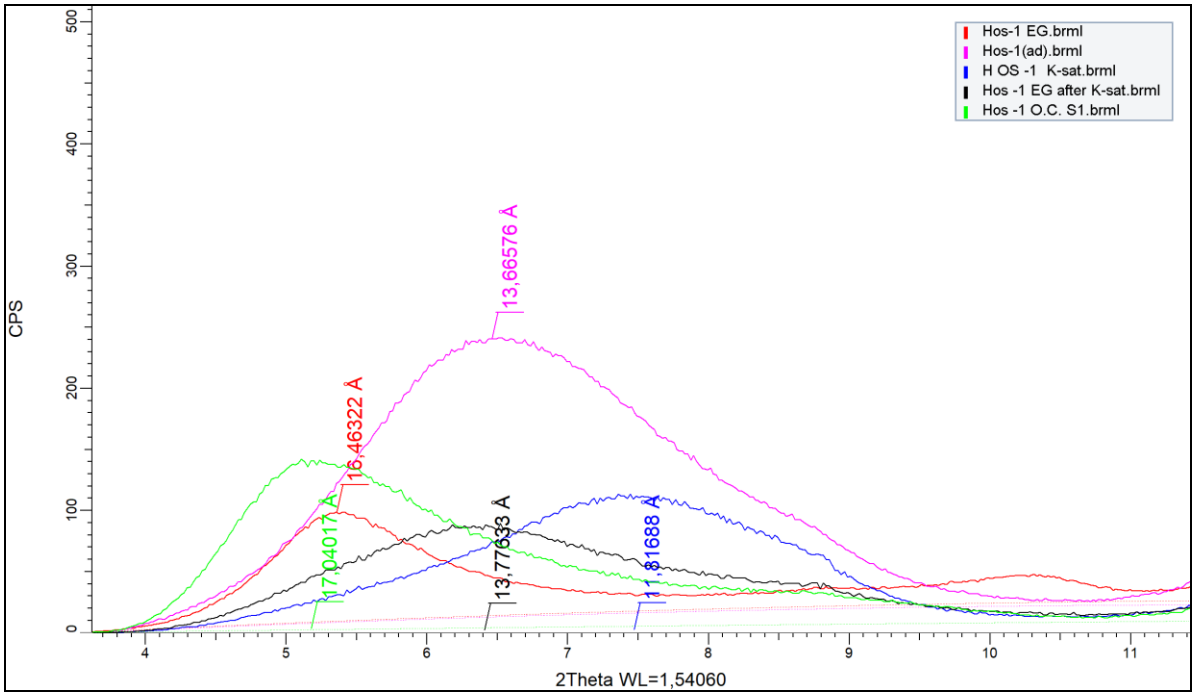
Hos-1 EG.brml
Hos-1(ad).brml
H OS -1 K-sat.brml
Hos -1 EG after K-sat.brml
Hos -1 O.C. S1.brml
CPS
13,66576 Å
16,46322 Å
17,04017 Å
13,77633 Å
11,81688 Å
2Theta WL=1,54060

I

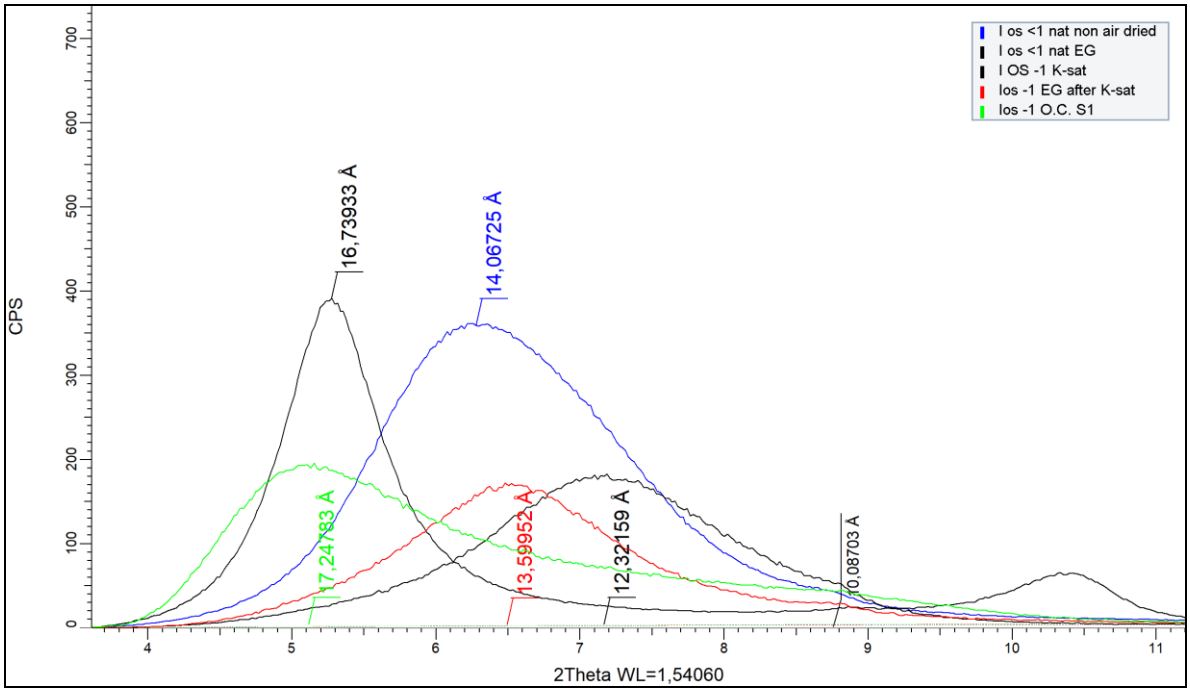
I os <1 nat non air dried
I os <1 nat EG
I OS -1 K-sat
Ios -1 EG after K-sat
Ios -1 O.C. S1
CPS
16,73933 Å
14,06725 Å
17,24783 Å
13,59952 Å
12,32159 Å
10,08703 Å
2Theta WL=1,54060

J

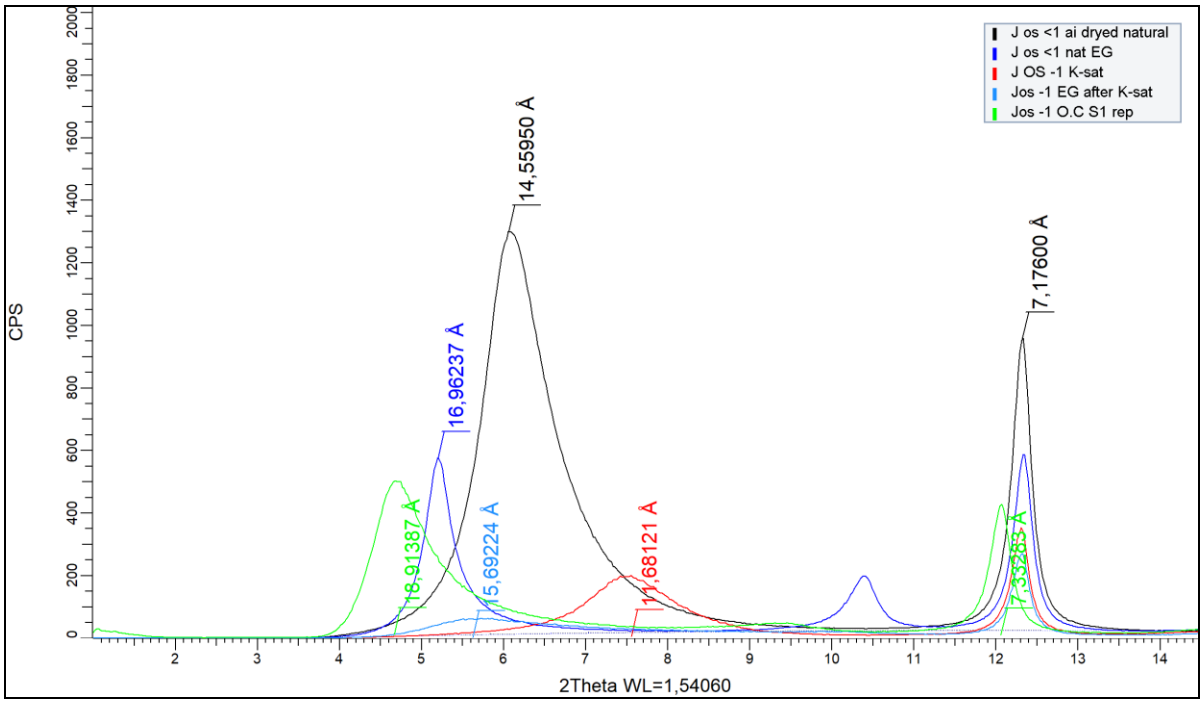
J os <1 ai dryed natural
J os <1 nat EG
J OS -1 K-sat
Jos -1 EG after K-sat
Jos -1 O.C S1 rep
14,55950 Å
16,96237 Å
7,17600 Å
18,91387 Å
15,69224 Å
11,68121 Å
7,33885 Å
CPS
2Theta WL=1,54060

K

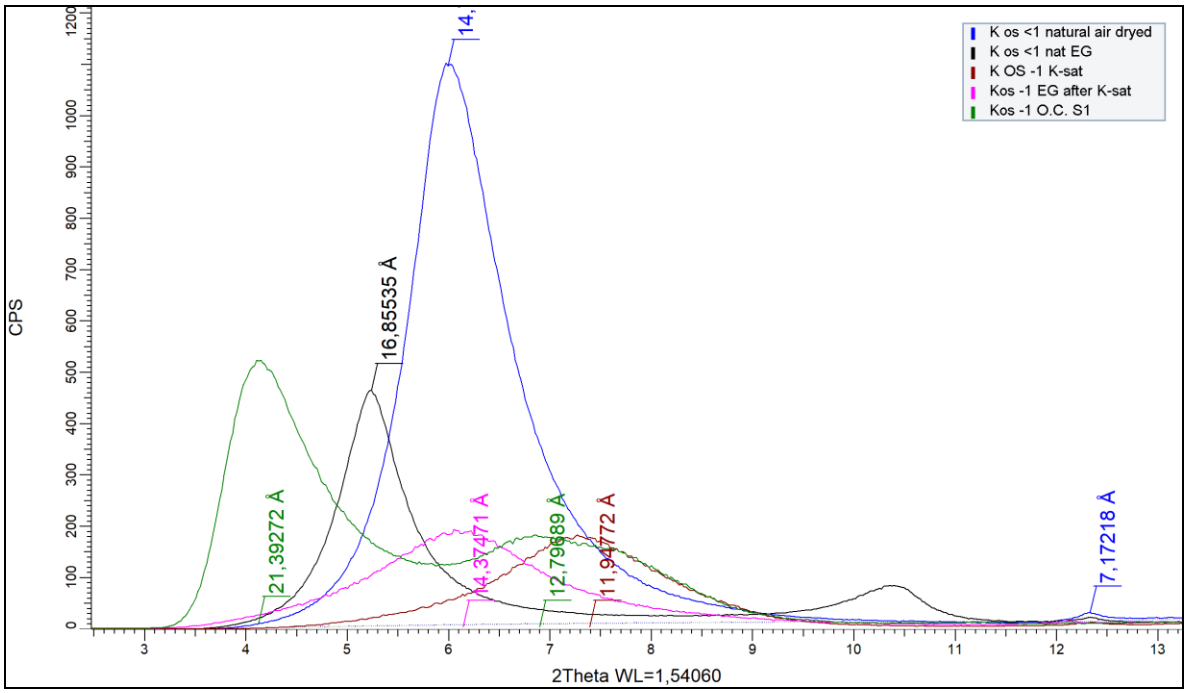
K os <1 natural air dryed
K os <1 nat EG
K OS -1 K-sat
Kos -1 EG after K-sat
Kos -1 O.C. S1
16,85535 Å
21,39272 Å
14,37471 Å
12,79689 Å
11,94772 Å
7,17218 Å
CPS
2Theta WL=1,54060

L

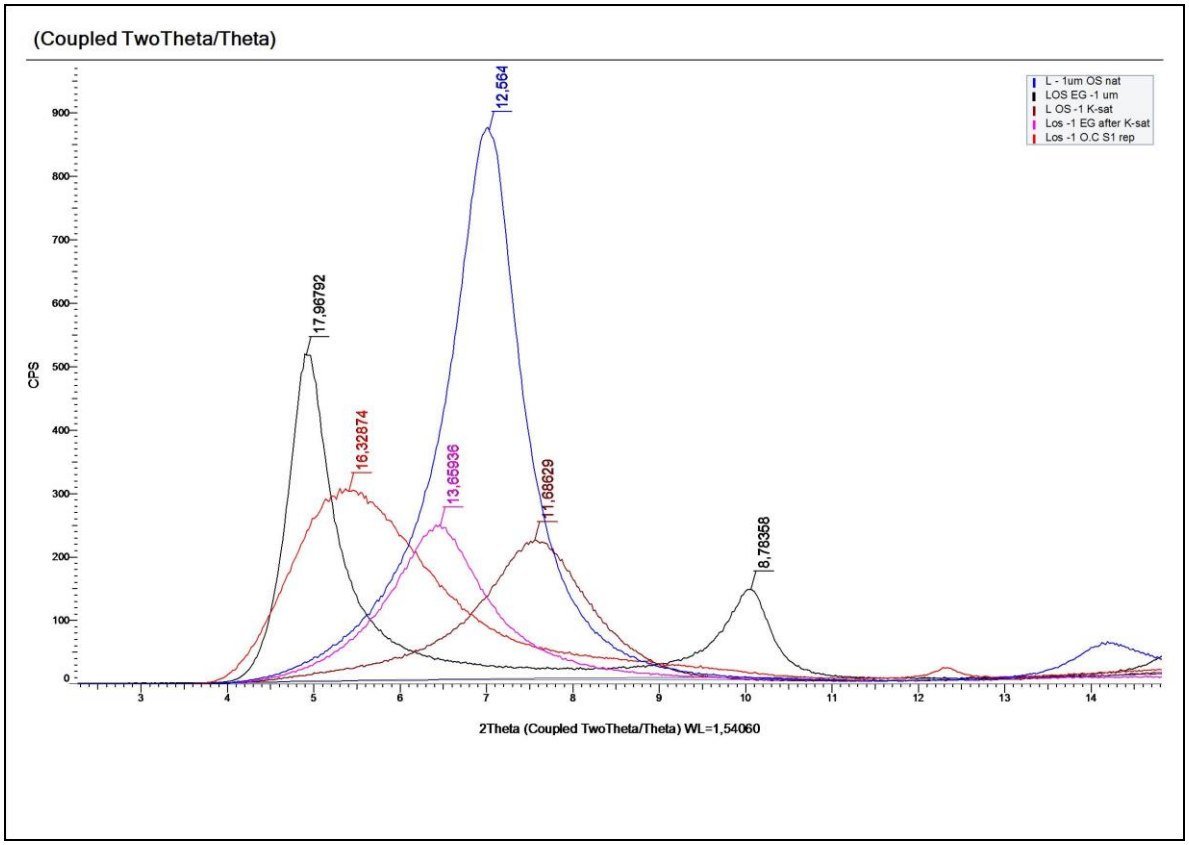
(Coupled TwoTheta/Theta)
L - 1um OS nat
LOS EG -1 um
L OS -1 K-sat
Los -1 EG after K-sat
Los -1 O.C S1 rep
12,564
17,96792
16,32874
13,65936
11,68629
8,78358
CPS
2Theta (Coupled TwoTheta/Theta) WL=1,54060

APPENDIX F

BENTONITE PURIFICATION BY WET CLASSIFICATION

An important remark, has to do with the processability of Na bentonites, for their rheological properties may cause particle dragging distorting concentration effect on hydrocyclone, consequently, some results are presented in Figure F1 aiming to outstand the effect of previous treatment to particle separation/concentration in wet media processing.

Figure F1 - Size distribution analyses for 3 types of pre-treatments to hydrocyclone size separation, for solid concentrations= 5%, 7.5% and 10%.

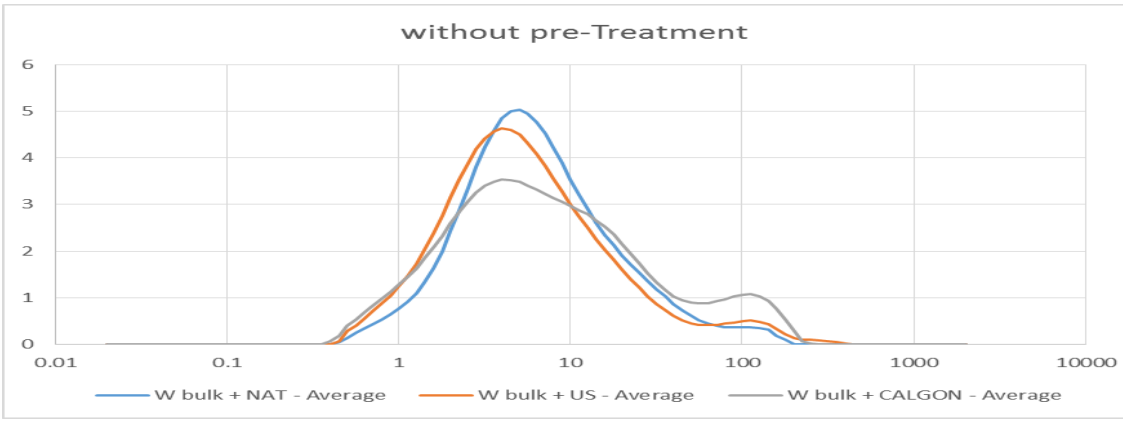

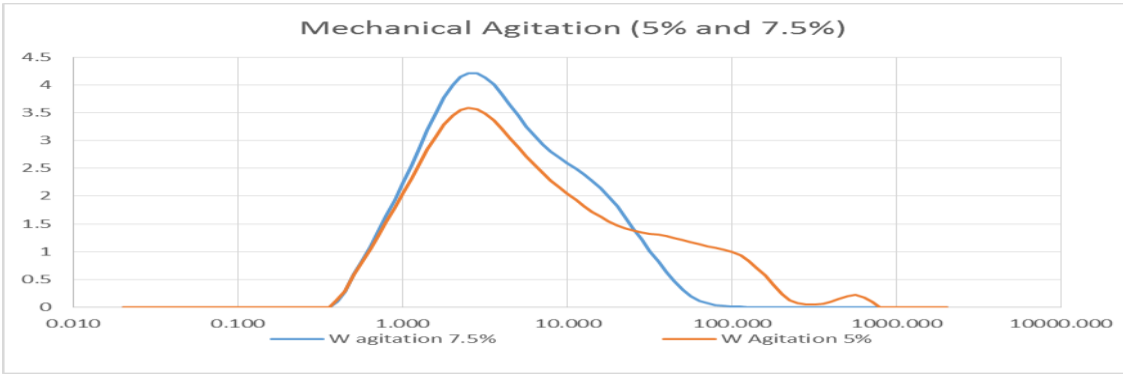

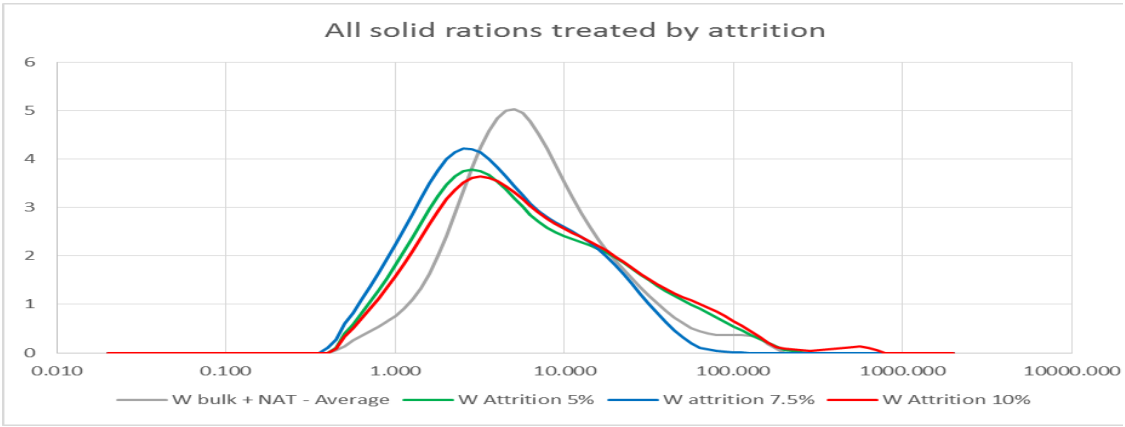

Plenty of information can be extracted from the series of particle size distribution charts over Figure F. Using Union process vertical attritor 1S, for 15 minutes in higher solid concentration (10%), we found the best pre-treatment arrangement to split size population before high pressure hydrocyclone, apparently desegregation of particles tend to shift mean size near 1 um. Smectite enrichment efficiency1 in wet media, and its correlation with the predominant compensating cations.